



LOW-ENERGY HIGH-THROUGHPUT MICROPOROUS EMULSIFICATION FOR LEMON OIL ENCAPSULATION

Wael Kaade

ADVERTIMENT. L'accés als continguts d'aquesta tesi doctoral i la seva utilització ha de respectar els drets de la persona autora. Pot ser utilitzada per a consulta o estudi personal, així com en activitats o materials d'investigació i docència en els termes establerts a l'art. 32 del Text Refós de la Llei de Propietat Intel·lectual (RDL 1/1996). Per altres utilitzacions es requereix l'autorització prèvia i expressa de la persona autora. En qualsevol cas, en la utilització dels seus continguts caldrà indicar de forma clara el nom i cognoms de la persona autora i el títol de la tesi doctoral. No s'autoritza la seva reproducció o altres formes d'explotació efectuades amb finalitats de lucre ni la seva comunicació pública des d'un lloc aliè al servei TDX. Tampoc s'autoritza la presentació del seu contingut en una finestra o marc aliè a TDX (framing). Aquesta reserva de drets afecta tant als continguts de la tesi com als seus resums i índexs.

ADVERTENCIA. El acceso a los contenidos de esta tesis doctoral y su utilización debe respetar los derechos de la persona autora. Puede ser utilizada para consulta o estudio personal, así como en actividades o materiales de investigación y docencia en los términos establecidos en el art. 32 del Texto Refundido de la Ley de Propiedad Intelectual (RDL 1/1996). Para otros usos se requiere la autorización previa y expresa de la persona autora. En cualquier caso, en la utilización de sus contenidos se deberá indicar de forma clara el nombre y apellidos de la persona autora y el título de la tesis doctoral. No se autoriza su reproducción u otras formas de explotación efectuadas con fines lucrativos ni su comunicación pública desde un sitio ajeno al servicio TDR. Tampoco se autoriza la presentación de su contenido en una ventana o marco ajeno a TDR (framing). Esta reserva de derechos afecta tanto al contenido de la tesis como a sus resúmenes e índices.

WARNING. Access to the contents of this doctoral thesis and its use must respect the rights of the author. It can be used for reference or private study, as well as research and learning activities or materials in the terms established by the 32nd article of the Spanish Consolidated Copyright Act (RDL 1/1996). Express and previous authorization of the author is required for any other uses. In any case, when using its content, full name of the author and title of the thesis must be clearly indicated. Reproduction or other forms of for profit use or public communication from outside TDX service is not allowed. Presentation of its content in a window or frame external to TDX (framing) is not authorized either. These rights affect both the content of the thesis and its abstracts and indexes.

Wael Kaade

Low-energy high-throughput
microporous emulsification for lemon oil
encapsulation

DOCTORAL THESIS

Supervised by:

Dr. Carme Güell Saperas

Co-supervised by:

Dr. Montserrat Ferrando Cogollos



UNIVERSITAT ROVIRA I VIRGILI

Universitat Rovira i Virgili

Department of Chemical Engineering

Tarragona, 2020

UNIVERSITAT ROVIRA I VIRGILI

LOW-ENERGY HIGH-THROUGHPUT MICROPOROUS EMULSIFICATION FOR LEMON OIL ENCAPSULATION

Wael Kaade

UNIVERSITAT ROVIRA I VIRGILI

LOW-ENERGY HIGH-THROUGHPUT MICROPOROUS EMULSIFICATION FOR LEMON OIL ENCAPSULATION

Wael Kaade

UNIVERSITAT ROVIRA I VIRGILI

LOW-ENERGY HIGH-THROUGHPUT MICROPOROUS EMULSIFICATION FOR LEMON OIL ENCAPSULATION

Wael Kaade



UNIVERSITAT
ROVIRA i VIRGILI

Departament d'Enginyeria Química, ETSEQ
Avinguda Països Catalans 26
Campus Sescelada, Spain
tel: + 34 977 55 8504

I STATE that the present study, entitled "Low-energy high-throughput microporous emulsification for lemon oil encapsulation", presented by Wael Kaade for the award of the degree of Doctor, has been carried out under my supervision at the Department of Chemical Engineering of Universitat Rovira i Virgili and that it fulfils all the requirements to obtain the doctoral degree.

Tarragona, February 10, 2020

Doctoral Thesis Supervisor/s

Dr. Carme Güell Saperas

Dr. Montserrat Ferrando Cogollos

Thesis committee

Dr. Lidieta Giorno

(President)

University of Calabria

Institute on Membrane Technology of the National Research Council

Calabria, Italy

Dr. Isabel Hernando Hernando

(Secretary)

Universidad Politécnica de Valencia

Escuela Técnica Superior de Ingenieros Agrónomos

Valencia, Spain

Dr. Susana Simal Florindo

(Vocal)

Universitat de les Illes Balears

Facultad de Ciencias

Palma, Spain

Acknowledgments

Carme, my supervisor, has picked me up at the airport on my first day in Spain and drove me home. I knew from that moment that I am in good hands. Thank you, Carme, for these four years and the opportunities you gave me to grow both on an academic and personal level.

Montse, was the voice of reason at many times during my PhD. Many a times I found myself wishing I had listened to your advice sooner. Thank you, Montse, for our conversation in Nantes and these four years under your supervision.

Sílvia, if there's anything I can learn from knowing you, is your ambition and driving energy for the whole group. I am truly grateful and proud to have been around to see your new projects flourish.

Tamara, I was very sad not to see you around our lab in my last year but I can say that working with you has taught me proficiency and responsibility. Thank you for being the first person to force the Spanish language unto me, I think you would be a bit proud of my improvement.

Miriam and Victor, I don't know where to start thanking you both. Miriam thank you for preparing me a meal on my first day in Tarragona (I regret saying no to it). Victor thank you for driving me on my first day to university. I wish you both all the success and happiness you deserve.

To Assad, Carmen and Aurélie, sorry if I worked you too hard at times but thank you because your work is part of the reason I am where I am now. Carmen I am very glad to have seen you again in our group and good luck in your confidential work.

To Esther, Pepa, Montse, Ana, Carmen and Susana thank you for everything. And to Núria Juanpere thank you for always receiving us with a smile.

To all the people I got to know at the university: Pau, Lola, Paula, Ariadna, Jordi, Miriam M., Anna, Ricardo, Aida, Monti, Morane, and Halima, thank you for the good times. And to Laura, Lina, Marni, Nihad, Samar, Noha, Sofia, Kamilla, Vibol, Nora, Helena, and Hande, thank you for being a part of my life during these years.

Gracias Luis por los cafés, las conversaciones y tu amistad.

Eduardo, thank you for being my food friend, my trip friend and life friend.

To my FoodIE friends that during my last year have become my second family: Junjing, Jorge, Nerea and Jitesh, Andrea and Carmen (again), I am very bad at showing emotions but I want you to know that I love you guys.

I am also grateful to Dr. Karin and Dr. Claire from Wageningen University for having me work in their group. It was an absolute honor. I had a one of a kind fruitful stay abroad experience and for that I also have to thank Emma.

Thank you Dr. Montse Mestres for your help with GC analysis and Dr. Carles Torras for your help characterizing my membranes.

I cannot but be grateful to the wonderful people at the Coral de la URV and Cor DaCapo and the Conservatory of Tarragona for filling my life with music and basically being my social life. I would like to specially thank Cristina, Francisco, Jaume and Michelle for their friendships.

Rita and Marie-Anne, thank you for being the bestest of friends.

Carole and Elie, thank you for always being there. One can't get cousins that are any better.

Dad, mom, Mario and Elie, I love you so much and thank you for being my backbone.

I finally wish to thank God because He guides my way with His love. Also, thank You God for giving me all these people to thank. Glory to your name.

UNIVERSITAT ROVIRA I VIRGILI

LOW-ENERGY HIGH-THROUGHPUT MICROPOROUS EMULSIFICATION FOR LEMON OIL ENCAPSULATION

Wael Kaade

UNIVERSITAT ROVIRA I VIRGILI

LOW-ENERGY HIGH-THROUGHPUT MICROPOROUS EMULSIFICATION FOR LEMON OIL ENCAPSULATION

Wael Kaade

Contents

Abstract	
List of symbols	
List of abbreviations	
1. Introduction	1
1.1. General introduction	3
1.1.1. Membrane emulsification	3
1.1.2. Premix membrane emulsification	4
1.1.3. Dynamic membrane emulsification	10
1.1.4. Essential oil encapsulation	14
1.1.5. Emulsifiers	15
2. Objectives	19
2.1. Objectives	21
3. Emulsifying lemon oil with inorganic membranes: Impact of interfacial properties on the volatile profile	23
3.1. Introduction	25
3.2. Materials and methods	28
3.2.1. Materials	28
3.2.2. Whey protein and electrostatic complex preparation	28
3.2.3. Premix membrane emulsification	29
3.2.4. Membrane cleaning	30
3.2.5. Droplet size distribution measurement	31
3.2.6. Zeta-potential measurement	31
3.2.7. Emulsion stability	31
3.3. Results and discussion	34
3.3.1. SPG membrane	34
3.3.2. Ceramic membrane	41
3.4. Conclusion	44

4. Low-energy high-throughput emulsification with nickel micro-sieves for essential oils encapsulation	45
4.1. Introduction	47
4.2. Material and methods	49
4.2.1. Microstructured nickel sieves	49
4.2.2. Contact angle test	50
4.2.3. Premix membrane emulsification	50
4.2.4. Micro-sieve cleaning procedure and water flux recovery	52
4.3. Results and discussion	52
4.3.1. Lemon oil emulsification using high-throughput premix ME with nickel micro-sieves	52
4.3.2. Micro-sieve integrity during premix ME and impact on productivity and emulsion properties	57
4.3.3. Effect of transmembrane pressure and pore size and geometry on droplet break-up	61
4.4. Conclusion	66
5. Dynamic membranes of tunable pore size for lemon oil encapsulation	69
5.1. Introduction	71
5.2. Materials and methods	72
5.2.1. Dynamic membrane of tunable size	72
5.2.2. Dynamic membrane cleaning	75
5.2.3. Emulsification	75
5.2.4. Emulsion stability	76
5.3. Results and discussion	76
5.3.1. Effect of coarse emulsion and DMTS characteristics on droplet size distribution and stability of LO emulsions	76
5.3.2. Effect of DMTS characteristics on emulsification throughput	84
5.3.3. Effect of tuning the system porosity on the emulsion characteristics and productivity: layered DMTS	88
5.4. Conclusion	89
6. Production of lemon oil emulsions stabilized by biopolymers with dynamic membranes of tunable pore size	91
6.1. Introduction	93
6.2. Materials and methods	94
6.2.1. Continuous phase preparation	95
6.2.2. Interfacial tension measurement	95

6.2.3. Emulsification	95
6.2.4. Particle size distribution measurement	97
6.2.5. Stability	97
6.3. Results and discussion	98
6.3.1. Effect of the DMTS system characteristics on the droplet size distribution of lemon oil emulsions stabilized with biopolymers	98
6.3.2. Effect of the DMTS system characteristics on the emulsification flux	103
6.3.3. Emulsions stability	105
6.3.4. Scaling equation for droplet size versus applied pressure in the DMTS system	110
6.3.5. Tailored design of the DMTS system	111
6.4. Conclusions	116
7. Pea protein for the stabilization of O/W emulsions: A microfluidics approach	117
7.1. Introduction	119
7.2. Materials and methods	120
7.2.1. Preparation of pea protein solution	120
7.2.2. Microfluidics experiments	120
7.3. Results and discussion	122
7.3.1. Effect of pea protein concentration on droplet stability	122
7.3.2. Effect of meandering channel length on droplet stability	124
7.3.3. Effect of continuous phase flow rate on droplet stability	125
7.4. Conclusion	126
8. Conclusion	127
8.1. General conclusion	129
8.2. Future work	131
References	133

UNIVERSITAT ROVIRA I VIRGILI

LOW-ENERGY HIGH-THROUGHPUT MICROPOROUS EMULSIFICATION FOR LEMON OIL ENCAPSULATION

Wael Kaade

List of Symbols

φ	[g s ⁻¹]	Mass flow rate
ρ_e	[kg m ⁻³]	Emulsion density
ρ_o	[kg m ⁻³]	Dispersed phase density
ρ_c	[kg m ⁻³]	Continuous phase density
ρ_p	[kg m ⁻³]	Particle density
ρ_d	[kg m ⁻³]	Bulk density
ϵ	[-]	Bed porosity
τ	[-]	Bed tortuosity
θ_d	[-]	Dispersed phase volume fraction
$\sigma_{w,p}$	[Pa]	Shear stress
σ	[mN m ⁻¹]	Droplet interfacial tension
η_e	[Pa.s]	Emulsion viscosity
ξ	[-]	Nickel micro-sieve tortuosity
a	[-]	fitting parameter
A	[cm ²]	Nickel micro-sieve effective area
A_{column}	[mm ²]	Area of emulsification column
A_f	[μ m ²]	Mean droplet area
A_i	[μ m ²]	Initial droplet area
A_o	[unit ²]	GC peak area on emulsification day
A_t	[unit ²]	GC peak area on sampling day
A_v	[m ⁻¹]	Particle surface area to particle volume ratio
b	[-]	fitting parameter
c	[-]	fitting parameter
d_{10}	[μ m]	10% of droplets are below this size
$d_{3,2}$	[μ m]	Area-volume mean size diameter
$d_{32,i}$	[μ m]	Incoming droplet size
$d_{32,o}$	[μ m]	Outgoing droplet size
$d_{4,3}$	[μ m]	Volume weighted mean diameter
d_{50}	[μ m]	50% of droplets are below this size
d_{90}	[μ m]	90% of droplets are below this size
d_{coarse}	[μ m]	Size of coarse emulsions droplets
d_h	[μ m]	Nickel micro-sieve hydraulic diameter

d_m	[μm]	Nickel micro-sieve mean pore diameter
d_p	[m]	Silica beads diameter
d_v	[m]	Bed interstitial void diameter
H	[mm]	Silica beads bed height
J	[$\text{m}^3 \text{m}^{-2} \text{h}^{-1}$]	Transmembrane flux
l_p	[μm]	Nickel micro-sieve pore length
N	[-]	Number of emulsification cycles
N_{coal}	[-]	Number of coalescence occurrences
P_{dis}	[kPa]	Pressure used to disrupt droplets
P_{flow}	[kPa]	Pressure used to push emulsion
P_m	[kPa]	Applied pressure
P_{ratio}	[-]	Dimensionless pressure
v_p	[m s^{-1}]	Average pore velocity
We	[-]	Webber number
w_p	[μm]	Nickel micro-sieve pore width
ΔP	[kPa]	Transmembrane pressure

List of abbreviations

CMC	Carboxymethylcellulose
DMTS	Dynamic membrane of tunable pore size
ESEM	Environmental scanning electron microscope
FID	Flame ionization detector
GC	Gas chromatography
HS-SPME	Head space-solid phase microextraction
L	Layered DMTS or layering
LO	Lemon oil
ME	Membrane emulsification
NaCaS	Sodium caseinate
O/W	Oil-in-water emulsion
PB	Packed bed
PP	Pea protein
Rep	Emulsification replicate
SPG	Shirasu porous glass
UV	Ultraviolet
W/O/W	Water-in-oil-in-water emulsion
WFR	Water flux recovery
WP	Whey protein

UNIVERSITAT ROVIRA I VIRGILI

LOW-ENERGY HIGH-THROUGHPUT MICROPOROUS EMULSIFICATION FOR LEMON OIL ENCAPSULATION

Wael Kaade

Abstract

Essential oils, such as lemon oil, are highly utilized in the food industry as flavorings. Lemon oil, is rich in unsaturated and oxygen functionalized terpenes making it susceptible to oxidation caused by oxygen, light and heat. Manufacturing and storage processes, packaging materials and ingredients in foods often cause modifications in overall flavor by reducing aroma compound intensity or producing off-flavor components. To limit aroma degradation or loss during processing and storage, encapsulation of essential oils prior to use in foods or beverages is a common practice. Also, encapsulation through microencapsulation and emulsification facilitates the incorporation of lemon oil into foods.

In this thesis, lemon oil-in-water emulsions were produced by means of a novel dynamic membrane of tunable pore size system and stabilized by a protein-polysaccharide electrostatic complex.

To produce stable emulsions, many factors are to be controlled including the type of emulsifier. First, using a protein-polysaccharide electrostatic complex, the impact of electric surface charge and the interfacial thickness on the physical and chemical stability of the emulsions was studied. Although an increase in droplet size was observed after 2 weeks, the color of the original emulsion as well as the aromatic profile were maintained in comparison with the emulsions stabilized with only a protein layer. The reason behind that might be the thickness of the emulsifier and the increased viscosity of the emulsion.

Aiming for producing emulsions with high-throughput, conventional emulsification technologies are highly energy intensive, causing damage to shear and heat sensitive products. Therefore, the a high-throughput low-energy emulsification system based on micro-structured nickel sieves to produce food-grade lemon oil in water emulsions was assessed. Results showed that emulsification is possible however certain limitations makes it difficult to maintain the integrity of the micro-

sieves and refine emulsions with oil fractions higher than 5%wt. The cleaning protocol was optimized to reduce the amount of wear caused on the micro-sieves.

A layer of silica glass beads was then added on top of the nickel micro-sieves to form what is called a dynamic membrane of tunable pore size (DMTS). This new system allowed to overcome the limitations pre-mentioned with the nickel micro-sieves, and by that stable lemon oil emulsions were produced with 40%wt oil fraction. Tuning the height of the silica beads layer and the size of the beads, allow to easily control the size and dispersion of the oil droplets in the emulsions. Also, a modified version of the DMTS system, produced emulsions with narrow size distribution ($\text{span} \leq 1$). Also, results obtained with the modified DMTS showed that major cutbacks in the system energy requirements can be done without compromising the quality of the emulsions (droplet size and dispersion, stability, flux).

Results from the DMTS system and those from emulsions stabilized with the protein-polysaccharide electrostatic complex encouraged testing the combined effect. For that reason, the effect of a protein-polysaccharide emulsifying complex, as compared to standard dairy proteins, on lemon oil emulsions properties and stability, using a DMTS system was assed. In addition to that, a modified DMTS was also tested for emulsification. Unlike the standard DMTS system, the modified DMTS contained two superimposed layers of silica beads of different sizes. First, results showed that using the DMTS system, and the modified DMTS in particular, resulted in the lowest reported droplet break-up for premix membrane emulsification ($0.05 < d_{3,2} / d_v < 0.2$). Also, emulsions stabilized with the complex had the lowest reported span value of 0.82. Similarly with the results from emulsions produced with conventional membranes, the emulsions produced with the DMTS system and stabilized with the protein-polysaccharide complex conserved the initial color of the emulsion.

Resumen

Los aceites esenciales, como el aceite de limón, son muy utilizados en la industria alimentaria como aromatizantes. El aceite de limón es rico en terpenos insaturados y funcionalizados con oxígeno, lo que lo hace susceptible a la oxidación causada por el oxígeno, la luz y el calor. Los procesos de fabricación y almacenamiento, los materiales de envasado y los ingredientes en los alimentos a menudo causan modificaciones en el sabor general al reducir la intensidad del compuesto aromático o producir componentes de sabor desagradable. Para limitar la degradación o pérdida de aroma durante el procesamiento y el almacenamiento, la encapsulación de aceites esenciales antes del uso en alimentos o bebidas es una práctica común. Además, la encapsulación a través de microencapsulación y emulsificación facilita la incorporación de aceite de limón en los alimentos.

En esta tesis, se produjeron emulsiones de aceite de limón en agua por medio de una nueva membrana dinámica de sistema de tamaño de poro regulable y estabilizadas por un complejo electrostático de proteína-polisacárido.

Para producir emulsiones estables, se deben controlar muchos factores, incluido el tipo de emulsificación. Primero, usando un complejo electrostático de proteína-polisacárido, se estudió el impacto de la carga superficial eléctrica y el grosor interfacial en la estabilidad física y química de las emulsiones. Aunque se observó un aumento en el tamaño de gota después de 2 semanas, el color de la emulsión original así como el perfil aromático se mantuvieron en comparación con las emulsiones estabilizadas con solo una capa de proteína. La razón detrás de esto podría ser el grosor del emulsionante y el aumento de la viscosidad de la emulsión.

Con el objetivo de producir emulsiones con alto rendimiento, las tecnologías de emulsificación convencionales requieren mucha energía, causando daños a los productos sensibles al calor y al cizallamiento. Por lo tanto, se evaluó un sistema de emulsión de baja energía y alto rendimiento basado en tamices de níquel

microestructurados para producir emulsiones de aceite de limón en agua de calidad alimentaria. Los resultados mostraron que la emulsificación es posible; sin embargo, ciertas limitaciones dificultan el mantenimiento de la integridad de los micro tamices y el refinado de las emulsiones con fracciones de aceite superiores al 5% en peso. El protocolo de limpieza fue optimizado para reducir la cantidad de desgaste causado en los micro tamices.

Seguidamente, se agregó una capa de esferas de vidrio de sílice en la parte superior de los micro tamices de níquel para formar lo que se llama una membrana dinámica de tamaño de poro regulable (DMTS). Este nuevo sistema permitió superar las limitaciones mencionadas anteriormente con los micro tamices de níquel, gracias a los cuáles se produjeron emulsiones estables de aceite de limón con una fracción de aceite del 40% en peso. Ajustar la altura de la capa de esferas de sílice y el tamaño de las esferas, permite controlar fácilmente el tamaño y la dispersión de las gotas de aceite en las emulsiones. Además, una versión modificada del sistema DMTS produjo emulsiones con una distribución de tamaño estrecha ($\text{span} \leq 1$). Los resultados obtenidos con el DMTS modificado mostraron que se pueden realizar importantes recortes en los requisitos de energía del sistema sin comprometer la calidad de las emulsiones (tamaño de gota y dispersión, estabilidad, flujo).

Los resultados del sistema DMTS y de las emulsiones estabilizadas con el complejo electrostático proteína-polisacárido alentaron a probar el efecto combinado. Por esa razón, se evaluó el efecto de un complejo emulsionante de proteína-polisacárido, en comparación con las proteínas lácteas estándar, sobre las propiedades y la estabilidad de las emulsiones de aceite de limón, utilizando un sistema DMTS. También, se probó un sistema DMTS modificado para la emulsificación. A diferencia del sistema DMTS estándar, el DMTS modificado contenía dos capas de esferas de sílice de tamaños diferentes. Primeramente, los resultados mostraron que el uso del sistema DMTS, y del DMTS modificado en particular, resultó en la ruptura de gotas más baja reportada para la emulsificación con membrana de premix ($0.05 < d_{3,2} / d_v < 0.2$). Además, las emulsiones estabilizadas con el complejo tuvieron el valor de dispersión más bajo reportado de 0.82. De manera similar con los resultados de las emulsiones producidas con membranas convencionales, las emulsiones producidas con el sistema DMTS y estabilizadas con el complejo proteína-polisacárido conservaron el color inicial de la emulsión.

UNIVERSITAT ROVIRA I VIRGILI

LOW-ENERGY HIGH-THROUGHPUT MICROPOROUS EMULSIFICATION FOR LEMON OIL ENCAPSULATION

Wael Kaade

UNIVERSITAT ROVIRA I VIRGILI

LOW-ENERGY HIGH-THROUGHPUT MICROPOROUS EMULSIFICATION FOR LEMON OIL ENCAPSULATION

Wael Kaade

1. Introduction

UNIVERSITAT ROVIRA I VIRGILI

LOW-ENERGY HIGH-THROUGHPUT MICROPOROUS EMULSIFICATION FOR LEMON OIL ENCAPSULATION

Wael Kaade

1.1. General introduction

Emulsions are a mixture of two immiscible liquids in which one is present as droplets, called the dispersed phase, distributed in the other the phase, that is referred as continuous phase. In that sense, simple emulsions would be in the form of oil-in-water (O/W) emulsions or water-in-oil (W/O) emulsions. Emulsions are not spontaneously formed. They require energy inputted into the system so the dispersed phase would break into microscopic sized droplets and suspend in the continuous phase. However, emulsions are thermodynamically unstable and they are bound to separate, which is referred to as the destabilization of an emulsion. A crucial element for the formation and kinetic stabilization of an emulsion is the emulsifier or surfactant. This latter is soluble in the continuous phase and contains a hydrophilic and a lipophilic group. For instance, for the production of an O/W emulsion, the emulsifier will dissolve in water and arrange its lipophilic site around and towards the oil droplets while leaving the hydrophilic site towards the water. The emulsifier layer around the oil droplets forms a protective layer stopping said droplets from coalescing that ultimately leads to the destabilization of the emulsion. Another function of the emulsifier is to reduce the interfacial tension between the two immiscible liquids and by that facilitates breaking up the dispersed phase into fine droplets.

Factors that affect an emulsion's stability include the dispersed phase droplets' size and size distribution, the mass/volume fraction of the dispersed phase, the type and amount of the emulsifier, the viscosity of the continuous phase and the emulsion's storage conditions.

1.1.1. Membrane emulsification

Emulsions can be produced by several methods such as rotor stator mixers, colloid mills, high-pressure homogenizers and ultrasonic homogenizers. These technologies, however, have some limitations controlling the dispersion of the final droplet size of the emulsion and use much higher energy input than required for droplet break-up, thus submitting the product to high shear stress and over-heating. Membrane emulsification (ME) is a dispersion technique that has gained advantage over traditional methods. It involves, depending on the type of ME, the permeation of either a pure dispersed phase through the microporous system into a continuous phase forming monodispersed suspended droplets, or the permeation of a coarse/premix emulsion through the micro-channels to reduce the size and size distribution of the preformed droplets. The main advantage of ME is that it requires lower energy input¹. Besides, this technique allows the control of the final droplet size of the emulsion by selecting the pore size, geometry and morphology of the membranes². To prepare O/W emulsions, a hydrophilic

membrane is required and for W/O emulsions a hydrophobic membrane is required. In any case, for successfully producing the emulsion, the membrane must remain well wetted by the continuous phase during the emulsification process. If the membrane becomes wetted by the continuous phase large droplet size distributions can be expected.

Comparing high-energy emulsification methods with ME, a microfluidizer for instance, which passes a coarse emulsion under high pressure through an orifice and breaks droplets by shear, impact and cavitation forces, produces emulsions with large droplet size dispersions while membranes are very efficient at refining an emulsion³. With such broad size distribution, a later addition of more stabilizers might be needed to make the emulsions more stable kinetically⁴.

More importantly, ME requires much less energy than the traditional emulsification methods. The energy input per unit volume in high-energy emulsification methods is about 5-20 kJ/dm³ while in membrane emulsification it is about 0.05-5 kJ/dm³⁵. It has been shown that in systems like high pressure homogenizers more than 99.9% of the energy is mostly converted into heat causing an increase in temperature⁶, therefore potentially damaging some of the emulsion's components. A recent study⁷ showed that no substantial degradation to heat sensitive nutrients occurs in the short time that the emulsion pass through the valve of a high pressure homogenizer; however the authors did recommend a rapid cooling step after emulsification to avoid degradation downstream. In food emulsions, the loss of volatile compounds is highly possible with the sudden increase of temperature caused by the extra energy introduced in the system by conventional emulsification methods.

In brief membrane emulsification allows to control of emulsions' droplet size and obtain narrow droplet size distribution. Also, less energy is invested and low shear values are registered resulting in no raise in emulsion temperature. These strong points are clearly advantageous for applications demanding stable emulsions with shear or heat sensitive compounds, such as food aromas.

1.1.2. Premix membrane emulsification

Membrane emulsification is a low-energy technology that branches into two types: direct⁸⁻¹⁹ and premix^{4,8,20-26} ME. Direct ME is when a pure disperse phase is passed through a membrane into a flowing or agitated continuous phase (Figure 1.1a). Control of droplet formation is achieved by passing a low amount of disperse phase through the membrane, resulting in low productivity and limiting scale-up of the process.

Premix ME, on the other hand (Figure 1.1b), is the passage of a premix or a coarse emulsion through a membrane to refine it resulting into a stable monodispersed emulsion. The advantages of premix ME over direct ME are in small droplet sizes and higher throughput for a given pore size²⁷, even though this might be related with a lower degree of monodispersity in the final product. Also, in general, a premix ME setup is simpler and easier to operate and control and the energy needed is one order of magnitude lower than in direct ME²⁷.

Premix ME is a well-established emulsification technique where many types of microstructured systems have been utilized. Corn²⁸ and sunflower oil^{4,25} emulsions have been produced by conventional membranes like the Shirasu porous glass (SPG) membranes. These membranes were first used for direct emulsification in 1988²⁹ and for premix emulsification in 1996³⁰. Because of their low-energy consumption and simplicity, they have gained popularity and the studies that use SPG membrane emulsification are innumerable^{2-4,27,28,31,31-37}. However, SPG membranes are expensive and have an extensive and time-consuming cleaning and regeneration procedure. Moreover, although the SPG membranes have large effective areas (3.2 - 30.7 cm²³³), the fluxes (flow rate per unit area) obtained with these membranes lie on the low range of the fluxes obtained with high-throughput ME systems.

More studies include other types of membranes used in premix ME. Trentin *et al.* (2009)²⁴ also have produced sunflower oil emulsions but using commercial polymeric microfiltration membranes (polycarbonate, nylon, polyethersulfone and nitrocellulose). These authors concluded that not all polymeric membranes are suitable to produce stable emulsions and factors like emulsifier type and emulsion pH could strongly control this aspect. This is a disadvantage when it comes to the production of food emulsions because they contain proteins at specific pH and that is difficult, and sometimes impossible, to change. Other polymeric membranes reported include polytetrafluoroethylene¹³⁹, polyethylene¹⁴⁰ and cellulose acetate¹⁴¹. Also, ceramic¹⁴² and glass¹⁴³ membranes were reported to be used in premix membrane emulsification. Although emulsification was possible with these membranes, fluxes remained low (0.45 - 13 m³m⁻²h⁻¹) and the setup was not simple or easily manipulated. In addition, these membranes have interconnected channels and foul easily especially when using proteins and they are difficult to clean²¹. For that reason it would be useful to utilize membranes with straight-through pores such as nickel membranes^{20,21}.

Nickel micro-engineered membranes, a.k.a. nickel sieves, are produced by the galvanic deposition of nickel onto a substrate that is fabricated by photolithography and etching. This technique is highly cost effective and accurate, producing highly porous nickel sieves with homogenous pore size distribution^{8,15}.

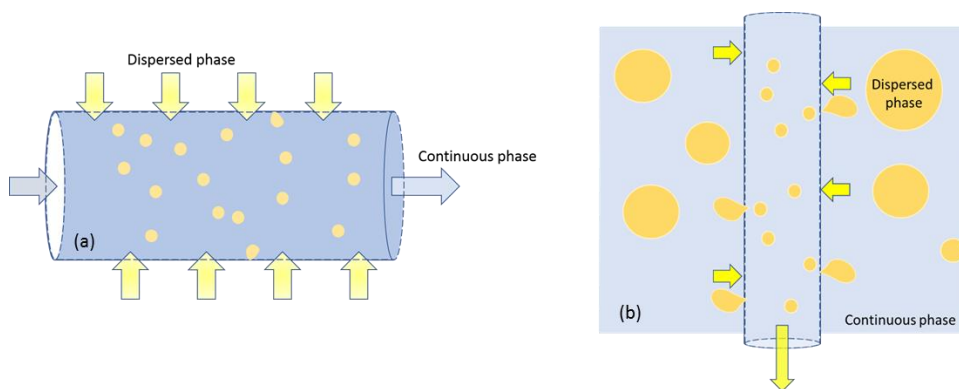


Figure 1.1. Scheme of a direct membrane emulsification

Unlike conventional membranes which have a deep and intricate network of pores, nickel sieves have straight-through pores that can be easily cleaned when fouled. Moreover, their metal properties allow them to be used under pressures to 500 kPa²¹, which would otherwise break more vulnerable membranes (e.g. flat ceramic membranes) having the same shape and dimensions. Thus, nickel micro-sieves combine mechanical resistance and pores in the micron range that make them suitable for emulsification.

Nickel micro-sieves have been employed in both direct and premix ME. Table 1.1 summarizes the studies that have used nickel micro-sieves to produce emulsions and the experimental conditions. In direct emulsification, a Micropore Dispersion Cell is reported to be used where the to-be-dispersed phase is pumped up through the micro-sieve into a tank containing the aqueous phase. This tank contains a rotating paddle, right above the nickel micro-sieve, which agitates the continuous phase thus helping in the break-up of the oil droplets. Dragosavac *et al.* (2012)¹² have prepared pumpkin oil double emulsions using this technique attaining fluxes up to 3.2 m³.m⁻².h⁻¹. Kosvintsev *et al.* (2005)¹⁵ and Egidi *et al.* (2008)¹⁷ reported the possibility of producing sunflower oil emulsions with fluxes of 0.9 and 2.64 m³.m⁻².h⁻¹ respectively. All these studies also mention that the produced emulsions have monosized droplets. Santos *et al.* (2015)⁸ produced lemon oil emulsions with fluxes between 0.1 and 1 m³.m⁻².h⁻¹, while the emulsions obtained were polydisperse. In all cases the authors agree that nickel micro-sieves require surface modification to change them from hydrophobic to hydrophilic to be used in the production of O/W emulsions.

Table 1.1. Literature review on the use of nickel micro-sieves for producing emulsions.

Emulsion type	Provider	Nickel Micro-Sieve				Porosity (%)	Surface Area (cm ²)	Surface treatment	Emulsification type	Micro-Sieve Shape	Ref.
		Length/Diameter	Width	Thickness	Pore size (µm)						
O/W	Micropore	5	-	-	-	0.05	52	-	Direct	Cylindrical	9
		10	-	-	-	0.2	-				
		20	-	-	-	0.9	-	Pre-soaked in proprietary wetting agent 30 min to increase hydrophilicity	Direct	Flat	12
		30	-	-	-	2	-				
O/W	Micropore	40	-	-	-	3.6	-				
		10	-	-	-	0.2	8.4		Direct	Flat	13
O/W	Micropore	10	-	-	-	0.2	26			Cylindrical	
		10	-	-	-	0.2	26				
		10	-	-	-	0.2	26	Pre-soaked in wetting agent for 30 mins to increase hydrophilicity	Direct	Cylindrical	14
		20	-	-	-	0.9	26				
O/W	Micropore	10	-	-	-	0.26	8.5	Treated with wetting agent to render surface hydrophilic	Direct		
		20	-	-	-	0.9	8.5		Premix	Flat	8
									Direct		
									Premix		

Continuation to Table 1.1

Emulsion type	Provider	Nickel Micro-Sieve				Surface Area (cm ²)	Surface treatment	Emulsification type	Micro-Sieve Shape	Ref.
		Length/Diameter	Pore size (µm)	Width	Thickness					
		9								
O/W	Micropore	18	-	-	-	-	-	Direct	Flat	¹⁵
		40								
O/W	Micropore	15	-	-	-	-	Soaked in polyalkyleneoxide modified heptamethyltrisiloxane	Direct	Flat	¹⁶
O/W	Micropore	20	-	-	-	5.6	-	Direct	Flat	¹⁷
O/W	Micropore	20	-	-	-	0.9	-	Direct	Flat	¹⁷
O/W	Micropore	10	-	-	-	-	-	Direct	Flat	¹⁸
O/W	Veco	405	10	-	-	4	-	Premix	Flat	³⁸
		336.9	13.2	80	-	4.79	-			
		329.3	12.8	200	-	4.37	-			
O/W	Veco	331.1	11.6	350	-	3.95	-	Premix	Flat	³⁹
		330.2	10.6	400	-	3.62	-			

Continuation to Table 1.1

Emulsion type	Provider	Nickel Micro-Sieve			Porosity (%)	Surface Area (cm ²)	Surface treatment	Emulsification type	Micro-Sieve Shape	Ref.	
		Length/Diameter	Pore size (μm)	Thickness							
O/W	Veco	3	-	50	-	-	Deposition of 50 nm layer of silicon oxide to render surface hydrophilic	Direct	Flat	19	
O/W	Veco	3	-	50	-	-	Plasma enhanced chemical vapor deposition influences membrane surface properties	Direct	Flat	10	
O/W	Veco	4	4	60	2.65	1.43					
		413.2	7.1	200	1.53	1.43					
		330.2	10.6	400	3.62	1.43					
		331.1	11.6	350	3.95	1.43		-	Premix	Flat	21
		329.3	12.8	200	4.37	1.43					
O/W	Veco	336.9	13.2	80	4.79	1.43					
O/W	Veco	331.1	11.6	350	3.95	1.43	-	Premix	Flat	40	
O/W	Veco	331.1	11.6	350	3.95	1.43	-	Premix	Flat	41	
O/W	Veco	331.1	11.6	350	3.95	1.43	-	Premix	Flat	22	

A stirred cell has also been used in a premix ME setup to refine a coarse emulsion. Santos *et al.* (2015)⁸ produced lemon oil in water emulsions using a stirred cell with a hydrophilic nickel micro-sieve. The stirred cell module has low fluxes and the authors reported that emulsification and droplet break-up was possible only when nickel micro-sieves' surface properties were previously modified, resulting in polydisperse emulsions. Moreover, nickel micro-sieves have also been used in premix ME with high-throughput system. In this system, the coarse emulsion is pressed through the micro-sieve at higher pressures than in the stirred cell, and droplet break-up mainly occurs in the membrane channels. This system has been used without any surface modification of the nickel micro-sieve to produce n-hexadecane/water emulsions^{20,21,26} and sunflower oil/water emulsions⁴². For n-hexadecane/water emulsions, Nazir *et al.* (2011)²⁰ reported fluxes up to 1500 m³.m⁻².h⁻¹ at 200 kPa. As far as the author knows there are no other previous applications for the production of food grade O/W emulsions with nickel micro-sieves using a high-throughput premix ME system.

1.1.3. Dynamic membrane emulsification

A new system, named dynamic membrane, DM, was first reported by Van Der Zwan *et al.* (2008)²⁶. This membrane is made of a bed of hydrophilic silica glass micro-beads supported by a nickel micro-sieve (Figure 1.2) and it is referred to as "dynamic" because the micro-beads size and bed height may be selected to tune the porosity and the thickness of this microporous system, respectively.

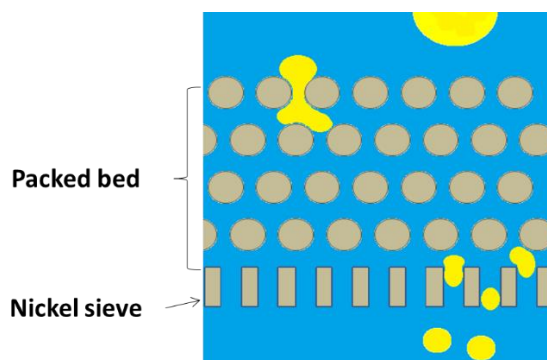


Figure 1.2. Dynamic membrane of tunable pore size system

The DM system is cheap and easily disassembled, cleaned and reused. This system is reported to yield high throughput ($\approx 1000 \text{ m}^3 \cdot \text{m}^{-2} \cdot \text{h}^{-1}$) and produce monodispersed emulsions⁴⁰. Dynamic membranes have been reported for the production of both non-food^{22,26,40,43} and food grade emulsions^{42,44–46}. Sunflower oil simple O/W^{42,44} and W/O/W double⁴⁵ emulsions were reported in the literature to be produced with the DM system. Also, DM have been used for the production of food foams⁴⁶. From this point forward this system will be referred to as dynamic membranes of tunable pore size (DMTS) to stress the fact that microporous structure can be tailored. Table 1.2 shows the summary of all the emulsions produced with the DMTS system, reporting the characteristics of the bed, and operating conditions used in literature. As it is clear, silica beads sizes used ranged from 30 to 90 μm with only one case going up to 1000 μm and the most common bed height was that of 2mm. As for the applied emulsification pressure, the highest pressure used was 600 kPa⁴⁵, in the same range as the highest pressure of 500 kPa³⁹ used for emulsification with the nickel micro-sieves alone. Studies that used the DMTS systems for food applications report transmembrane fluxes that range between 65 - 800 $\text{m}^3 \cdot \text{m}^{-2} \cdot \text{h}^{-1}$ depending on the beads size used, the bed height, the applied pressure and also the composition of the emulsion, knowing that food emulsions can be quite viscous. Only one study⁴², reported using a protein, whey protein in particular, to stabilize sunflower oil-in-water emulsions. These emulsions were successfully refined at 300 kPa using a DMTS (72 μm beads size and 2 mm bed height) with little to no signs of bed fouling. This shows that the DMTS can be used for the production of food emulsions whose constituents are complex.

Table 1.2. Summary of operating conditions used for DMTS emulsification in literature.

	Emulsifier	Oil	PB		Ref.		
			Size (μm)	Height (mm)			
O/W polymer microcapsule	Poly-vinyl alcohol	Decane	$d_{50} = 30$	2	2		
			$d_{50} = 65$	2	2		
			$d_{50} = 78$	2, 5, 10, 20	2 ²²		
			$d_{50} = 78$	2	1, 2, 3, 4		
O/W	Tween80	Precirol	$d_{50} = 90$	2	2		
			$d_{50} = 30$	2	2		
			$d_{50} = 63$	2	2		
			$d_{50} = 63$	1, 3, 5	2		
			$d_{50} = 75$	2	0.5, 1, 1.25, 1.5		
			$d_{50} = 75$	2	2		
W/O/W	Whey protein	Sunflower	$d_{3,2} = 71$	2	2, 3, 4, 5		
			$d_{50} = 70, 100, 200, 300, 400, 1000$	100	47		
O/W	Pea protein	Sunflower 20%	$d_{3,2} = 71$	2	3		
						Whey protein	
							Lentil protein

Continuation to Table 1.2

	Emulsifier	Oil	PB			Ref.
			Size (μm)	Height (mm)	Pressure (bar)	
W/O/W	Glucose + Tween20	Sunflower 5%	$d_{3,2} = 30$	2	2,4,6	45
			$d_{3,2} = 55$	2	2,4,6	
			$d_{3,2} = 65$	2	2,3,4,5	
			$d_{3,2} = 65$	2,5,20,40	4	
			$d_{3,2} = 78$	2	4	
			$d_{3,2} = 90$	2	4	
O/W	Tween20	Hexadecane 5%	$d_{4,3} = 75.9$	1.9, 4.3, 9.5, 17.4	0.5 - 5	26
O/W	Tween20	Hexadecane	$d_{3,2} = 55$	2.5	3,5	41
			$d_{3,2} = 55$	2.5	2	
O/W	Tween20	Hexadecane 5%	$d_{3,2} = 55$	2.5	0.5 - 5	40
			$d_{3,2} = 65$	2.5	2	
			$d_{3,2} = 78$	1,2,5,5,10,20	2	
			$d_{3,2} = 90$	2.5	2	
Foam	Whey protein	Nitrogen	$d_{3,2} = 65$	2.5	1,2,3,4,5	46

1.1.4. Essential oil encapsulation

Essential oils, such as lemon oil, are highly utilized in the food industry as flavorings. Manufacturing and storage processes, packaging materials and other ingredients in foods often cause modifications in the overall flavor by reducing aroma compound intensity or producing off-flavor components. To limit aroma degradation or loss during processing and storage, encapsulation of essential oils prior to incorporation in foods or beverages is a common practice.

Lemon oil (LO), widely used in the food industry to flavor many products, from baked goods and soft drinks to dairy and confectionery products, is easily degraded by oxidation, heat and/or light⁴⁸. For those reasons, lemon oil emulsions and capsules have been produced as means to protect and facilitate the handling of this volatile oil^{8,48-53} as well as allow its dispersion in aqueous foods like soft drinks. Additionally, studies on LO emulsification are becoming more relevant since, d-limonene, one of its major constituents, is an environmental friendly chemical that has been assessed in the production of green emulsions with applications in agrochemical products^{54,55}. Also, recently an interest in the antimicrobial, antifungal and antioxidant properties of lemon oil has been rising⁵⁶.

As for LO emulsification, a study of the literature shows that both high energy (shear intensive) as well as low energy techniques were used (Table 1.3). The latter techniques, which require low energy inputs, are microchannel emulsification⁵³, membrane emulsification with a stirred cell module⁸ and spontaneous emulsification⁵⁷. Since LO, contains many volatile compounds that are heat sensitive, it will benefit of using a low energy – low shear membrane emulsification technique. However, these systems used in the literature so far, are far behind industrial requirements. Microchannel emulsification, for instance, applies a direct emulsification technique with very low flow rates ($5 \text{ mL}\cdot\text{h}^{-1}$). The stirred cell module, and although it works for premix emulsification, rendered fluxes that are still low ($0.1 - 1 \text{ m}^3\cdot\text{m}^{-2}\cdot\text{h}^{-1}$) and the emulsions produced were polydispersed. As for spontaneous emulsification, it needs high concentrations of emulsifiers and still the emulsions are not stable for more than 24 hours. All these drawbacks point towards the need of a low energy – low shear membrane emulsification technique for lemon oil emulsification that can produce stable emulsions with narrow size distributions and at industrial fluxes. This is important not only for scaling up purposes but also for post-emulsification processes like spray drying that gives the best results with monodispersed stable emulsions⁵⁸.

Table 1.3. Techniques used to encapsulate lemon oil

Microcapsules	Polymer microcapsules	52,59
	Spray drying	48,50
	β – Cyclodextrin capsules	51,60–63
	Freeze drying	64
Emulsions	Shear homogenizer	65–67
	High pressure homogenizer	68–71
	Microfluidizer	49,72,73
	Microchannel emulsification	53
	Stirred cell	8
	High intensity ultrasonic processor	74,75

1.1.5. Emulsifiers

Lemon essential oil emulsions in literature, have been stabilized with sophorolipids⁶⁵ (a surface active glycolipid), non-ionic (e.g.: sucrose monopalmitate⁶⁹, Span80⁷⁴, Tween20⁵³ and Tween80^{69,76}) and anionic (Sodium dodecyl sulfate⁵³) surfactants, polysaccharides (e.g.: gum Arabic, corn fiber gum and beet pectin⁴⁹) and milk protein (bovine serum albumin⁵³ and sodium caseinate⁶⁴).

Polyoxyethylene (20) sorbitan monolaurate, commercially known as Tween20, is a conventional emulsifier used to prepare O/W emulsions (Table 1.2). This nonionic surfactant is FDA approved for human consumption as a food additive (Code of Federal regulations, Title 21, Chapter 1, Subchapter B, Part 172, Subpart F, Sec. 172.515). However, in aim of improving interfacial structures and chemical stability, a different stabilizer is required to better stabilize the lemon oil emulsions and protect the oil from oxidation. It was reported that whey protein (WP) significantly lowered β -carotene emulsions degradation compared to Tween20⁷⁷. Also, other authors stress that WP at controlled pH, whether acidic or basic) can control the chemical stability of the emulsions^{78,79}. Besides, the presence of proteins themselves, present an added nutritional value to emulsions.

Traditional food grade emulsifiers are dairy proteins like whey protein and sodium caseinate (NaCaS). Proteins are considered as good emulsifiers because of their amphiphilic nature. The main components of WP are the globular proteins β -lactoglobulin and α -lactalbumin forming 50% and 20% respectively of the total protein content. NaCaS contains a mixture of α_{S1-} , α_{S2-} , β - and κ -casein proteins in a weight proportion of 4:1:4:1^{80,81}.

Proteins contain hydrophobic parts that adsorb onto the oil phase while their hydrophilic parts remain in the aqueous phase forming a bulky barrier at the interface⁸². However proteins have their limitations due to their complicated structures, the interactions they have between their own molecules and the way they adsorb to the interface changes resulting in a less coherent protein layer structure⁸³.

Therefore, other studies have reported using mixtures of proteins and polysaccharide that forms a bulkier complex⁸⁴⁻⁸⁶. One kind of complexation is electrostatic where the oppositely charged biopolymers interact. For example, Berendsen, Güell, Henry, & Ferrando, (2014)⁸⁷ have successfully produced a water soluble 0.5%wt whey protein – 0.25%wt carboxymethyl cellulose complex (WP-CMC) at a pH of 3.8. Below its isoelectric point (pH \approx 5.2), WP is positively charged and the polysaccharide (CMC) is negatively charged. Upon mixing, an over-all negatively charged complex is formed. In addition to having a thicker layer protecting the oil droplets and preventing their coalescence in O/W emulsions, CMC increases the viscosity of the continuous phase making it more difficult for droplets to move and retarding creaming. Another advantage of WP-CMC electrostatic complex is the possibility, in the presence of CMC, to reduce the concentration WP needed to stabilize an emulsion. Moreover, it has been reported that the WP-CMC complex increases the stability of emulsions^{84,87}.

To the author's knowledge, only two studies used another type of protein-polysaccharide covalent complexation known as a Maillard conjugate (sodium caseinate-lactose and soy protein-gum acacia) to stabilize lemon oil emulsions^{70,71} and no studies report the use of the WP-CMC electrostatic complex.

Nevertheless, a recent interest in plant-based proteins has been on the rise. With the increase of the global human population to 9.5 billion by 2050, the demand for protein is expected to double. For that reason, research is turning to plant proteins as another protein source. Plant proteins are safer for human consumption (low allergenicity) and more sustainable, not to mention they are a preference for people following a vegan or vegetarian diet. A downside to plant proteins is their strong taste and low solubility in water. In the last year alone more than fifteen studies have reported using plant proteins as emulsifiers to stabilize O/W emulsions. Some of these studies are reported in Table 1.4.

One kind of plant protein that stands out in Table 1.4, is pea protein (PP). PP's major components (65-80%) are the globular proteins: 11S legumin, 7S vicilin^{88,89}. Compared to other plant proteins like soy, PP have lower allergenic potential and higher nutritional value. Similarly to milk proteins, PPs are amphiphilic and by that can be used to stabilize emulsions as it is clear in Table 1.4. Burger & Zhang, (2019)⁸⁹ report that the process for PP to stabilize an oil/water interface starts by

migration of the protein to the interface, adhesion, partial denaturation and reorientation (the hydrophilic portion facing the water and the hydrophobic one inside the oil) and finally the formation of a viscoelastic film at the interface. This film stabilizes oil droplets through electrostatic repulsion and steric hindrance.

Table 1.4. Literature review on the use of plant proteins as emulsifiers.

O/W Emulsions	Emulsifier	Ref.
10% wt. sunflower oil	Whey-pea protein blends	90
	Sodium caseinate-pea protein blends	
2% wt. corn oil	Pea protein-gum Arabic maillard conjugates	91
5% wt. rapeseed oil	Fava bean protein isolate	92
5% wt. flaxseed oil	Flaxseed protein	93
	Flaxseed protein-flaxseed mucilage complex	
10% wt. sunflower oil	Brown rice protein	94
	Hemp protein	
	Pea protein	
	Soybean protein	
10% wt. soybean oil	Sunflower seeds protein	95
10% wt. soybean oil	Rice protein-chlorogenic acid complex	95
	Quillaja saponin protein	
5% wt. medium chain triglyceride oil/flaxseed oil mixture	Gum arabic	96
25% vol. corn oil	Cumin protein isolate	97
10% wt. sunflower oil	Sunflower seeds derived complexes	98
15%wt sunflower oil	Pea protein	99
	Soy protein	
	Milk- pea protein and milk-soy protein mixtures	
2.5% wt. caprylin oil	Flaxseed protein	100
	Flaxseed protein-flaxseed mucilage complex	
10% wt. corn oil	Lotus seedpod proanthocyanidin-whey protein complex	101
5% wt. canola oil	Pea protein	102
50% wt. canola oil	Lentil protein	103
	Lentil protein-carboymethyl cellulose complex	
	Lentil protein-gum Arabic complex	
	Lentil protein-alginate complex	
10% vol. rapeseed oil	Lentil protein-l-carrageenan complex	104
	Soy protein	
	Peanut protein	

UNIVERSITAT ROVIRA I VIRGILI

LOW-ENERGY HIGH-THROUGHPUT MICROPOROUS EMULSIFICATION FOR LEMON OIL ENCAPSULATION

Wael Kaade

2. Objectives

UNIVERSITAT ROVIRA I VIRGILI

LOW-ENERGY HIGH-THROUGHPUT MICROPOROUS EMULSIFICATION FOR LEMON OIL ENCAPSULATION

Wael Kaade

2.1. Objectives

The purpose of this work is to assess the use of novel low-energy high-throughput emulsification techniques, based on microporous systems, to encapsulate lemon oil in stable and narrow droplet size emulsions. The effect on the performance of the emulsification system and emulsion stability of several emulsifiers, from a low molecular weight non-ionic surfactant to biopolymers, is studied. These general goals can be reached by fulfilling the following specific objectives:

- To use a protein-polysaccharide electrostatic complex to stabilize lemon oil emulsions produced with a conventional premix membrane emulsification system, based on inorganic membranes, and to assess the improvement in the chemical stability of target volatile compounds of lemon oil.
- To produce lemon oil emulsions, stabilized with Tween 20, with nickel micro-sieves and ascertain advantages and limitations of this microporous system.
- To test a novel microporous system based on a bed of silica beads supported by a nickel micro-sieve (dynamic membranes of tunable size, DMTS) to produce lemon oil emulsions with oil fractions of 20 and 40%, stabilized with Tween 20.
- To evaluate the effect of the DMTS characteristics, thickness and interstitial void fraction, and the porosity of the nickel micro-sieve support in droplet break-up, emulsion productivity and emulsion stability for Tween 20 stabilized emulsions.
- To determine if the DMTS system enables to produce lemon oil emulsions stabilized with biopolymers such as whey protein, sodium caseinate and whey-protein – carboxymethyl cellulose electrostatic complex. The effect of the DMTS characteristics on droplet break-up, emulsion productivity and emulsion stability are studied.
- To implement modifications in the DMTS system, by tuning the microporous structure, to obtain stable and narrow droplet size distribution lemon oil emulsions stabilized with Tween 20 or biopolymers, while reducing the energy input to the system.
- To use microfluidics to study the use of a plant-based protein, pea protein, as an alternative to dairy proteins to stabilize food emulsions.

UNIVERSITAT ROVIRA I VIRGILI

LOW-ENERGY HIGH-THROUGHPUT MICROPOROUS EMULSIFICATION FOR LEMON OIL ENCAPSULATION

Wael Kaade

3. Emulsifying lemon oil with inorganic membranes: Impact of interfacial properties on the volatile profile

This chapter has been submitted as:

Kaade, W., Sánchez, C.M., Güell, C., De Lamo-Castellví, S., Mestres, M. and Ferrando, M., *“Emulsifying lemon oil with inorganic membranes: Impact of interfacial properties on the volatile profile”*, *Food Chemistry*

UNIVERSITAT ROVIRA I VIRGILI

LOW-ENERGY HIGH-THROUGHPUT MICROPOROUS EMULSIFICATION FOR LEMON OIL ENCAPSULATION

Wael Kaade

3.1. Introduction

Essential oils are known to deteriorate quickly producing off-flavors and by that reducing their shelf-life ⁷⁹. Lemon oil, a natural flavoring and food additive, which consumers nowadays highly seek, is rich in unsaturated and oxygen functionalized terpenes making it susceptible to oxidation caused by oxygen, light and heat. The main components of lemon oil are d-limonene, γ -terpinene, β and α – pinene and the isomers of citral, neral and geranial (Table 3.1). These two latter, dominate the over-all flavor profile of fresh lemon oil over more than 130 volatiles found in lemon oil ¹⁰⁵.

Table 3.1. Principal compounds present in lemon essential oil ^{106,107}

Compound	Quantities in fresh cold-pressed LO (%)	Classification
d-Limonene	45.0-80	Cyclic monoterpene
γ-Terpinene	2.9-15.6	Cyclic monoterpene
β-Pinene	2.2-15.0	Cyclic monoterpene
α-Pinene	0.4-5.3	Cyclic monoterpene
β-Myrcene	0.9-12.7	Linear monoterpene
E-Citral (Geranial)	0.6-2.3	Aldehyde
Z-Citral (Neral)	0.4-1.9	Aldehyde
Sabinene	0.5-1.7	Bicyclic monoterpene
Terpilonene	0.6-1.3	Cyclic monoterpene
Neryl acetate	0.1-0.9	Acetate ester
Geranyl acetate	0.1-1	Acetate ester
β-Caryophyllene	0.3-0.8	Bicyclic sesquiterpene
α-Terpinene	0.7	Cyclic monoterpene
<i>p</i>-Cymene	0.6-1.1	Cyclic monoterpene
α-Terpineol	0.2-0.5	Monoterpene alcohol
Linalool	0.08-0.2	Terpene alcohol

d-Limonene, is the main constituent of lemon oil making up 45-80% of it. This cyclic monoterpene is susceptible to degradation by acid-catalyzed hydration-dehydration and oxidation reactions. By-products of these reactions include carvone, carveol, 2,8-menthadiol and limonene oxide (Figure 3.1) ⁷¹. Likewise, citral, a monoterpene aldehyde and key contributor to citrus flavor, decomposes rapidly during storage at acidic pH by a series of cyclization and oxidation reactions (Figure 3.1). As a result of citral degradation, the level of fresh lemon-like aroma decreases and off-flavors are generated. To reduce the occurrence of these reactions and extend the self-life of lemon oil, a protection technique is needed.

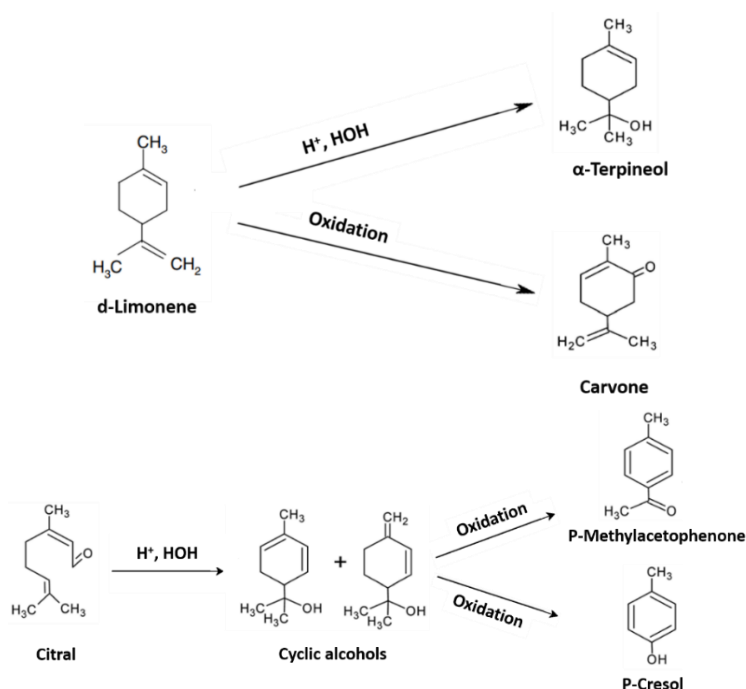


Figure 3.1. Degradation pathways of d-Limonene and citral^{71,108}

Lemon oil, and citrus oils in general, have been used for flavoring purposes of soft drinks, dairy products and confectionaries. Because citrus oils are not fully water-soluble, they are added to many food and beverages as oil-in-water (O/W) emulsions, which in turn become a way of protecting volatile and/or active ingredients. Many studies have examined some of the major factors influencing the production and stability of O/W emulsions encapsulating lemon oil, citral or limonene. Recently the impact of high- and low-energy emulsification technologies on the properties of lemon oil emulsions has been reported. However, little to no information is present on process productivity. While high-energy technologies, such as high-pressure homogenization or sonication, apply high shear forces and cavitation to obtain stable lemon oil emulsions with a droplet size that can be below 100 nm^{68,109}, low-energy emulsification technologies, particularly membrane emulsification, produce emulsions with a narrow droplet size distribution at low shear stress conditions.

Moreover, the role of interfacial properties of lemon oil emulsions on controlling their physical and chemical stability as well as the release of encapsulated aroma compounds has been widely investigated. Special attention has been paid to biopolymers because of their capacity to both form layers/coatings able to stabilize the oil-water interface and reduce the access of H^+ and prooxidant metals to the

interface and by that, the conditions promoting chemical degradation. Accordingly, whey proteins (WP) were found to decrease oxidative reactions in citral emulsions at pH 3 and that was linked to their ability to form a cationic emulsion interface able to repel prooxidative metals and/or the presence of amino acids in whey proteins capable to scavenge free radical and chelate prooxidative metals ⁷⁹.

More recently, engineered interfaces with proteins combined to polysaccharides have been explored to control chemical degradation in citral, limonene and lemon oil emulsions. Maillard conjugates of sodium caseinate and lactose ⁷¹ partially inhibited off-flavors formation from lemon oil emulsions compared to those stabilized with the single protein, while soy protein-polysaccharides Maillard conjugates improved the physical stability of citral emulsions during prolonged storage ¹¹⁰. Furthermore, interfacial stabilization using the layer-by-layer technique, in which oppositely charged polymers, such as proteins and polysaccharides are adsorbed onto the droplet surface to create a bi-layered interfacial membrane, has produced stable emulsions with a better control of lemon oil degradation. In particular, dairy proteins, e.g. lactoferrin, α -lactalbumin, β -lactoglobulin or sodium caseinate, were used to adsorb at the droplet surface while anionic polysaccharides like pectin or gum Arabic, were added to the system to electrostatically interact with the already positively charged interface ¹¹¹⁻¹¹³. Likewise, lecithin, which works as an anionic emulsifier because of the functional head groups of various phospholipids, has been used to create negatively charged droplets subsequently coated by positively charged polysaccharides such as chitosan ¹¹⁰. Although the electrical surface charge of the oil droplets has been suggested as an efficient strategy to reduce the access of prooxidant cations to the interface ⁷³, it may not be the only factor to consider seeing as both negatively and positively charged interfacial bi-layers have been found to reduce the chemical degradation of citral and limonene emulsions. Apparently the thicker interfacial bi-layer formed by proteins and polysaccharides, as well as the enhanced viscosity of the continuous phase in these emulsions contribute to prevent the access to prooxidant cations to the interface.

An alternative approach to stabilize lemon emulsions with thick interfacial layers made of protein and polysaccharides is through using electrostatic complexes as emulsifiers. Soluble protein-polysaccharide complexes, resulting from electrostatic interactions between oppositely charged macromolecules at certain conditions of pH and ionic strength, have been successfully used to stabilize oil-in-water interfaces in single O/W ^{86,114} and multiple W/O/W emulsions ^{115,116}. Berendsen *et al.* (2014)⁸⁷ reported that sunflower O/W emulsions stabilized with a whey-protein – carboxymethyl cellulose (WP-CMC) electrostatic complex maintained a more stable droplet size distribution than O/W emulsions stabilized with a monolayer of WP or those stabilized by a bi-layer made of positively charged WP coated by

negatively charged CMC. Nevertheless, sunflower oil oxidized much faster in emulsions stabilized with WP-CMC electrostatic complex than in those with just WP, what was attributed to the negatively charged droplet surface obtained with the electrostatic complex.

The aim of this work was to determine how both the electric surface charge and the interfacial thickness impact the physical and chemical stability of lemon O/W emulsions when stabilized with a WP-CMC electrostatic complex and WP at neutral and acidic conditions. To do so, emulsions were obtained using premix Shiratsu porous glass (SPG) membrane emulsification and low-cost ceramic membranes. To assess to what extent each interfacial structure affected the physical and oxidative stability of O/W emulsions, droplet size distribution and the evolution of some key components of the lemon oil volatile profile at accelerated oxidative conditions were monitored over two weeks.

3.2. Materials and methods

3.2.1. Materials

For the production of the simple O/W emulsions, distilled water was used and the lemon oil was purchased from Dallant, Spain. The emulsifiers used were Tween20 (Sigma Aldrich, CAS: 9005-64-5), whey protein (Davisco Foods International, USA) and a protein-polysaccharide electrostatic complex: whey protein-carboxymethyl cellulose. CMC (Sigma-Aldrich, San Luis, Misuri, CAS: 900-32-4) was purchased from Sigma-Aldrich Quimica SL, Spain. For emulsification, a High-speed mini kit, a 1 μm hydrophilic SPG membrane (tubular membrane of 125 mm length \times 10 mm external diameter \times 0.8 mm wall thickness, SPG Technology Co., Japan) and a low-cost ceramic membrane (Instituto de Tecnología Cerámica, Universidad Jaume I, Castellón) were utilized. Hydrochloric acid (HCl) was purchased from Fisher Scientific (UK).

3.2.2. Whey protein and electrostatic complex preparation

The continuous phase containing whey protein was prepared one day before using it for emulsification and stored in the refrigerator (4 °C) overnight. The three emulsifiers used in this study were 1%wt WP (pH: 6.8), 1%wt WP (pH: 3.8) and 0.5%wt WP - 0.25%wt CMC electrostatic complex (pH: 3.8). 200 ml of 2%wt WP solution was prepared and diluted on the day of the experiment to 1%wt. Also, on the emulsification day, the pH of the WP with the neutral pH (pH: 6.8) was only measured while the WP that needed pH modification to 3.8, that was done using 1M HCl. As for the WP-CMC complex, 2%wt WP and CMC solutions were prepared the day before, and the day of the experiment 200 ml of the complex were

prepared by mixing the following: 22.5g of 2%wt CMC, 22.5g of distilled water, 90g of 20mM acetic acid buffer and finally 45g of 2%wt WP. At this point the pH of the complex was adjusted to 3.8 with 1M HCl. Berendsen, *et al.* (2014)⁸⁷ have shown that this protein-polysaccharide 2:1 proportion is soluble at pH 3.8 and that the complex is negatively charged.

3.2.3. Premix membrane emulsification

Lemon oil coarse emulsions to be refined with SPG membranes had 20% oil fractions while those meant for low-cost ceramic membranes had 5% oil fraction. Table 3.2 details the experimental conditions and combinations tested in this chapter. All coarse emulsions (a.k.a premix) were first homogenized with a high shear mixer (IKA® T-18 basic Ultra-turrax) at 15,500 r.p.m with a 30 seconds break after each minute to avoid overheating. A 1ml sample of the coarse emulsions was then taken for droplet size distribution analysis as described in section 3.2.5.

Table 3.2. Membranes' properties and coarse emulsions characterization

Membrane	Membrane pore size (μm)	Emulsifier	Pressure (kPa)	Oil fraction (%)	Coarse emulsion	
					$d_{3,2}$ (μm)	Span (-)
Low-cost Ceramic	3.84	2% Tween20	150	5	5.28 ± 0.08	1.10 ± 0.02
SPG	1	1% WP (pH: 6.8)	850	20	13.87 ± 0.55	0.99 ± 0.02
		1% WP (pH: 3.8)	850	20	13.76 ± 0.15	0.99 ± 0.02
		0.5% WP – 0.25% CMC (pH: 3.8)	850	20	19.38 ± 0.49	0.98 ± 0.04

To refine the coarse emulsion, it was placed in the pressure tank (Figure 3.2) and pushed with nitrogen gas through the membrane. The membrane module shown in Figure 3.2 is that of an SPG membrane. For low-cost ceramic membranes, the whole setup was the same except that the membrane module was circular. Emulsions were passed through the membrane three consecutive times (three cycles) to further refine the emulsions. After each cycle a sample was taken for droplet size distribution analysis.

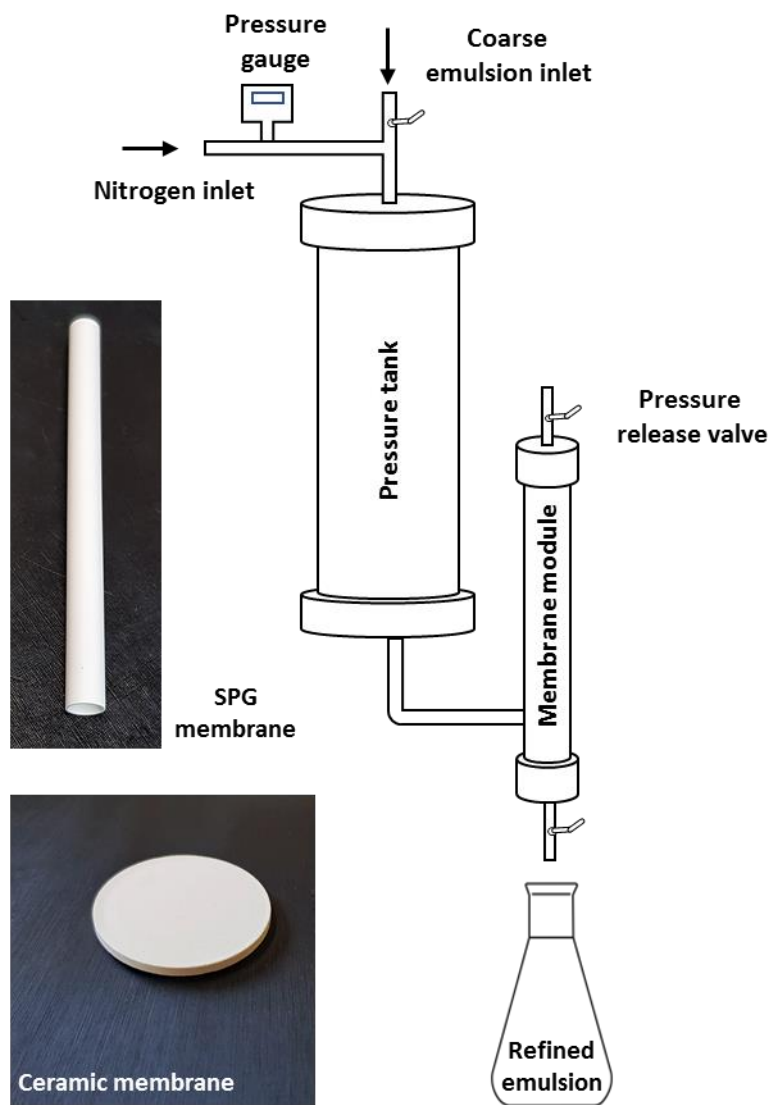


Figure 3.2. Emulsification setup for conventional premix membrane emulsification

3.2.4. Membrane cleaning

The low-cost ceramic membrane was cleaned by soaking in ethanol and sonicating for 15 minutes. After that the membrane was sonicated in distilled water for another 15 minutes. As for the SPG membrane, and after using it for emulsification, it was soaked and sonicated in acetone for 15 minutes then baked in a furnace at 500 °C for 8 hours. To restore the hydrophilicity of the membrane, it was soaked

and sonicated in 2N HCl for 1 hour. Then, the membrane was sonicated in distilled water, three times, for 30 minutes, changing the water every time.

3.2.5. Droplet size distribution measurement

Emulsion characterization consisted of droplet size and droplet size distribution analysis using a laser diffraction equipment (Malvern Mastersizer 2000). The emulsion sample was diluted to 1:10 ratio and three measurements were performed in the Mastersizer. For each sample introduced (measurement), the Mastersizer performs three readings. This resulted in nine total readings for each sample. An average of all readings was calculated, and the area-volume mean diameter or Sauter mean diameter ($d_{3,2}$) was calculated using Equation (3.1)

$$d_{3,2} = \frac{\sum_{i=1}^N z_i D_i^3}{\sum_{i=1}^N z_i D_i^2} \quad (3.1)$$

where, z_i is the number of droplets with diameter D_i . Also, to know the width of the size distribution, the droplet span was calculated using Equation (3.2).

$$Span = (D_{90} - D_{10}) / D_{50} \quad (3.2)$$

D_{10} and D_{90} are the 10th and 90th percentiles in the size distribution curve and D_{50} is the median.

3.2.6. Zeta-potential measurement

Laser Doppler micro-electrophoresis (Zetasizer Nano ZS , Malvern Instruments, Ltd., Worcestershire, UK) was used to measure ζ -potential of the lemon oil droplets in emulsions stabilized with 1%wt WP (pH: 6.8), 1%wt WP (pH: 3.8) and 0.5%wt WP - 0.25%wt CMC electrostatic complex (pH: 3.8). Measurements were done by diluting a 0.5mL emulsions sample with 20mL of water. All measurements, of fresh emulsions and for the stability study, are an average of nine measurements and calculated by the Smoluchowski equation. All measured ζ -potential distributions gave a monomodal distribution.

3.2.7. Emulsion stability

Every emulsion prepared was divided onto ten glass tubes of 12ml. Five of these tubes were used for the physical stability measurements and the other five for the chemical stability measurements. For an accelerated stability test, all ten of the tubes were placed in closed wooden box that contains a UV light (Philips TL 8W/108 ultraviolet) source on the inside. The box also had a thermometer inside to monitor the temperature and the temperature was on average $25 \pm 2^\circ\text{C}$.

On a sampling day, two tubes were removed from the box (one for physical and the other for chemical stability measurements). Sampling was done after 2, 3, 7, 10 and 14 days.

3.2.7.1. *Physical stability*

The physical stability of the emulsions was followed by taking pictures of the emulsions over time noting any changes in color or form. Also, the droplet size distribution was measured as described in section (3.2.5) and the Z-potential was measured as described in section (3.2.6).

3.2.7.2. *Chemical stability*

The emulsions' chemical stability was measured by evaluating the volatile profile evolution. The analytical technique used was the gas chromatography (GC) so a pretreatment of the emulsion was necessary to separate the volatile fraction. Among the different sample preparation techniques, the most appropriate to the present study was the solid-phase microextraction applied to the headspace of the sample (HS-SPME). This is a solvent-free technique that allows the extraction and concentration of the volatile compounds from a complex mixture with minimal manipulation of the sample and avoiding the interferences that may cause nonvolatile compounds. This is possible because SPME only uses a fiber coated with a sorbent where volatile compounds are retained when this device is exposed to the headspace generated by a sample.

Prior to the analysis of the samples and to obtain and ensure reproducible results, the different parameters that affect the microextraction process were optimized: temperature and time of extraction, sample volume and fiber coating. The best results were obtained when the analyses were performed as follows:

- 1) 0.380 ± 0.005 g of homogenous emulsion were diluted in a 100mL volumetric flask and homogenized using a vortex.
- 2) 0.250 mL of this diluted sample were placed in a 20ml glass vial with a magnet bar inside.
- 3) 10mL of an 8% sucrose solution was added to the vial, it was then sealed hermitically with a PTFE/silicone septum and finally shaken manually to homogenize the mixture.
- 4) the vial was thermostatted at 40 °C under constant medium stirring for 15 minutes to promote the volatile compounds to move to the headspace.
- 5) a 50/30 μm divinylbenzene/Carboxen/polydimethylsiloxane on a 2 cm StableFlex fiber was then inserted into the headspace of the vial by using a special syringe device. The fiber is kept into the headspace for another 15 minutes to extract the volatile compounds.

6) The syringe needle that houses the fiber was inserted into the gas chromatograph injection port and, once there, the fiber was exposed at 270°C during 3 minutes to guarantee the release of all the volatile compounds into the GC.

Regarding the GC separation, it was performed using a gas chromatograph (Hewlett-Packard 5890) equipped with a flame ionization detector (FID). The sample injection was carried out in splitless mode for 1 min and using an inlet of 0.75 μm I.D. to minimize peak broadening. Chromatographic separation was made using an HP-5 M.S. (Crosslinked 5% Ph Me Silicone) (30 m x 0.25 mm I.D., 0.25 μm film thickness) fused silica capillary column. The carrier gas was helium (1.5 mL/min) and the FID detector was supplied with air (447 mL/min), hydrogen (40 mL/min) and helium (22 mL/min). The oven temperature was set at 40 °C for 2 minutes, then increased to 200 °C at 20 °C /min and finally at 50°C/min to 275 °C (50 °C /min) temperature that was held for 7 min. The temperature of the detector was maintained at 200 °C.

The supplier of lemon oil provided a chromatographic profile obtained when analyzing it by GC-FID together with the peaks identification. Once the lemon oil arrived to our lab, these identities were verified by using a gas chromatograph (Hewlett-Packard 6890) coupled to a mass selective detector Hewlett-Packard HP-5973. Separation was achieved under the same conditions above-described and using the same column used in the GC-FID analysis in order to identify the odorant compounds using the retention time parameter. The mass spectrometer operated in the electron impact ionization mode (70 eV). Interface, source and quadrupole temperatures were 250°C, 230° C and 150°C, respectively. Mass range was from 35 to 300 amu and the mass spectra library used was NIST14.L .

To monitor the evolution of the different lemon oil emulsions, the chromatographic response of each peak corresponding to the different volatile compounds was considered. Specifically, the change (either an increase or a decrease) of each peak (in percentage) was evaluated by comparing the peak area on the sampling day (A_t) versus that obtained on the day of the emulsification (A_0) according to Equation (3.3).

$$\text{Variation (\%)} = \frac{A_t}{A_0} \times 100 \quad (3.3)$$

3.3. Results and discussion

3.3.1. SPG membrane

3.3.1.1. Properties of lemon O/W emulsions produced with SPG membranes

Coarse emulsions containing 20%wt. lemon oil and stabilized with 1%wt WP (pH: 6.8), 1%wt WP (pH: 3.8) and 0.5%wt WP - 0.25%wt CMC electrostatic complex (pH: 3.8) were refined by premix ME with SPG membranes. The droplet reduction pattern was similar for all of them: the highest droplet break-up occurred in the first emulsification cycle with little to no change in the consecutive cycles (Figure 3.3). As for the span, it has improved with the cycles for emulsions produced with only WP reaching a span less than 0.8. The span of the refined emulsions produced with the WP-CMC complex, however, was higher (≈ 1.37) than that of the coarse emulsion (≈ 0.98) indicating a less efficient capacity of the WP-CMC complex either to reduce interfacial tension or to reach the oil-in-water interface during the emulsification process.

Berendsen *et al.* (2014)⁸⁷ have produced 20%wt. sunflower oil-in-water emulsions with 10 μm SPG membrane and stabilized with 1%wt WP-pH: 3.8 and 0.5%wt WP-0.25%WP-CMC-pH: 3.8. These authors report a similar trend in droplet break-up to the one obtained in this study; however, the span values they report were much higher (1.7 for WP and 3.6 for WP-CMC). This might be due to the higher viscosity of sunflower oil or also that their SPG membrane had larger pore sizes. Bigger sizes of the membrane pores may lead to different mechanisms of droplet break-up and further recoalescence, thus leading to less monodisperse emulsions.

Regarding zeta potential, it clearly depended on the interfacial composition (Figure 3.4c). Lemon emulsions stabilized with 1%wt. WP at pH 6.8 exhibited a negative charged surface of -48 mV, while at pH 3.8 were positively charged with a z-potential of $+24$ mV.

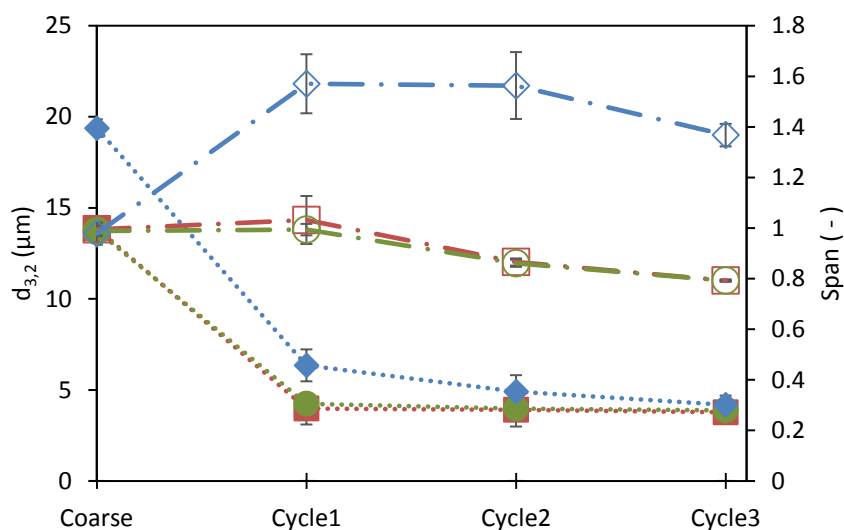


Figure 3.3. Effects of emulsification cycles and emulsifier type on oil droplet size ($d_{3,2}$) and span. (■, □) WP-pH: 6.8, (●, ○) WP-pH: 3.8, (◆, ◇) WP-CMC-pH: 3.8. Filled markers refer to droplet size and empty markers refer to droplets span

In contrast, lemon oil droplets in emulsions stabilized with 0.5%wt WP - 0.25%wt CMC electrostatic complex at pH 3.8 showed a negative droplet surface charge of -41 mV. In a previous work, Berendsen *et al.* (2015)¹¹⁵ found that water-in-oil-in-water (W/O/W) emulsions formulated with sunflower oil and 0.5%wt WP - 0.25%wt CMC electrostatic complex at pH 3.8 as hydrophilic emulsifier, had a zeta-potential of the oil droplets of -24 mV. Also, measuring the z-potential of the WP-CMC complex in aqueous solution (before using it for emulsification) gave a value of -28 mV, which is quite close to that of the W/O/W emulsion⁸⁷. This difference between the z-potential of lemon and sunflower oil droplets stabilized by the same WP-CMC complex at pH 3.8 may be attributed to the variations in the composition and polarity of the oil phases, that can modify the distribution of the positively/negatively charged patches of the hydrocolloids when adsorbed to the oil-in-water interface, and, in turn, their electrical surface charge.

In the case of lemon oil emulsions stabilized by the layer-by-layer technique, z-potential ranged between -15 mV and -25 mV for oil droplets coated by a primary layer of positively charged protein, like whey proteins and sodium caseinate, followed by a secondary external layer of a negatively charged polysaccharide, such as pectin or gum Arabic, at a pH between 3 and 4¹¹¹⁻¹¹³. Accordingly, using a WP-CMC electrostatic complex enabled to significantly reduced the interfacial zeta-potential compared to that obtained by the reported layer-by-layer technique.

3.3.1.2. Physical stability of lemon O/W emulsions produced with SPG membranes

The stability of lemon emulsions was examined for 14 days of storage at accelerated oxidation conditions induced by UV light. For what regards physical stability, droplet size distribution, zeta-potential and change in color were monitored. The emulsions stabilized with WP-pH: 3.8 seem to maintain the same droplet size over the whole stability period but the size dispersion started increasing linearly after three days (Figure 3.4a). However, emulsions stabilized with WP in acidic conditions shows higher stability when compared to those stabilized with WP at pH: 6.8. These latter reached span value after 14 days that is five times the original value. This observation goes in the same direction as that of Djordjevic *et al.* (2008) when comparing the effect of emulsifier pH⁷⁹. These authors found that during homogenization, emulsions stabilized by WP at pH: 7 showed a smaller droplet size distribution than those at pH: 3. However, at pH: 7 the mean particle diameter increased considerably after 1 day of storage, what was attributed to droplet flocculation caused by an increase in the surface hydrophobicity of the lipid droplets when the adsorbed proteins underwent surface denaturation. Another reasoning could be the formation of disulfide bonds between adsorbed proteins on different oil droplets¹¹⁷. McClements *et al.* (1993)¹¹⁸ reports that WP stabilizing O/W droplets may interact with WP molecules on neighboring droplets or even a single WP molecule adsorbing to two oil droplets. This interaction leads to the formation of disulfide bonds.

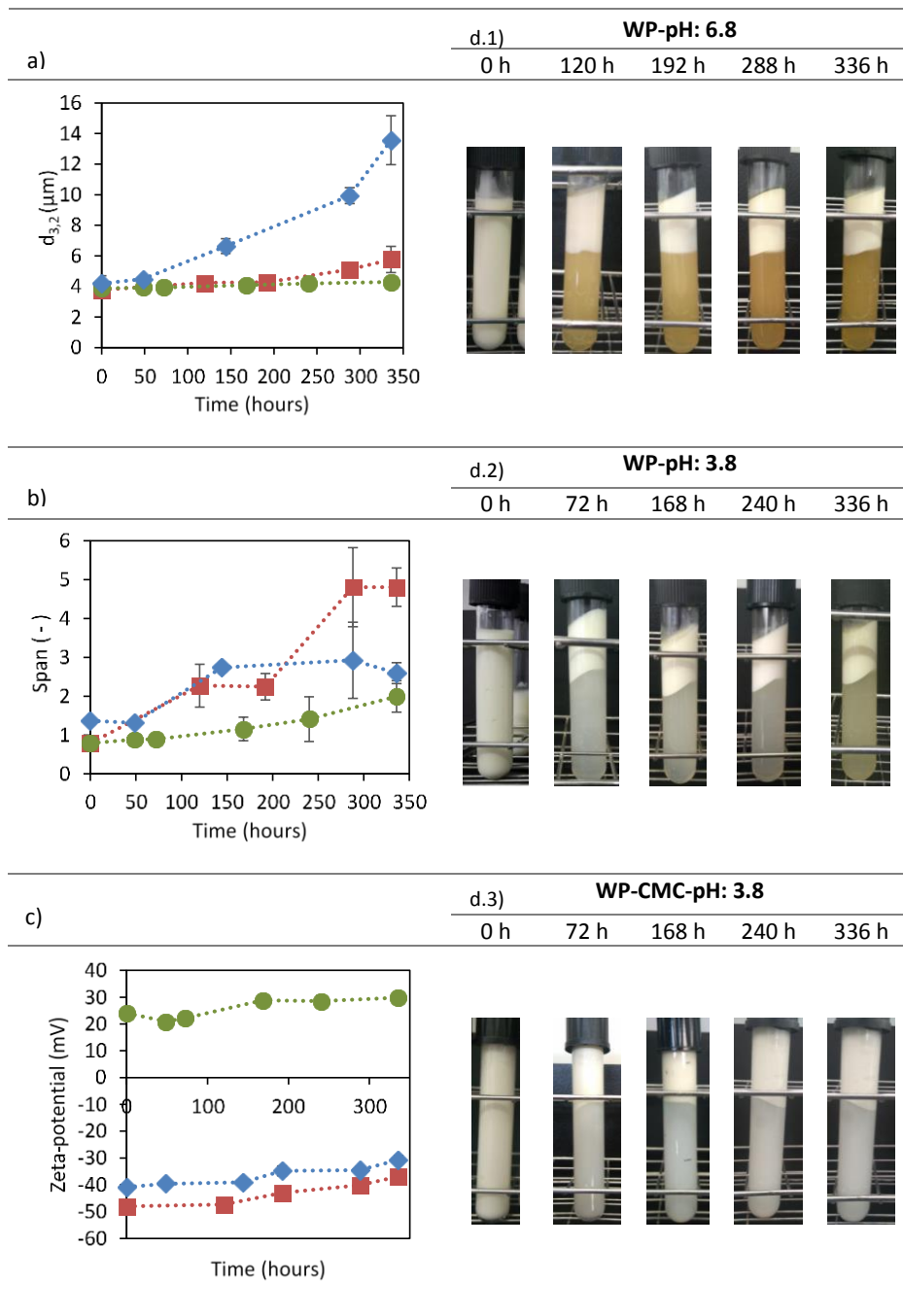


Figure 3.4. Physical stability of emulsions with (■) WP-pH: 6.8, (●) WP-pH: 3.8 and (◆) WP-CMC-pH: 3.8 interfaces in terms of (a) droplet size, (b) span, (c) z-potential and (d) color evolution during storage

As for emulsions stabilized with the electrostatic complex, Figures 3.4a and 3.4b show that droplet size distribution and span started increasing after 48 hours. With a span value ≈ 1.4 , the emulsion already had a somewhat polydisperse droplet size distribution from the first day. This is certainly a factor in increasing the potential of coalescence. After 14 days the span of the emulsion was ≈ 2.6 which is in line with the value (≈ 2.5) reported by Berendsen *et al.* (2014)⁸⁷ for sunflower oil emulsions after 14 days under UV light. These results are in the range of those shown by Su *et al.* (2018)¹¹² for O/W emulsions containing d-limonene and stabilized with a bilayer made of β -lactoglobulin and gum Arabic, in which after two weeks of storage at 25°C the droplet size increased almost two times with respect to the initial value. Similarly, Xiang *et al.* (2015)¹¹¹ reported that the physical stability of citral emulsions coated by an interfacial bilayer formed by whey proteins and pectin was lower than that found in single-layered emulsions.

Regarding a visual assessment of stability, all the emulsions underwent the formation of a top thick layer, a process otherwise known as creaming. This meant that once a sample was collected for physical or chemical stability measurements, the emulsions were manually and gently homogenized by repetitively rotating the tubes. Another interesting factor to be noted is the yellow color evolution in the emulsions. The emulsion with the most popping color change is the one stabilized with WP-pH: 6.8 (Figure 3.4d.1). The emulsion stabilized with WP at acidic medium didn't show a change until after 14 days of storage (Figure 3.4d.2) and no change in color was noted in the emulsion stabilized with WP-CMC (Figure 3.4d.3). A change in color is often linked to oxidation of polyphenolic compounds, after all citrus fruits are rich in phenolics like the compound eriocitrin^{119,120} which is responsible for pigmentation in lemons. It is obvious that the low acidic pH, delays these oxidations to happen.

As for the surface charge of the droplets, Figure 3.4c shows very little change in the zeta-potential. The charge of the droplet stabilized with WP-pH: 6.8 and WP-CMC have increased slightly over the two weeks period but still remain under -30 mV, a value at which enough electrostatic repulsion should ensure physical stability. In that sense, other mechanisms than electrostatic stabilization seem to control the droplet size distribution of lemon oil emulsions stabilized with either protein-polysaccharides electrostatic complexes or multilayered hydrocolloids.

3.3.1.3. Stability of volatile compounds in lemon O/W emulsions produced with SPG membranes

To determine the impact of the interfacial composition on the encapsulated aroma of lemon oil, the degradation of citral and d-limonene was followed. In particular, we monitored, neral and geranial, the isomers of citral, as well as α – terpineol and

carvone, off-flavors result of the d-limonene degradation. Due to its unsaturated character, d-limonene can yield by-products such as carvone, via radical formation by oxidative pathways. Besides, d-limonene is highly susceptible to acid-catalyzed reactions which give rise to compounds such as α -terpineol. The HS-SPME-GC method was applied to follow the compositional changes of lemon oil components in emulsions encapsulated with 1%wt WP, pH 3.8 and 6.8, and a 0.5%wt WP - 0.25%wt CMC, pH 3.8, electrostatic complex and stored under UV-light for 14 days.

An example of an obtained chromatogram from analyzing the emulsion stabilized with WP-pH: 6.8 is shown in Figure 3.5. It should also be noted that the degradation of volatile components in lemon oil quantified by HS-SPME-GC during storage should be attributed to the deterioration of the emulsion as a whole, independently from its origin (either from the oil or the water phase). As explained in section 3.2.7.2, the evolution of the volatile compound content was monitored from the ratio of the peak area of each compound during storage to the corresponding initial peak area (A_t/A_0).

The production/release rate of α -terpineol and carvone was dramatically affected by the interfacial composition (Figure 3.6). 1%wt WP-stabilized emulsions at pH 3.8 exhibited a very fast production of α -terpineol. The increase of α -terpineol was particularly abrupt as of 72 h of storage reaching an A_t/A_0 value of 300% and by the end of the storage period reaching a value of 780%. At the same acidic conditions, pH 3.8, emulsions with WPI-CMC electrostatic complex showed a much slighter increase of A_t/A_0 from 157% to 203% after 7 and 14 days of storage, respectively. So, the production/release rate at low pH of α -terpineol, recognized as a major unpleasant off-flavor in citrus juices and result of the acidic pathway of limonene degradation, was reduced when stabilizing the oil-water interface by a 0.5%wt. WP - 0.25%wt. CMC electrostatic complex. This occurred despite that the interfacial surface was negatively charged and the total WP content was reduced by a 50%. For carvone, a degradation product of terpenic compounds such as d-limonene under aerobic conditions, we also observed the fastest production rate in emulsions stabilized with WPI at pH 3.8 with a A_t/A_0 value of 300% over the whole storage period. Similarly to α -terpineol, the carvone produced/released was drastically reduced by using 0.5%wt WP - 0.25%wt CMC electrostatic complex at pH 3.8 or 1%wt. WP at pH 6.8 as emulsifiers. Similar trends were reported by Sabik *et al.* (2014)⁷¹ in lemon oil emulsions stabilized by Maillard conjugates of sodium caseinate and lactose.

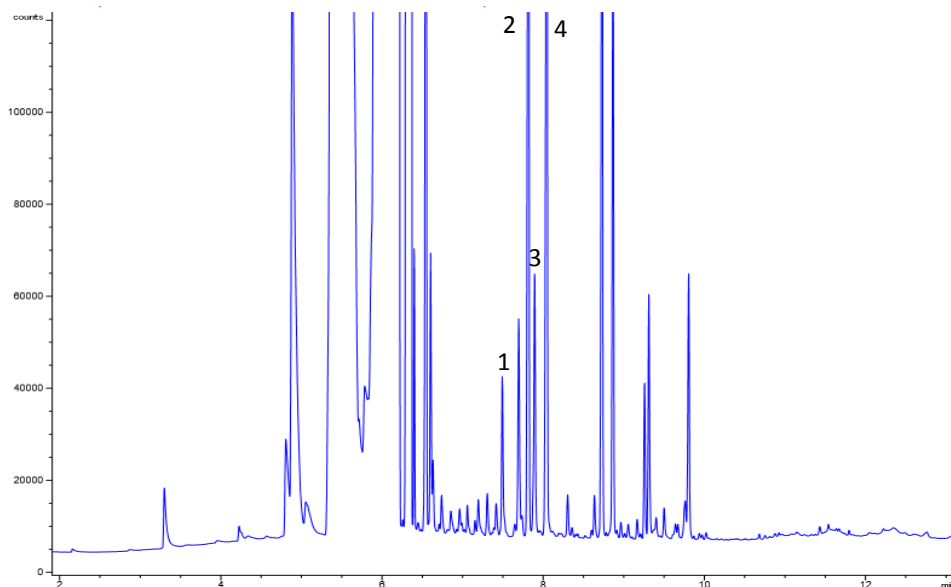


Figure 3.5. Chromatogram of an emulsion stabilized with WP-pH: 6.8. The numbered peaks refer to the compounds: 1) α – terpineol, 2) neral, 3) carvone, and 4) geranial

In the case of the citral isomers, we observed a faster degradation of neral in lemon emulsions at pH 3.8 than in those at pH 6.8 (Figure 3.6), although the final A_t/A_0 (after 14 days of storage) was about 33% regardless of the emulsion pH. Results for geranial showed a fast decrease rate for WPI-stabilized emulsions at pH 3.8, which showed a final A_t/A_0 value of 28%, significantly lower than the 49% and 43% showed by emulsions stabilized with WP at pH 6.8 and WP-CMC at pH 3.8, respectively. These results would confirm a major effect of acid-catalyzed cyclization on the deterioration of these two isomers, that, for geranial, it was partially inhibited by the WP-CMC complex at pH 3.8.

It is not clear why this is the case since, at this pH, WP is positively charged and can repel cationic catalysts. Djordjevic *et al.* (2008) made a similar observation where less oxidation levels of citral were reported with emulsions stabilized with WP-pH: 7 than with WP-pH: 3⁷⁹. The authors explain that this might be due to the antioxidant properties in some whey protein amino acids. Also, in emulsions stabilized with subsequent interfacial coatings of whey proteins and pectin¹¹¹, negatively charged interface and obtained by the layer-by-layer technique, a slight reduction in neral and geranial degradation was observed when compared to emulsions with a positively charged single interfacial layer of whey protein. In light of all that, it seems that the electrical charge of the interfacial surface is not the only parameter affecting the degradation rate of citral and d-limonene, the main compounds responsible for lemon aroma. An additional factor that may affect both the accessibility of the prooxidants to the interface but also how easily

the already formed products of degradation are released should be considered. Interfacial physical properties such as thickness and viscosity probably play a significant role. In a previous work by Berendsen *et al.* (2014)⁸⁷, it was found that the thickness of an interfacial layer made of WP was notably lower (0.6 nm) than that formed by the WPI-CMC complex (2.2 nm), both at pH 3.8. Additionally, the presence of CMC in the complex significantly increases the viscosity. Consequently, a negatively charged but thicker and more viscous interface of WPI-CMC complex would prevent the access of prooxidant cations, reducing the rate of acid-catalyzed hydration-dehydration reactions while hindering the release of the deterioration products.

3.3.2. Ceramic membrane

Since ceramic membranes are about 10 times cheaper than SPG membranes, it was an obvious choice to test them for emulsification. For that reason, a simple coarse emulsion of 5%wt. lemon oil and 2%wt. Tween20 was produced and refined by the ceramic membrane at 150kPa as described in section 3.2.3. These membranes are fragile with a thickness of a few millimeters making going to higher pressure impossible without breaking the membrane.

3.3.2.1. Droplet size distribution and flux

Results of the droplet size distribution are reported in Figure 3.7a. The largest droplet break-up of 36% happened in the first cycle with little change afterwards reaching a droplet break-up of 52% by the third cycle. Also, the final droplet size of the emulsion (3rd cycle) was 34% smaller than the average pore size of the membrane. As for the droplet size dispersity, it was possible to reduce the span of the coarse emulsions from 1.1 to 0.8 showing that ceramic membranes are very efficient at breaking the oil droplets.

Fluxes obtained with the ceramic membrane, as shown in Figure 3.7b, were around $2.5 \text{ m}^3 \cdot \text{m}^{-2} \cdot \text{h}^{-1}$. This value is in the same range as the flux values reported with stirred-cell emulsification model. This model has been used for both direct and premix membrane emulsification^{8,12,15,17} and the attained fluxes were in the range of $0.1 - 3.2 \text{ m}^3 \cdot \text{m}^{-2} \cdot \text{h}^{-1}$. These values are on low end of the fluxes reported for membrane emulsification.

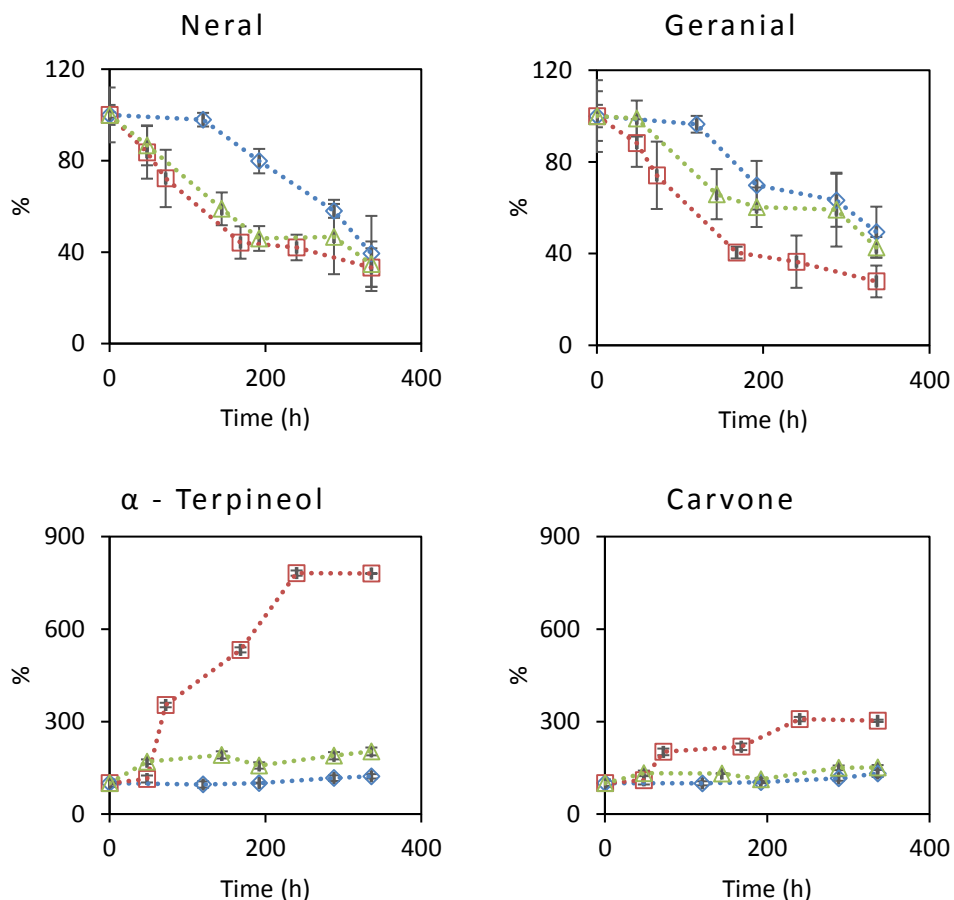


Figure 3.6 Progression of the percentages of compounds detected in lemon oil emulsions stabilized with (\diamond) WP-pH: 6.8, (\square) WP-pH: 3.8 and (\triangle) WP-CMC-pH: 3.8, over the period of two weeks under UV light.

Moreover, when looking at the refined emulsions, it was noted that the emulsions were too watery and the membranes had an oily look. For that reason, the stability study described in section 3.2.7 was not performed. Instead, the tubes with the emulsions were wrapped in aluminum foil, and stored in the lab at room temperature. Pictures were taken over the following 7 days. Figure 3.8 shows that slowly but surely, creaming was taking place but the cream layer is very small, even though the initial oil fraction was only 5%wt. This might indicate that the membrane has partially retained some oil. This not uncommon since the literature reports many studies where ceramic membranes are used for filtration and to break emulsions ¹²¹. With the low fluxes obtained and the oil retention, it was decided not to move to more complex emulsifiers.

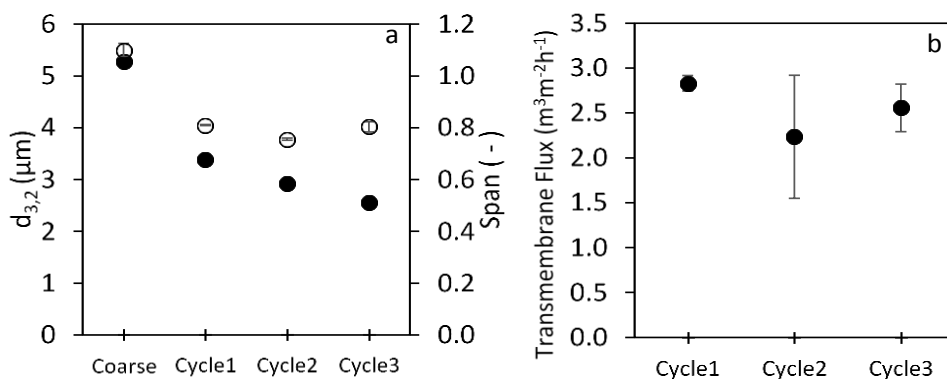


Figure 3.7. Progress of a) droplet size distribution and b) transmembrane flux during emulsification of Tween 20-stabilised O/W emulsions refined with low-cost ceramic membranes. Markers in figure a: empty: span; filled: $d_{3,2}$

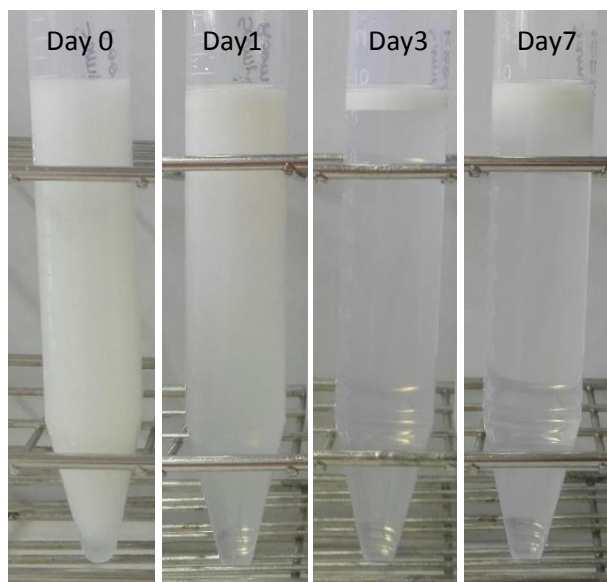


Figure 3.8. Evolution of a 5%wt lemon oil emulsion refined with a ceramic membrane

3.4. Conclusion

In lemon O/W emulsions, both the interfacial surface charge and the barrier properties of a single layer of whey protein can be tailored with a WP-polysaccharide electrostatic complex. With it, a thicker interfacial coating than that obtained with single WP along with a negatively charged interface at acidic conditions were formed to stabilize emulsions produced by premix membrane emulsification. Although the physical stability of these emulsions in terms of droplet size distribution was not improved using the tailor-made electrostatic WP-CMC complex, other physical characteristics like emulsion color were maintained. Regarding chemical stability, the electrostatic WP-CMC complex decreased the production/release of off-flavors resulting from the deterioration of d-limonene while hindering the reduction of citral isomers under acidic and accelerated oxidation conditions.

All in all, interfacial engineering with food biopolymers (i.e. proteins and polysaccharides) together with a low energy emulsification technique able to preserve the interfacial structure, like premix membrane emulsification, seems to be an effective strategy to control the complex chemical reactions underpinning the degradation of aroma compounds in lemon oil.

4. Low-energy high-throughput emulsification with nickel micro-sieves for essential oils encapsulation

This chapter has been published as:

W. Kaade, M. Ferrando, A. Khanmohammed, C. Torras, S. De Lamo-Castellví, and C. Güell, "Low-energy high-throughput emulsification with nickel micro-sieves for essential oils encapsulation," *J. Food Eng.*, vol. 263, pp. 326–336, Dec. 2019.

UNIVERSITAT ROVIRA I VIRGILI

LOW-ENERGY HIGH-THROUGHPUT MICROPOROUS EMULSIFICATION FOR LEMON OIL ENCAPSULATION

Wael Kaade

4.1. Introduction

Essential oils, such as lemon oil, are highly utilized in the food industry as flavorings. Manufacturing and storage processes, packaging materials and other ingredients in foods often cause modifications in the overall flavor by reducing aroma compound intensity or producing off-flavor components. To limit aroma degradation or loss during processing and storage, encapsulation of essential oils prior to incorporation in foods or beverages is a common practice. Lemon oil, widely used in the food industry to flavor many products, from baked goods and soft drinks to dairy and confectionery products, is easily degraded by oxidation, heat and/or light⁴⁸. For those reasons, lemon oil emulsions and capsules have been produced as means to protect and facilitate the handling of this volatile oil^{8,48-53}. Additionally, studies on lemon oil emulsification are becoming more relevant since, D-limonene, one of its major constituents, is an environmental friendly chemical that has been assessed in the production of green emulsions with applications in agrochemical products^{54,55}.

Emulsions can be produced by several methods such as rotor stator mixers, colloid mills, high-pressure homogenizers and ultrasonic homogenizers. These technologies can have some limitations to control the dispersion of the final droplet size of the emulsion and use much higher energy input than required for droplet break-up, thus submitting the product to high shear stress and overheating. Membrane emulsification (ME) is a dispersion technique that has gained advantage over traditional methods since it requires lower energy input¹; besides, membrane selection will allow controlling the final droplet size of the emulsion. These strong points are clearly advantageous for applications demanding stable emulsions with shear or heat sensitive compounds, such as food aromas.

Membrane emulsification is a low-energy technology that branches into two types: direct⁸⁻¹⁹ and premix^{4,8,20-26} ME. Direct ME is when a pure disperse phase is passed through a membrane into an agitated continuous phase. Control of droplet formation is achieved in direct ME by passing through the membrane a low amount of disperse phase, resulting in low productivity and limiting scale-up of the process. Premix ME, on the other hand, is the passage of a premix or a coarse emulsion through a membrane to refine it resulting into a stable monodispersed emulsion. The advantages of premix ME over direct ME are in small droplet sizes and higher throughput for a given pore size²⁷, even though this might be related with a lower degree of monodispersity in the final product.

Premix ME is a well-established emulsification technique where many types of microstructured systems have been utilized. Corn²⁸ and sunflower oil^{4,25} emulsions have been produced by Shirasu porous glass (SPG) membranes. Trentin *et al.* (2009)²⁴ also have produced sunflower oil emulsions but using commercial

polymeric microfiltration membranes (polycarbonate, nylon, polyethersulfone and nitrocellulose). n-Hexadecane was emulsified by the previously mentioned polycarbonate membrane²³ and also with metal nickel membranes^{20,21}. Further information on how emulsion properties, operating conditions and characteristics of the microporous system impact the emulsification performance can be found in several reviews^{122,123}.

Nickel micro-engineered membranes, a.k.a. nickel sieves, are produced by the galvanic deposition of nickel onto a substrate that is fabricated by photolithography and etching. This technique is highly cost effective and accurate, producing highly porous nickel sieves with homogenous pore size distribution^{8,15}. Nickel sieves have straight-through pores that can be easily cleaned when fouled. Moreover, their metal properties allow them to be used under pressures to 500 kPa²¹, which would otherwise break more vulnerable membranes (e.g. flat ceramic membranes) having the same shape and dimensions. Thus, microstructured nickel sieves combine mechanical resistance and pores in the microns range that make them suitable for emulsification.

Microstructured nickel sieves have been employed in both direct and premix ME. In direct emulsification, a Micropore Dispersion Cell is reported to be used where the to-be-dispersed phase is pumped up through the micro-sieve into a tank containing the aqueous phase. This tank contains a rotating paddle, right above the nickel micro-sieve, which agitates the continuous phase thus helping in the break-up of the oil droplets. Dragosavac *et al.* (2012)¹² have prepared pumpkin oil double emulsions using this technique attaining fluxes up to $3.2 \text{ m}^3\text{m}^{-2}\text{h}^{-1}$. Kosvintsev *et al.* (2005)¹⁵ and Egidi *et al.* (2008)¹⁷ reported the possibility of producing sunflower oil emulsions with fluxes of 0.9 and $2.64 \text{ m}^3\text{m}^{-2}\text{h}^{-1}$. All these studies also mention that the produced emulsions have monosized droplets. Santos *et al.* (2015)⁸ produced lemon oil emulsions with fluxes between 0.1 and $1 \text{ m}^3\text{m}^{-2}\text{h}^{-1}$, while the emulsions obtained were polydisperse. In all cases the authors agree that nickel micro-sieves require surface modification to change them from hydrophobic to hydrophilic to be used in the production of O/W emulsions.

The stirred cell has also been used in a premix ME setup to refine a coarse emulsion. Santos *et al.* (2015)⁸ produced lemon oil in water emulsions using a stirred cell with a hydrophilic nickel micro-sieve. The stirred cell module has low fluxes and the authors reported that emulsification and droplet break-up was possible only when nickel micro-sieves' surface properties were previously modified, resulting in polydisperse emulsions. Moreover, nickel micro-sieves have also been used in premix ME with high-throughput system. In this system, the coarse emulsion is pressed through the micro-sieve at higher pressures than in the stirred cell, and droplet break-up mainly occurs in the membrane channels. This

system has been used without any surface modification of the nickel micro-sieve to produce n-hexadecane/water emulsions emulsions^{20,21,26} and sunflower oil/water emulsions⁴². For n-hexadecane/water emulsions, Nazir et al., (2011)²⁰ reported fluxes up to $1500 \text{ m}^3\text{m}^{-2}\text{h}^{-1}$ at 200 kPa. As far as the authors know there are no other previous applications for the production of food grade O/W emulsions with nickel micro-sieves using a high-throughput premix ME system.

This chapter will assess the use of a high-throughput low-energy emulsification system based on microstructured nickel sieves to produce food-grade lemon oil in water emulsions to gain knowledge for process scale-up. The novelty of this study is the use of premix ME with nickel sieves of two different pore geometries and no surface treatment to produce food-grade lemon oil in water emulsions. Moreover, we assessed how the potential changes in membrane integrity and wettability affected productivity and emulsion properties, such as droplet size distribution. Special attention was paid to mechanisms of droplet break-up during premix emulsification with the nickel micro-sieves to facilitate scale-up of the process.

4.2. Material and methods

4.2.1. Microstructured nickel sieves

The nickel micro-sieves, from now on micro-sieves, (Stork Veco, Eerbeek, The Netherlands) used in this study have straight through pores. One set of sieves has rectangular pores ($\approx 4.5 \mu\text{m} \times 291.2 \mu\text{m}$) while the other has more square-like ($\approx 17.7 \mu\text{m} \times 20.6 \mu\text{m}$) pores. For convenience the micro-sieves will subsequently be referred to as rectangular and square pore sieves. Both set of micro-sieves have a thickness of $90 \mu\text{m}$. Figure 4.1 shows images, taken by an environmental scanning electron microscope (FEI ESEM Quanta 600, USA), of the morphology of the different pore sizes.

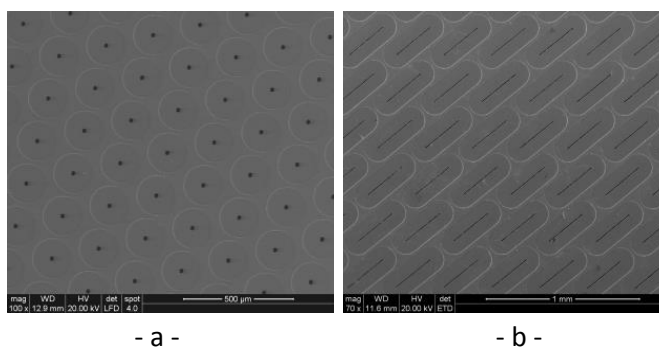


Figure 4.1. ESEM images of brand new a) square and b) rectangular pore sieves

Using the ESEM, three pores were chosen randomly from three random and different regions of a micro-sieve and an image of each pore was taken. These images were analyzed with the software ImageJ to collect the pore's length (l_p) and width (w_p). Also, from the three images an average pore area was obtained which, with the total number of pores, allowed the calculation of the micro-sieve porosity.

For each pore geometry, the hydraulic diameter (d_h) was calculated according to Equation (4.1).

$$d_h = (2 \cdot l_p \cdot w_p) / (l_p + w_p) \quad (4.1)$$

4.2.2. Contact angle test

Contact angle measurements for all the micro-sieves were performed by sessile drop technique using the automatic video-based analysis system OCA 35 (Dataphysics). Measurements were carried-out dispensing 10 μ L distilled water drops on the surface of the micro-sieves. After absorption was recorded, measurement was taken at 3-6 seconds after the drop contacted the surface, since this is the time at which the steady state angles were typically reached. Three measurements were performed for each sieve. Contact angle was measured for the brand new micro-sieves and also after these sieves had gone through emulsification and cleaning. It should be noted that the angles reported are the result of not only the interaction of water with the surface but possibly also liquid moving through the pores.

4.2.3. Premix membrane emulsification

All the emulsions produced were O/W emulsions. Lemon oil (Dallant, Spain) was the oil phase and Tween20 (polyoxyethylene sorbitan monolaurate, Sigma Aldrich, CAS: 9005-64-5) was the emulsifier used. This latter formed 2%wt of the total emulsion weight, while the oil phase formed 5%. Some initial trials used a lemon oil fraction of 20%wt.

The lemon oil coarse emulsion (200-350 g) was produced using an Ultra-turrax homogenizer (IKA® T-18 basic) at 15500 rpm for 3 minutes. Another coarse emulsion was prepared for preliminary testing with the Ultra-turrax homogenizer at 7000 rpm for 3 minutes. The droplet size of these premix emulsions was measured using a light scattering equipment as it was explained in section 3.2.5. The first and second mechanical emulsifications conditions rendered a droplet size of about 5 μ m and 20 μ m, respectively.

Once the coarse emulsion was ready it was placed in the pressure tank (3 in Figure 4.2) where, using nitrogen gas, it was then pushed under pressure through the membrane (premix) module (4 in Figure 4.2). The micro-sieve was placed at the bottom of the module. The emulsion was collected in an Erlenmeyer flask placed on a digital balance (6 in Figure 4.2) that was connected to a computer (7 in Figure 4.2). A computer software collected mass versus time data each second while the emulsion was flowing. This allowed the calculation of the mass flow rate, φ , and the transmembrane flux (J) using Equation (4.2),

$$J = \varphi / (\rho_e \cdot A) \quad (4.2)$$

where ρ_e is the emulsion density (can be taken to be equal to that of the continuous phase, 1000 kg/m^3 , since the oil fraction is low) and A is the sieve effective area (2.2 cm^2). Then, a sample of the emulsion was collected to measure the droplet size distribution (DSD). This process was repeated 5 times (cycles) maintaining the sieve in the holder. The pressures used in the experiments were 150, 300 and 450 kPa.

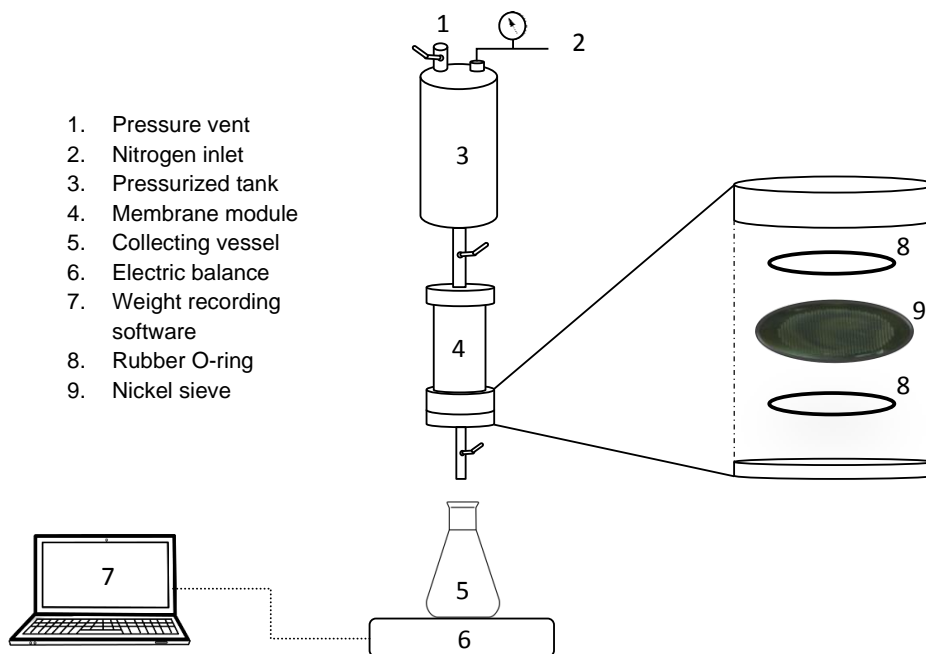


Figure 4.2. Membrane emulsification setup

Emulsion characterization was carried in the exact way described in chapter 3.2.5. A dimensionless ratio between the $d_{3,2}$ and the hydraulic diameter of the micro-sieve has been defined as d_{ratio} in Equation (4.3).

$$d_{ratio} = d_{3,2} / d_h \quad (4.3)$$

4.2.4. Micro-sieve cleaning procedure and water flux recovery

After emulsification each micro-sieve was cleaned. The cleaning protocol was based on that used by Santos *et al.*, (2015)⁸. The micro-sieves were cleaned in an ultrasonic bath with (1) 4M NaOH (Fisher Scientific) for 5 minutes; (2) 2%wt citric acid (Fisher Scientific) for 5 minutes and (3) distilled water for 5 minutes. After the micro-sieve integrity tests (section 4.3.2), the final cleaning protocol excluded the citric acid step.

It should be noted that before using a nickel sieve for emulsification, the initial water flux was calculated by passing 2000 g of distilled water through the new sieve 5 times at 50 kPa. After emulsification and cleaning, the same procedure was repeated, and the final water flux was compared to the initial one and the water flux recovery (*WFR*) was calculated (Equation 4.4). *WFR* was taken as an indicator of the effectiveness of the cleaning method.

$$WFR = \frac{\text{final water flux}}{\text{initial water flux}} \times 100 \quad (4.4)$$

4.3. Results and discussion

4.3.1. Lemon oil emulsification using high-throughput premix ME with nickel micro-sieves

Since this is the first time that micro-sieves, without wettability modification, were used in a high-throughput premix emulsification to produce lemon oil/water emulsions, preliminary tests were required to assess their feasibility and select the operating conditions. In the following sub-sections, the impact of nickel micro-sieve properties (pore size and geometry, wettability), process conditions (transmembrane pressure, number of emulsification cycles) and emulsion formulation (oil fraction) on productivity and emulsion stability are presented.

Since the only reported literature on the use of micro-sieves in high-throughput premix ME studied n-hexadecane/water emulsions^{20,21,26} and sunflower oil/water emulsions stabilized with legume proteins⁴², initial trials were performed with n-hexadecane. The emulsion formulation maintained the oil fraction used by Nazir *et al.*, (2011)²⁰, 5% oil, even though the droplet size of the coarse emulsion was

bigger. As shown in Table 4.1, using square pore micro-sieves it was possible to refine an n-hexadecane/water emulsion of 48 μm at 150 kPa.

Comparing these results with the ones reported by Nazir et al., (2011)²⁰ the fluxes in the present case are ten times smaller for the same pressure, which could be due to the fact that we used a thicker micro-sieve with a much lower porosity. Nonetheless, the droplet size after two passes through the micro-sieve is quite similar to the one reported by these authors, and the throughput of the premix ME system is significantly higher than the one reported with the stir cell in premix ME⁸, proving the benefits of this kind of operation for industrial scale-up.

Following these initial trials, micro-sieves were assessed for the refinement of lemon oil/water emulsions. For this particular application oil fractions of 5 and 20% were selected and emulsions were refined using rectangular pore micro-sieves, the ones with higher porosity in our case (Table 4.1), at different pressures. The size of the coarse emulsion was another variable considered to test the feasibility of micro-sieves for the refinement of lemon oil emulsions, selecting sizes of about 20 and 6 μm . As it can be seen in Table 4.1, with a 5% lemon oil coarse emulsion of a size of 20 μm ($d_{ratio} = 3.5$) the flux in the first emulsification cycle increases when increasing the applied pressure from 150 to 450 kPa. Moreover, the droplet size reduction after the first pass through the micro-sieve is in both cases significant, reaching a droplet size of about 8 μm and 5 μm at 150 kPa and 450 kPa, respectively. However, when refinement continued with a second emulsification cycle, there was no emulsion passing through the micro-sieve for the lowest pressure and the flux obtained at the highest pressure dropped by a factor of ten (Table 4.1). These findings can be linked to fouling of the micro-sieves, which was confirmed by optical microscopy. Looking at the fouled micro-sieves used to refine the lemon oil emulsions, a thin wax-like layer could be seen covering the surface of the sieves, and under the microscope the pores seem blocked. Sahin *et al.*, (2016)¹²⁴, when discussing sunflower oil in water emulsions, describe how its main constituent, triglyceride, may form tightly bound films on the glass surface of the of micro-fluidic EDGE emulsification apparatus, consequently hindering the formation of monodisperse droplets. Similar observations were made by the work of Schroën *et al.*, (2016)¹²⁵ where sunflower oil bonded to the surface of polyethersulfone and nitrocellulose membranes thus forming a film and fouling said membranes. In the present case, the micro-sieves as shown by the contact angle test (see section 4.2.2), are more hydrophobic than hydrophilic causing terpenic and unsaturated oils like lemon oil to interact with the metal surface and reduce the available open area of the micro-sieve. Moreover, it has been reported^{126,127} that metals catalyze both oxidation and polymerization reactions in fatty acids.

Table 4.1. Initial conditions tested for lemon oil/water emulsions produced with nickel micro-sieves.

Oil phase and fraction	d_{coarse}	Nickel Micro-sieve	ΔP (kPa)	Sieve Porosity (%)	d_h	d_{ratio}	Cycle1		Cycle2	
							J	$D_{3,2}$ (μm)	J	$D_{3,2}$ (μm)
Lemon (5%)	20	Rectangular (thickness: 90 μm)	150	0.90	5.72	3.50	167.4	7.71	NEC*	NEC*
Lemon (5%)	20	Rectangular (thickness: 90 μm)	450	0.90	5.72	3.50	261.8	5.12	24.55	3.55
Lemon (20%)	5.9	Rectangular (thickness: 120 μm)	100	0.83	7.75	0.76	232.0	4.66	196.2	4.02
Hexadecane (5%)	48	Square (thickness: 120 μm)	150	0.45	18.2	2.82	129.9	16.9	89.2	11.9

*NEC: No Emulsion Collected at the outlet of the premix ME

Since lemon oil is known to be rich in unsaturated fatty acids¹²⁸, the large molecules formed as a result of these reactions might also be a reason for the micro-sieve fouling. On the other hand, n-hexadecane, which is a hydrocarbon doesn't seem to cause similar problems. Since changing the wettability of the micro-sieves was out of the scope of this study, adjustments in the emulsion formulation were planned.

Using a 20% lemon oil fraction and a coarse emulsion of about 6 μm ($d_{ratio} = 0.76$), it was possible to refine a lemon oil emulsion using a rectangular pore micro-sieve at low pressure (Table 4.1). The fluxes during two consecutive emulsification cycles were about 200 $\text{m}^3 \text{m}^{-2} \text{h}^{-1}$, with a slight decrease in the second cycle, and there was almost a 40% reduction in the droplet size by the end of cycle 2. The reduction in the flux continued during emulsification, and after 5 cycles (results not shown) the flux had dropped by a factor of 10, which is thought to be due to fouling of the micro-sieves. From these initial tests it seems that using a d_{ratio} below 1 should allow to use unmodified nickel micro-sieves to refine lemon oil/water emulsions with a high-throughput premix ME system. It is worthy to mention that in the previous studies using a high-throughput premix ME system with micro-sieves the d_{ratio} was close to 1 for emulsification of a 10% sunflower oil/water emulsion⁴² and ranged from 1 to almost 7 for a 5% n-hexadecane/water emulsion^{20,21}. Therefore, to study the influence of pore size and geometry, the oil fraction was set at 5% to avoid excessive fouling when using low porosity micro-sieves such as the ones used in the present study (Table 4.2).

Table 4.2. Characterization of all the micro-sieves used for emulsification

Transmembrane Pressure (kPa)	Square (S) pore sieves		Rectangular (R) pore sieves	
	SA		RA	
150	Pore dimensions: (17.04 x 20.76) μm	Pore dimensions: (4.94 x 288.66) μm		
	Thickness: 90 μm	Thickness: 90 μm		
	Hydraulic diameter: 18.77 μm	Hydraulic diameter: 9.71 μm		
	Porosity: 0.83%	Porosity: 1.44%		
	Initial water flux: 134.36 $\text{m}^3 \cdot \text{m}^{-2} \cdot \text{h}^{-1}$	Initial water flux: 277.23 $\text{m}^3 \cdot \text{m}^{-2} \cdot \text{h}^{-1}$		
	SB	RB		
300	Pore dimensions: (19.23 x 19.59) μm	Pore dimensions: (4.15 x 291.62) μm		
	Thickness: 90 μm	Thickness: 90 μm		
	Hydraulic diameter: 19.41 μm	Hydraulic diameter: 8.18 μm		
	Porosity: 0.70%	Porosity: 1.22%		
	Initial water flux: 160.54 $\text{m}^3 \cdot \text{m}^{-2} \cdot \text{h}^{-1}$	Initial water flux: 265.44 $\text{m}^3 \cdot \text{m}^{-2} \cdot \text{h}^{-1}$		
	SC	RC		
450	Pore dimensions: (16.81 x 21.56) μm	Pore dimensions: (4.47 x 293.33) μm		
	Thickness: 90 μm	Thickness: 90 μm		
	Hydraulic diameter: 18.89 μm	Hydraulic diameter: 8.81 μm		
	Porosity: 0.71%	Porosity: 1.21%		
	Initial water flux: 152.52 $\text{m}^3 \cdot \text{m}^{-2} \cdot \text{h}^{-1}$	Initial water flux: 242.53 $\text{m}^3 \cdot \text{m}^{-2} \cdot \text{h}^{-1}$		

4.3.2. Micro-sieve integrity during premix ME and impact on productivity and emulsion properties

Once the feasibility of using unmodified micro-sieves to produce lemon oil/water emulsions with a high-throughput premix ME system was proven, and the limitations were clear, replicates of 5% lemon oil / water emulsions with an initial $d_{3,2}$ diameter of $5.5 \pm 0.14 \mu\text{m}$ and a span of 1.1 ± 0.01 were refined at 150 kPa using one square (SA, $d_{ratio} = 0.29$) and one rectangular (RA, $d_{ratio} = 0.57$) pore micro-sieve (see Table 4.2). Nickel micro-sieves were characterized in terms of pore dimensions, hydraulic diameter, porosity, contact angle and initial water flux. The values are reported in Table 4.2 and 3. The experiments enabled to determine how the pore size and geometry affected the productivity and the droplet size distribution during emulsification, while assessing if the emulsification cycles and the required cleaning to restore permeability affected the micro-sieves integrity.

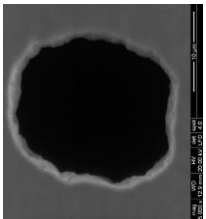
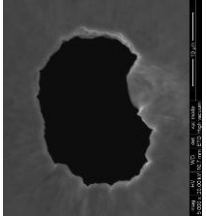
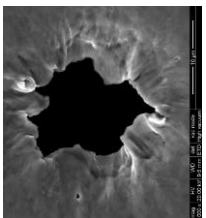
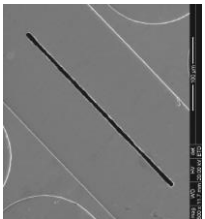
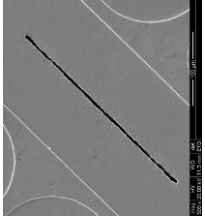
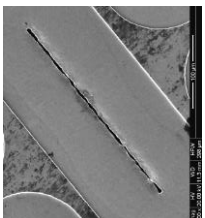
Table 4.3. Evolution of the micro-sieves' surface contact angle

	Brand new	After rep1 (after the first time the sieve was used for five emulsification cycles, cleaning (with acid and base) and WFR)	After rep2 (after the second time the sieve was used for five emulsification cycles, cleaning (with acid and base) and WFR)
Sieve SA	115°	99°	90°
Sieve RA	115°	81°	69°

The contact angles of the square and rectangular sieves used at 150 kPa were measured and the value (115°, Table 4.3) was the same for both of them indicating that the nickel surface was hydrophobic. Many contact angle measurements on nickel sieves from the same batch were done and the sieves were all hydrophobic. This assured that the other four sieves, also from the same batch (used at 300 and 450 kPa), and although their contact angle was not measured, were also hydrophobic.

Emulsification experiments in this study consist of five consecutive emulsification cycles, cleaning of the sieves and measurement of WFR. When performing the emulsification experiments it was clear that the WFR was continuously decreasing after each emulsification (Table 4). At this point it is important to define the term replicate (rep) used in this paper. A replicate (rep) refers to a complete set of emulsification (five passes of the emulsion through the micro-sieve), cleaning and WFR measurement. Therefore, rep1 refers to the first time the sieve was used for emulsification, cleaning and WFR cycle, rep2 to the second time the sieve was used for emulsification, cleaning and WFR cycle, and so on.

Table 4.4. Progression of pore morphology for micro-sieves SA and RA from their brand new state, to that after rep 1 and after rep 2

	Brand New	After rep1	After rep2
Sieve SA	 <p>For 5th emulsification cycle:</p> <ul style="list-style-type: none"> • φ_5: 10.8 g.s⁻¹ • $d_{3,2}$: 1.33 μm • Span: 1.29 • $\delta_{w,p}$: 27.84 Pa • WFR: 83 % 	 <p>For 5th emulsification cycle:</p> <ul style="list-style-type: none"> • φ_5: 10.1 g.s⁻¹ • $d_{3,2}$: 1.38 μm • Span: 1.34 • $\delta_{w,p}$: 26.12 Pa • WFR: 64 % 	 <p>For 5th emulsification cycle:</p> <ul style="list-style-type: none"> • φ_5: 20.9 g.s⁻¹ • $d_{3,2}$: 1.85 μm • Span: 1.49 • $\delta_{w,p}$: 107.29 Pa • WFR: 72 %
Sieve RA	 <p>For 5th emulsification cycle:</p> <ul style="list-style-type: none"> • φ_5: 17.8 g.s⁻¹ • $d_{3,2}$: 1.93 μm • Span: 1.54 • $\delta_{w,p}$: 90.83 Pa • WFR: 86 % 	 <p>For 5th emulsification cycle:</p> <ul style="list-style-type: none"> • φ_5: 20.9 g.s⁻¹ • $d_{3,2}$: 1.85 μm • Span: 1.49 • $\delta_{w,p}$: 107.29 Pa • WFR: 72 % 	 <p>For 5th emulsification cycle:</p> <ul style="list-style-type: none"> • φ_5: 20.9 g.s⁻¹ • $d_{3,2}$: 1.85 μm • Span: 1.49 • $\delta_{w,p}$: 107.29 Pa • WFR: 72 %

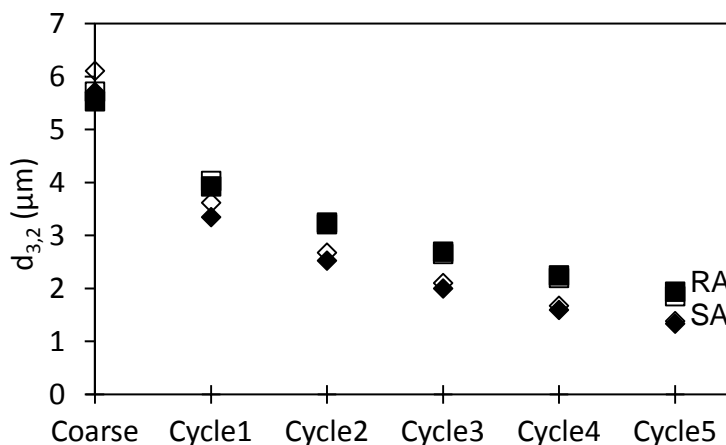


Figure 4.3. Effect of the replicate number on the Sauter mean diameter of emulsion produced with micro-sieves SA (\diamond , \blacklozenge) and RA (\square , \blacksquare). Filled markers refer to the first time the sieve was used for emulsification (rep1) and the empty marker refer to the second time the sieve was used for emulsification (rep2)

After rep2, the WFR decreased to 64% for sieve SA and to 72% for sieve RA. This however had no effect whatsoever neither on the emulsion mass flow rate, nor on the size of the oil droplets produced. In other words, had the WFR not been measured, no other indicator would have revealed any changes happening in the emulsification process (Figure 4.3).

Microscopic characterization (ESEM) and contact angle measurements were used for monitoring micro-sieves integrity during emulsification experiments. ESEM images were taken of each micro-sieve after each replicate. Table 4 shows the damage occurring on the pores and how it is progressive for both micro-sieves until the openings are practically closed. Santos et al., (2015)⁸, from whom the cleaning protocol was adapted, hasn't reported similar problems with their nickel sieves. They used the sieves for a direct and premix emulsification with a stirred cell where the shear stress, $\delta_{w,p}$ (Equation 4.5), is much lower (< 1 Pa) than that in the present case (26-162 Pa).

$$\delta_{w,p} = (8 \cdot \eta_e \cdot J \cdot \xi) / (\epsilon \cdot d_m) \quad (4.5)$$

In Equation 4.5, η_e is the emulsion viscosity, ξ the membrane tortuosity, ϵ the membrane porosity and d_m is membrane pore mean diameter. When the volume fraction of the dispersed phase is low (5-10%), the emulsion viscosity can be assumed to be that of the continuous phase. Moreover, the tortuosity is equal to 1 when the pores can be considered straight through. As for the membrane pore

mean diameter, the width of the pore, a.k.a. characteristic diameter (d_{char}), has been used instead in the calculations.

Moreover, Nazir et al., (2011)²⁰ that have used nickel sieves for premix emulsification with shear stress in the same order as in the present study, but applying a different cleaning technique, also haven't reported the micro-sieve damage problem. As a result, it was concluded that the combination of the NaOH/citric acid cleaning procedure and the emulsification at high shear stress was causing the nickel on the walls of the pores to soften and under pressure (150 kPa), the pore walls were being pushed inwards thus closing the opening. In fact, a brand-new nickel sieve was cleaned four consecutive times without using it for emulsification, while collecting ESEM pictures of the pores after each cleaning (Figure 4.4a and 4.4b). No changes whatsoever were observed, which backs up the conclusion that the combination of chemical cleaning plus the high shear were causing the damage.

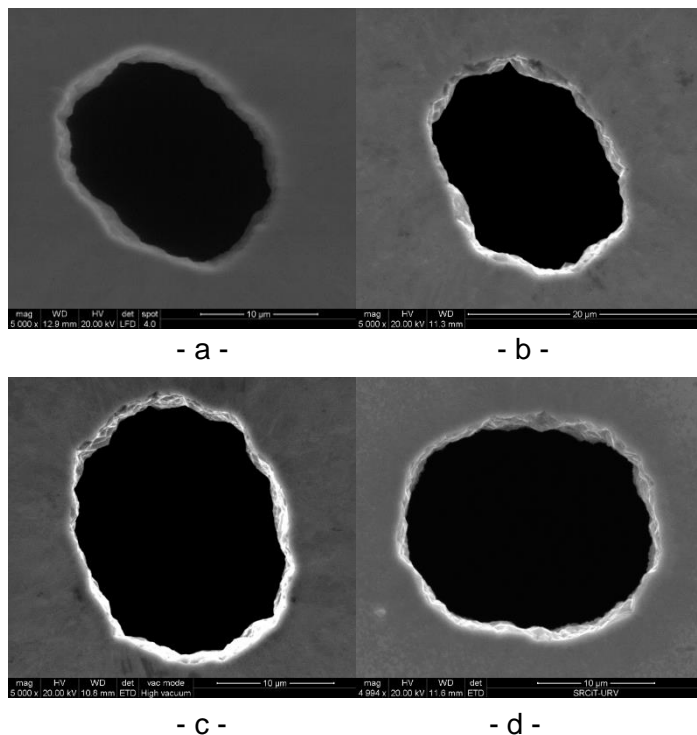


Figure 4.4. ESEM images of (a) a brand new micro-sieve pore and (b) after applying the acid-base-water cleaning protocol four consecutive times without being used for emulsification. Image (c) shows a brand new micro-sieve pore and (d) shows a pore after rep2 (while applying the modified cleaning protocol).

Regarding contact angle measurements, the two-brand new micro-sieves used for emulsification at 150 kPa were more hydrophobic than hydrophilic, as it is clear from contact angle values in Table 4.3. As they were used repetitively for emulsification and cleaned, the contact angle tended to decrease, indicating that emulsification and cleaning had an effect on their wettability. The effect of the contact angle variations on emulsification was not further investigated because it didn't seem to affect the flux and the droplet size of the emulsions obtained under the present working conditions.

In the current working conditions and aware of the changes that were happening to the micro-sieve pores from one replicate to the other, it was concluded that the use of the same micro-sieve for three replicates couldn't ensure reproducibility. However, modifying the cleaning protocol by removing the acid treatment, it was possible to clean the micro-sieves and reduce the damage on the pores allowing the use of the same micro-sieve for two replicates (rep 1 and rep 2), as shown in Figure 4.4c and 4.4d. In that sense, a different brand-new micro-sieve was used in the emulsification experiments rep 1 and rep 2 for each pressure. Due to the significant variability in the porosity among micro-sieves of the same nominal pore size, a thorough characterization was performed to select a final set having similar porosity and initial water flux. The final set of micro-sieves is presented in Table 4.2.

4.3.3. Effect of transmembrane pressure and pore size and geometry on droplet break-up

In order to scale-up the premix ME process, the relationship between the energy applied (pressure) and droplet break-up was investigated for this particular system. Firstly, we have studied the effect of transmembrane pressure applied on the fluxes during emulsification for the two different pore geometries, considering two different d_{ratio} values, 0.57 and 0.29 for rectangular and square micro-sieves, respectively (Equation 4.3).

The flux values (Figure 4.5) at the fifth cycle for the square pore sieves range from about $200 \text{ m}^3 \cdot \text{m}^{-2} \cdot \text{h}^{-1}$ at 150 kPa to about $360 \text{ m}^3 \cdot \text{m}^{-2} \cdot \text{h}^{-1}$ at 450 kPa, while for the rectangular pore sieves the values are from about $320 \text{ m}^3 \cdot \text{m}^{-2} \cdot \text{h}^{-1}$ to $780 \text{ m}^3 \cdot \text{m}^{-2} \cdot \text{h}^{-1}$ for 150 kPa and 450 kPa, respectively. From Figure 4.5 a decrease in the flux can be seen with the number of cycles, regardless of the pore size and geometry.

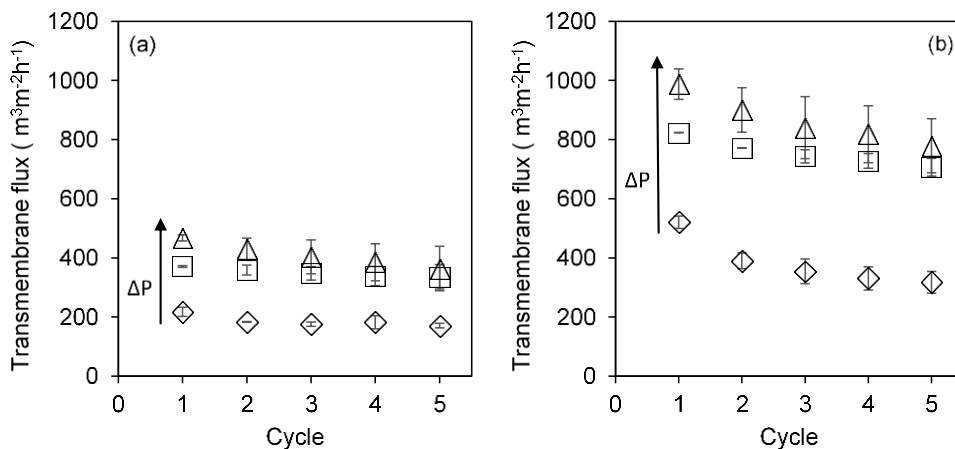


Figure 4.5. Transmembrane flux versus the number of cycles for emulsions produced with micro-sieves (a) SA and (b) RA at (\diamond) 150 kPa, (\square) 300 kPa and (\triangle) 450 kPa

As reported previously^{24,27} the pressure applied is used both to flow the emulsion through the microporous systems and to break the oil droplets. Therefore, when there is no significant reduction in the droplet size from one emulsification cycle to the next one, the pressure applied would be mainly invested in flowing the emulsion through the microporous system, resulting in constant flux if there were no fouling. In the present scenario, flux decreased or was kept almost constant when increasing the number of cycles while droplet size was simultaneously reduced (Figure 4.6). This behavior is mainly attributed to fouling of the microporous systems, which is thought to be caused by the wax layers that lemon oil can form on the hydrophobic surface of the nickel micro-sieves as mentioned before.

Regarding droplet size distribution during emulsification with the nickel micro-sieves of two different pore geometries, Figure 4.6 shows the effect of number of cycles and transmembrane pressure on $d_{3,2}$ and span. The coarse emulsion had a $d_{3,2}$ of about 5.5 μm for all the experiments. The droplet diameter ($d_{3,2}$) was reduced to 1.34 μm after 5 cycles at 150 kPa with the square micro-sieves, with a slight increase of the span value compared to the coarse emulsion (Figure 4.6). The droplet size at the 5th cycle decreased as the transmembrane pressure applied increased to a value of 0.55 μm at 450 kPa, while increasing the span. The results obtained with the rectangular micro-sieves followed the same trend, with a similar decrease in the $d_{3,2}$ with the number of cycles and the pressure applied. At a pressure of 150 kPa, a droplet breakup of 66% ($1 - d_{\text{cycle5}} / d_{\text{coarse}}$) was obtained after 5 emulsification cycles which is similar to the results reported by Nazir et al., (2011)²⁰, where at the same pressure, 69% droplet break occurred with hexadecane-in-oil emulsions and Tween20 as emulsifier.

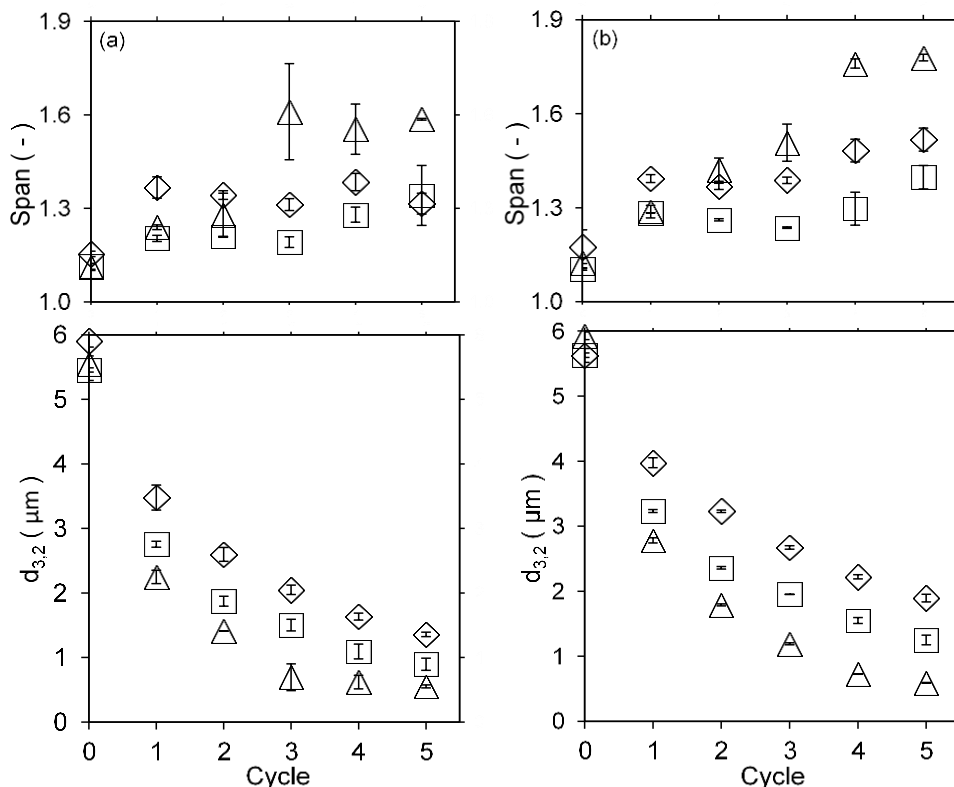


Figure 4.6. Sauter mean diameter versus the number of cycles for emulsions produced with micro-sieves (a) SA and (b) RA at (\diamond) 150 kPa, (\square) 300 kPa and (\triangle) 450 kPa

Santos et al. (2015)⁸, similarly to our work, produced lemon oil-in-water emulsions by premix membrane emulsification, however using a stirred cell which works with much smaller shear stress than in this study. That technique rendered polydispersed emulsions even after three cycles with a span ranging from 1.5 to 6. In our study however, using high-throughput premix ME has produced emulsions of span values of 1.2-1.7, which are improved values. It can be noticed from Figure 4.6 that with more cycles to refine the emulsion, the particle size was indeed decreasing as discussed previously and also, at high pressure especially, the span increased indicating that re-coalescence of the droplets occurs much faster than the stabilization of the newly created interfaces by the emulsifier^{8,20}.

In short, we observed that rectangular micro-sieves had significantly higher fluxes than the square ones. However, when we compared the average velocity inside the pore, v_p , (calculated using Equation 4.6) between the RA and SA micro-sieves, differences were significantly reduced (Figure 4.7).

$$v_p = J / \epsilon \quad (4.6)$$

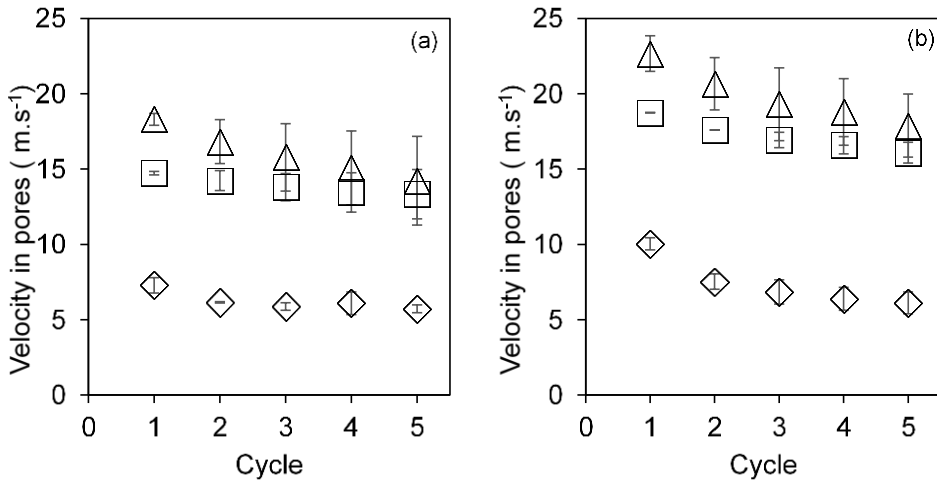


Figure 4.7. Velocity inside the pores versus the number of cycles for emulsions produced with a) micro-sieves SA and b) RA at (◇) 150 kPa, (□) 300 kPa and (△) 450 kPa

Consistently, no noticeable effect on the final droplet size distribution could be seen at the same transmembrane pressure in both sieves. Also, the higher shear stress generated in this system did not end up in a narrower droplet size distribution, probably because droplet disruption occurred faster than the time required for the emulsifier to travel to the created interfaces and stabilize the newly formed droplets.

Moreover, to identify the droplet break-up mechanisms, Webber number (We , Equation 4.7) is plotted versus the dimensionless pressure (P_{ratio} , Equation 4.8). The dimensionless Webber number, commonly used in membrane emulsification, represents the ratio of applied inertial force to the opposing interfacial tension force¹²⁹.

$$We = (d_{32,o} \cdot \rho_e \cdot v_p^2) / (2 \cdot \delta) \quad (4.7)$$

Here $d_{32,o}$ is the Sauter mean diameter of the outgoing droplets and δ is the droplet interfacial tension. Nazir et al., (2011)²⁰ have defined the dimensionless pressure, P_{ratio} , as the indicative of the applied energy and the minimum amount of energy needed to deform the droplet, and it can be calculated using Equation (4.8),

$$P_{ratio} = (d_{32,i} \cdot \Delta P) / \delta \quad (4.8)$$

where $d_{32,i}$ is the Sauter mean diameter of the ingoing droplets and ΔP is the transmembrane pressure. Large P_{ratio} values refer to excessive applied energy, more than that required to form and free the droplets and large We number

indicates the dominance of inertial effects^{20,21}. For these calculations a droplet interfacial tension of 4.3 mN.m^{-1} was obtained by the Drop Volume Method (ISO 9101:1987). In Figure 4.8, the data shown are those from all cycles of emulsification at all three pressures (150, 300 and 450 kPa) using the two sieves of different geometry.

At high P_{ratio} values, that are mainly attained at the first emulsification cycle, the results of the two types of sieves follow a different trend. It is clear that the rectangular pore micro-sieve, with the first cycle, puts forth more inertial effects than the square pore micro-sieve. These effects decrease as the ingoing droplet size decreases. The change of the slope of the curve possibly indicates a change in droplet break-up mechanism. However, it is important to point out that the geometry of the pores (square or rectangle) is not the factor responsible for this difference in trend but rather the characteristic diameter (d_{char}) of the pores. Calculating the ratio of the coarse emulsion diameter to d_{char} , for the square and rectangular micro-sieves, values of about 1.2 and 0.3 are obtained. Clearly, the coarse emulsion droplet size is larger (11 to 33%) than the width of the rectangular pores and much smaller (71-72%) than the dimensions of the square pores. Vladislavljević *et al.*, (2004)²⁷ has defined two droplet break-up mechanisms at high shear stresses, as we have in high-throughput system.

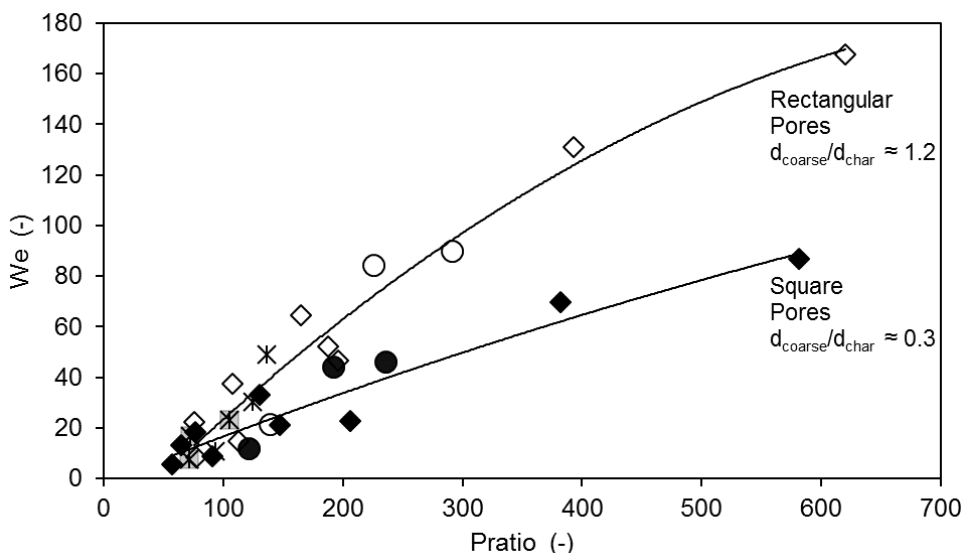


Figure 4.8. We number as a function of P_{ratio} : (\diamond, \blacklozenge) 1st, (\circ, \bullet) 2nd, (\square, \blacksquare) 3rd, (\ast, \boxtimes) 4th and ($\triangle, \blacktriangle$) 5th cycles. Filled markers refer to square pore sieves and empty markers refer to rectangular pore sieves.

Droplets bigger than the pores deform at the entrance, disrupt in the pores due to friction with the pore walls, and any further break-up is due to collisions between themselves and the pore walls. Based on this, it is expected with rectangular pores, that the droplets break first by friction with the pore walls and then, as they become smaller with every emulsification cycle (in this case after the first cycle), break-up happens solely due to collisions. Otherwise, for the square sieves, droplet break-up will most probably happen due to collisions only. This could explain the differences in the slope of the plots in Figure 4.8. The higher slope of the RA micro-sieves corresponds to the first emulsification cycles that could be linked to the disruption of droplets because of friction with the pore walls. As droplet break-up progresses and droplet size becomes much smaller than the pore size, the mechanism controlling droplet disruption for both micro-sieves becomes the collisions with the pore walls.

4.4. Conclusion

The results of this work have shown that a high-throughput low energy system based on hydrophobic nickel micro-sieves of different pore geometries can be used to successfully produce lemon oil/water emulsions. From the emulsification/cleaning tests, it is advised to use mild cleaning conditions for the micro-sieves to maximize their use, since this type of microstructured systems are highly attractive for processes requiring high emulsion productivity. More importantly, to refine lemon oil emulsions using nickel micro-sieves of different pore geometry, the oil fraction and the coarse emulsion size have to be adjusted depending on the porosity and the hydraulic diameter of the micro-sieves, respectively. It is advised for a successful operation to maintain low lemon oil fractions (5%) when the porosity of the unmodified micro-sieve is below 1.5%. Moreover, the ratio between the droplet size of the coarse emulsion and the hydraulic diameter of the micro-sieve has to be kept about 1 or below to refine emulsions at pressures ranging from 150-450 kPa. Under these conditions, the high fluxes obtained during emulsification show the potential of microstructured micro-sieves to scale-up this technology. All lemon oil emulsions produced by premix ME with unmodified micro-sieves had a $d_{3,2}$ of around 0.5 μm at the highest pressure used, this is a ten times reduction from the initial size; however, at this pressure droplet re-coalescence is prominent, which slightly increases the span value. Regarding droplet break-up mechanisms, the relationship between the We number and the P_{ratio} seems to indicate that lemon oil droplets are broken by friction with the pore walls during the first cycles, followed by break-up due to collisions when the droplets have been reduced in size for the rectangular pore micro-sieves. While for the square pore micro-sieves, the droplet break-up only occurs due to collisions with the walls. Knowledge of break-up mechanisms

resulting from the hydrodynamics of the system is significant for scale up of the process and for droplet size prediction.

This chapter dealing with the use of the nickel micro-sieve for lemon oil emulsification has highlighted the potentials and limitations of this system. The nickel sieve is the base of the dynamic membrane of tunable size system which will be used in the next chapter. In the DMTS system, as mentioned in section 1.1.3, a layer of glass beads is placed on top of the nickel micro-sieve and used as a membrane for emulsification. For that reason, the understanding of the function of the nickel sieve alone in lemon oil encapsulation was crucial.

UNIVERSITAT ROVIRA I VIRGILI

LOW-ENERGY HIGH-THROUGHPUT MICROPOROUS EMULSIFICATION FOR LEMON OIL ENCAPSULATION

Wael Kaade

5. Dynamic membranes of tunable pore size for lemon oil encapsulation

This chapter has been published as:

Kaade, W., Güell, C., Ballon, A., Mellado-Carretero, J., Lamo-Castellví, S. De, & Ferrando, M. (2020). Dynamic membranes of tunable pore size for lemon oil encapsulation. *LWT*, 109090.

UNIVERSITAT ROVIRA I VIRGILI

LOW-ENERGY HIGH-THROUGHPUT MICROPOROUS EMULSIFICATION FOR LEMON OIL ENCAPSULATION

Wael Kaade

5.1. Introduction

Lemon essential oil has been widely used for flavoring purposes but recently an interest in its antimicrobial, antifungal and antioxidant properties has been rising⁵⁶. Encapsulation through microencapsulation and emulsification has facilitated its incorporation into foods. A study of the literature shows that both high energy (shear intensive) as well as low energy techniques were used to emulsify lemon oil (LO). The latter techniques, which require low energy inputs, are microchannel emulsification⁵³, membrane emulsification with a stirred cell module⁸, spontaneous emulsification⁵⁷ and as discussed in chapter 4, premix emulsification with micro-structured nickel sieves, which has shown high-throughput. In that case, flux values up to $990 \text{ m}^3 \cdot \text{m}^{-2} \cdot \text{h}^{-1}$ were reported, which is an advantage over other low energy techniques.

Since LO, contains many volatile compounds that are heat sensitive, it will benefit of using a low energy – low shear membrane emulsification technique. In energy intensive emulsification techniques, more than 99% of the energy is dissipated as heat which causes an increase in the emulsion temperature⁶. This in turn leads to the damage of the aromatic profile of LO, unless more energy is spent in a post-emulsification cooling step. A new system named dynamic membrane, first reported by Van Der Zwan *et al.* (2008)²⁶ is an excellent substitute for energy intensive emulsification techniques, where there is no rise in temperature. This membrane is made of a bed of silica glass micro-beads supported by a nickel micro-sieve and it is referred to as “dynamic” because the micro-beads size and bed height may be selected to tune the pore size and thickness of this microporous system, respectively. Dynamic membranes have been reported for the production of both non-food^{22,26,40,43} and food grade emulsions^{42,44–46}. However, to the author’s knowledge, no studies have dealt with the encapsulation of LO with the dynamic membrane system.

In order to produce a more stable encapsulate, emulsification can be followed by a drying step (e.g. spray drying) to obtain solid microcapsules. Oil fraction, droplet size distribution and oil to wall material ratio are key parameters to enhance the encapsulation efficiency during spray-drying⁵⁸. Therefore, selecting an emulsification technique that allows to control the droplet size distribution in emulsions having an oil fraction above 20%, while reducing the heat stress over the product, will increase the overall industrial efficiency for encapsulation of LO.

The aim of this study is to produce stable LO emulsions with a narrow droplet size distribution, in the range of a few micrometers, using a low-energy high-throughput emulsification system to set the basis for an industrial application. Emulsions with oil fractions up to 40% were refined using dynamic membranes of

tunable pore size (DMTS) in premix emulsification mode. The effect of the DMTS (void fraction and height) and the micro-sieve characteristics on emulsification fluxes, droplet break-up and emulsion stability were studied. More importantly, a modification to the standard DMTS system, superimposing two layers of different micro-beads size, has been tested to improve the properties of the O/W emulsion and reduce the overall energy input.

5.2. Materials and methods

5.2.1. Dynamic membrane of tunable size

The DMTS is formed of a bed of silica glass micro-beads placed on top of a nickel metal micro-sieve (Figure 5.1). These nickel sieves (Stork Veco, Eerbeek, The Netherlands) have rectangular pores. The hydrophilic silica glass micro-beads used for emulsification were of three sizes (d_b) \approx 42, 68 (Microspheres-nanospheres, USA) and 99 μm (Unicorn Industrial Cleaning Solutions, The Netherlands). Table 5.1 reports the different combinations of micro-beads and micro-sieves utilized to produce the emulsions.

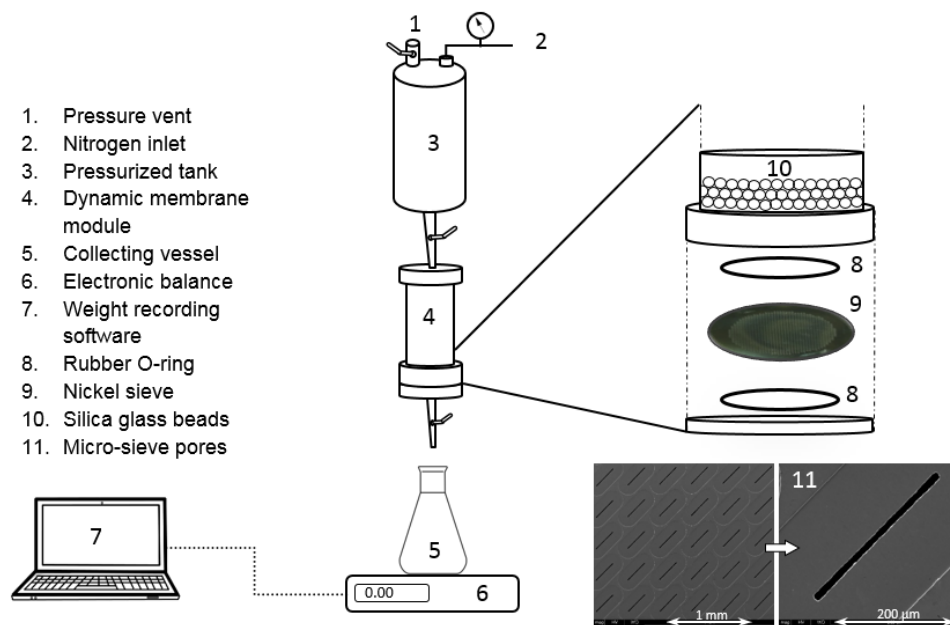


Figure 5.1. Dynamic membrane emulsification setup

Table 5.2. Physical properties and characteristics of the DMTS systems.

	Beads size, $d_{3,2}$, (μm)	Span of beads	Micro-beads density, ρ_d , (kgm^{-3})	Bulk density, ρ_b , (kgm^{-3})	Porosity of bed, ϵ , (%)	Interstitial void diameter, d_v , (μm)	Tortuosity (t)	Bed height (mm) / Amount (g)	Micro-sieves pore dimensions ($\mu\text{m} \times \mu\text{m}$)	Micro-sieve porosity (%)
DMTS 1	41.7	0.82	2466	1221	50.48	28.33	1.28	9.27 / 2	11.12 x 290.44	2.39
DMTS 2	67.5	0.65	2743	1474	46.28	38.79	1.32	7.68 / 2	11.12 x 290.44	2.39
DMTS 3								2.18 / 0.5	11.12 x 290.44	
DMTS 4								4.35 / 1	6.29 x 286.86	1.31
DMTS 5								8.70 / 2	6.29 x 286.86	1.31
DMTS 6	98.7	0.75	2446	1301	46.83	57.97	1.31	8.70 / 2	10.67 x 290.14	2.33
DMTS 7								8.70 / 2	13.79 x 281.62	2.82
DMTS 8								17.4 / 4	6.29 x 286.86	1.31
Layering										
	Top layer: 98.7	0.75	2446	1301	46.83	58.0	1.31	4.35 / 1		
	Bottom layer: 41.7	0.82	2466	1221	50.48	28.3	1.28	4.63 / 1	10.67 x 290.14	2.33

The sizes of the micro-beads obtained (42, 68 and 99 μm) are the result of sieving batches of polydispersed micro-beads using a series of trays with mesh sizes ranging between 25 and 200 μm . The samples collected after sieving were analyzed with a Mastersizer for the particle size distribution.

The particle (ρ_p) and dry bulk (ρ_b) densities of the micro-beads were measured using a pycnometer and a 5 mL graduated cylinder respectively and the values are shown in (Table 5.1). Porosity (ϵ) of the bed was calculated using Equation 5.1.

$$\epsilon = 1 - \frac{\rho_b}{\rho_p} \quad (5.1)$$

As for the tortuosity (τ) of the bed, it was calculated using Equation 5.2⁴⁰. Values of the porosity and tortuosity are found in Table 5.1.

$$\tau = 1 + 0.41 \ln\left(\frac{1}{\epsilon}\right) \quad (5.2)$$

The interstitial void diameter (d_v) is defined by Equation 5.3 where A_v is the specific surface area, a ratio of the surface area of a particle to its volume. A_v is related to a sphere's diameter by: $A_v = 6/d_b$ where d_b is the bead diameter.

$$d_v = \frac{4\epsilon}{A_v(1-\epsilon)} \quad (5.3)$$

The height of the silica micro-beads bed was controlled by controlling the mass of micro-beads laid on top of the nickel sieve. The height (H) is related to the mass of the micro-beads by Equation 5.4²⁶:

$$H = \frac{\text{mass of beads}}{\rho_p A_{\text{column}} (1-\epsilon)} \quad (5.4)$$

In our case the area of the column (A_{column}) used was 177 mm^2 .

To produce the silica micro-beads bed, a weighed mass of the micro-beads was placed on top of the nickel sieve and a few drops of water were added then vacuumed out slowly (the process of adding water was repeated 2-3 times) to pack the micro-beads and make sure the surface is flat and homogeneous.

A number of emulsification experiments were done with a combination of micro-beads of different sizes and these experiments were labeled "layering" (L). In these experiments 1 g of 42 μm micro-beads were placed on top of the micro-sieve and packed with water making sure the surface is flat. Then, 1 g of the 99 μm micro-beads were placed on top of the 42 μm micro-beads and also packed with water gently so as to not disturb the bottom bed. In this way, the dynamic membrane

was formed of, from bottom to top, the nickel sieve, 1 g of the 42 μm micro-beads and finally 1 g of the 99 μm micro-beads.

5.2.2. Dynamic membrane cleaning

After being used for emulsification, the system was disassembled and the silica glass micro-beads were cleaned with soap and water then dried in an oven at 100 $^{\circ}\text{C}$ overnight. As for the nickel sieve, as reported in section (4.2.2), the best way to clean it was by soaking it in an ultrasonic bath for 5 minutes, first in 4M NaOH (Fisher Scientific) and then in distilled water.

5.2.3. Emulsification

O/W emulsions were produced by dispersing LO (Dallant, Spain) into distilled water and stabilized with Polyoxyethylene sorbitan monolaurate (Tween20, Sigma Aldrich, CAS: 9005-64-5). The oil formed either 20%wt or 40%wt of the total emulsion weight and the surfactant formed 2%wt.

The coarse emulsion (160-270 g), or premix, was produced by means of a high shear homogenizer (IKA[®] T-18 basic Ultra-turrax) at 15500 r.p.m for 3 min (with a 30 s break after each minute to avoid over-heating). The resulting droplet size was quickly measured using a light scattering equipment (refer to section 3.2.5 for details). The O/W emulsion had a droplet size ($d_{3,2}$) of $5.7 \pm 0.2 \mu\text{m}$ and a span of 1.15 ± 0.03 . Also, another coarse emulsion with a $d_{3,2} \approx 24 \pm 2 \mu\text{m}$ and a span of 1.08 ± 0.04 was produced at 6000 r.p.m for 2 min followed by 7000 r.p.m for 1 min.

The coarse emulsion was subsequently poured into the pressure tank of the membrane emulsification setup shown in number 3 of Figure 5.1. The nitrogen supply was opened and the emulsion was pushed at 450 kPa down through the DMTS (4 in Figure 5.1) and collected in a recipient placed on an electronic balance. The balance transmits to a computer software the mass of emulsion per second, allowing the calculation of the mass flow rate, φ , and the transmembrane flux (J). This latter can be calculated using Equation (5.5):

$$J = \frac{\varphi}{\rho_e A_{column}} \quad (5.5)$$

where ρ_e is the density of the emulsion (969 kg/m^3) and is calculated from Equation 5.6

$$\rho_e = \theta_d \rho_d + (1 - \theta_d) \rho_c \quad (5.6)$$

θ_d , ρ_d , and ρ_c are the dispersed phased volume fraction, dispersed phase density (846.2 kg/m^3) and continuous phase density (1000 kg/m^3) respectively.

All emulsions were produced in duplicates.

5.2.4. Emulsion stability

After the final emulsification cycle, 6 tubes with 14 mL of the emulsion were saved for the stability study. Three of the tubes were placed in a refrigerator (4°C) and the other three were stored at room temperature (25°C). All the tubes were wrapped with aluminum foil to reduce oxidation caused by light. Two tubes (one refrigerated and another stored at room temperature) were collected after 1, 3 and 7 days (d) and the $d_{3,2}$ and span were measured for each.

5.3. Results and discussion

5.3.1. Effect of coarse emulsion and DMTS characteristics on droplet size distribution and stability of LO emulsions

The selection of the DTMS micro-beads size and their amount will allow to control the interstitial void diameter of the channels (d_v) and the height (H) of the microporous system, respectively. Both parameters influence the emulsification process in terms of the final droplet size distribution and the flux.

To study the effect of the micro-beads size (interstitial void diameter of the bed) in the emulsification process, a coarse emulsion with 20% LO was produced, as explained in section 2.2, having a $d_{3,2}$ of 5.7 μm . This coarse emulsion was refined by passing it five times (cycles) through a DMTS system composed of 2 g of silica micro-beads of 42, 68 or 99 μm . This amount of micro-beads results in a bed height of 8.55 ± 0.8 mm. Figures 5.2a and 5.2b show the $d_{3,2}$ and span variation during five consecutive emulsification cycles, respectively.

From Figure 5.2a, it is clear that when the DMTS system was made using the smallest micro-beads (42 μm) which have the smallest interstitial void diameter, the droplet size of the emulsion after 5 cycles was bigger than that obtained with the DMTS systems with bigger micro-beads. However, the DMTS system with the smallest micro-beads is the only one that enables to produce a final emulsion with a span value lower than 1 (Figure 5.2b), which is an indication of an emulsion with narrow size distribution. As seen in these two plots, there is an opposite effect of channels' size (d_v) of the DMTS system on the droplet size and on the span: a reduction of the d_v results in bigger droplets with lower dispersion. The DMTS system with 42 μm micro-beads reduced the droplet size from its initial value to about 3 μm (44% size reduction) in the first three cycles, remaining almost constant afterwards (Figure 5.2a). However, when the DMTS system was made with micro-beads of 68 or 99 μm there was a reduction of the droplet size with each cycle, reaching a value of about 2 μm (68% size reduction) after the fifth cycle. As it will

be explained in section 5.3.2, DMTS systems made up by micro-beads of small sizes present higher resistance to the emulsion flow because of their narrower channels, thus lower pore velocities and lower forces applied on droplets to break them, in turn leading to larger final droplets²². When increasing micro-beads size, high fluxes might not give enough time for the emulsifier to move to the oil-water interface of the newly formed droplets leading to their re-coalescence and resulting in higher spans. These observations regarding droplet break-up are in line with what has been reported in literature for the production of simple O/W emulsions with dynamic membrane emulsification^{22,40,43,47}.

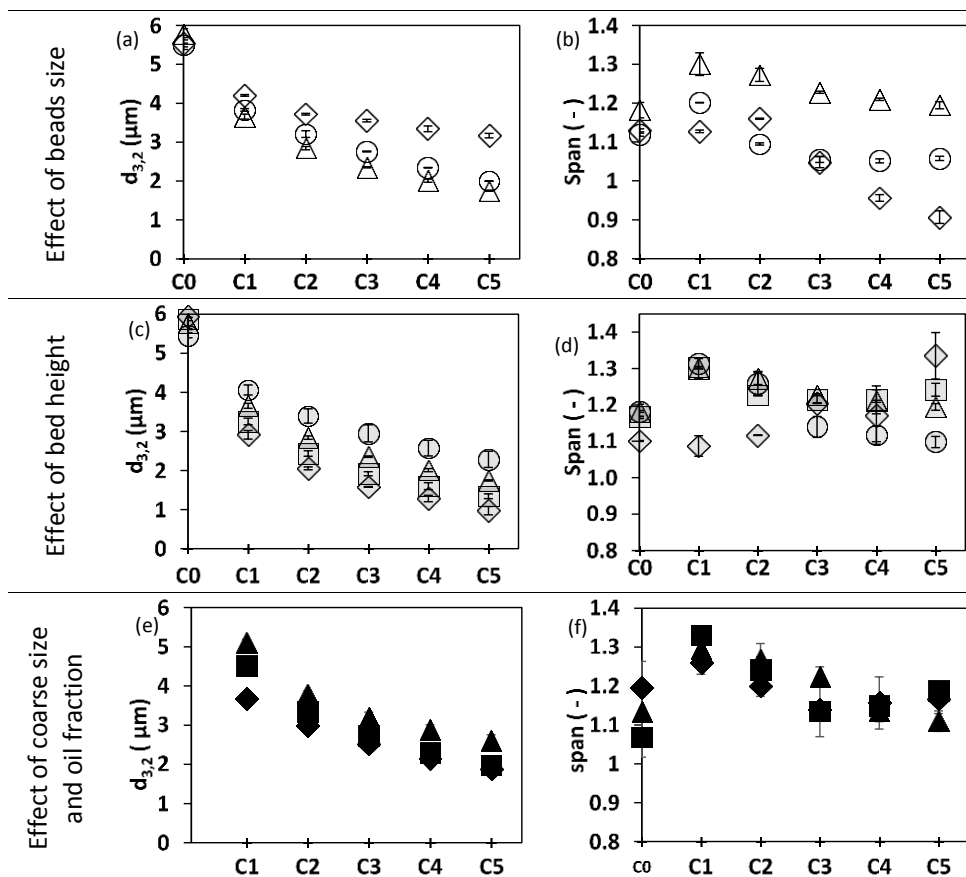


Figure 5.2. Effects on droplet size (a,c) and span (b,d) of micro-beads size (\diamond : $42 \mu\text{m}$, \circ : $68 \mu\text{m}$, Δ : $99 \mu\text{m}$) and bed height (\diamond : 0.5 g , \square : 1 g , \triangle : 2 g , \bigcirc : 4 g). Also, the effect on droplet size (e) and span (f) of coarse emulsion size and oil fraction (\blacklozenge : $99 \mu\text{m} - 5.7 \mu\text{m} - 20\% \text{ LO}$, \blacksquare : $99 \mu\text{m} - 24 \mu\text{m} - 20\% \text{ LO}$, \blacktriangle : $99 \mu\text{m} - 24 \mu\text{m} - 40\% \text{ LO}$). The legend in (e,f) forms three parts: the micro-beads size used ($99 \mu\text{m}$), the size of the coarse emulsion (5.7 or $24 \mu\text{m}$) and finally the lemon oil (LO) fraction (20 or 40%).

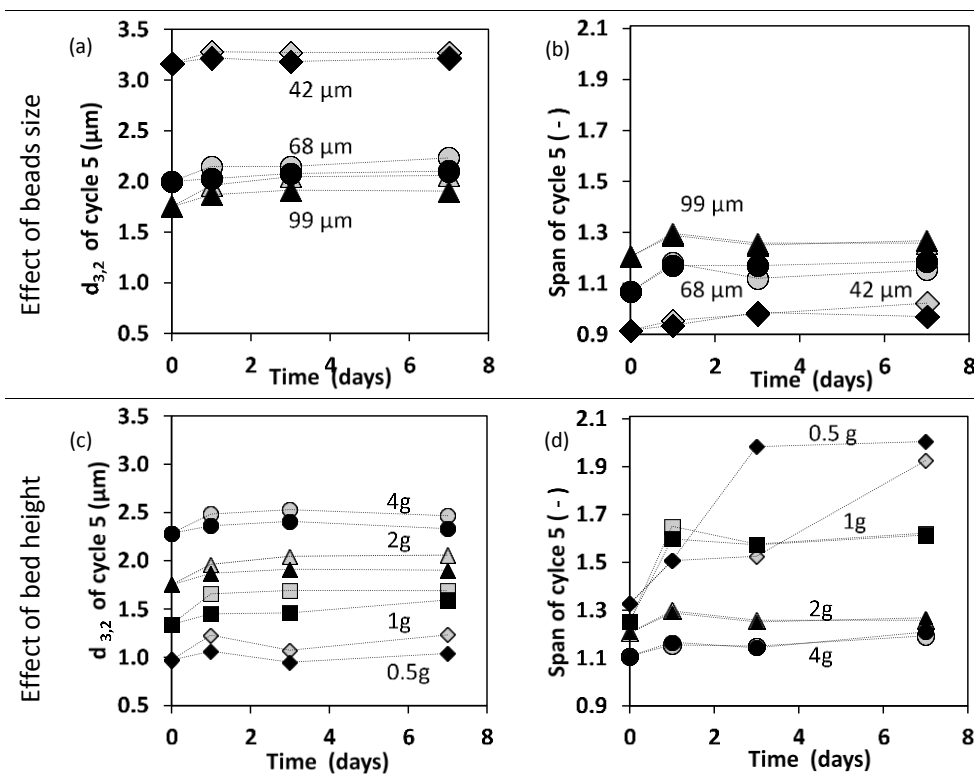
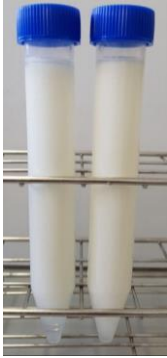
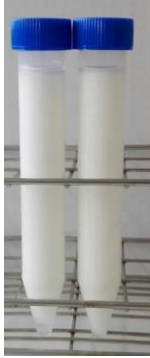


Figure 5.3. Effects of DMTS micro-beads size (a,b) and bed height (c,d) as well as storage temperature on emulsion stability. Grey markers refer to refrigerated samples and black markers refer to samples stored at room temperature.

As for the stability of these emulsions, the results seem to point out that changing micro-beads size in the DMTS system didn't have a great effect on the emulsions' stability (Figures 5.3a and 5.3b and Table 5.2 in supplementary materials), regardless of the starting droplet size; the emulsions maintained the $d_{3,2}$ value for 7 d at room temperature and under refrigeration ($T = 4\text{ }^{\circ}\text{C}$) (Figure 5.4). The span value (Figure 5.3b) slightly increased for the three emulsions after one day of storage, and it was almost constant for the remaining time in emulsions produced in the DMTS system with 68 or 99 μm micro-beads, while it was increasing with time in the emulsion produced in the DMTS system with 42 μm micro-beads, however still, in this case, the span was maintained at or below 1 after seven days of storage.

Table 5.2. Stability of a 20% lemon oil emulsion prepared at two different micro-beads sizes.

	Day 0		Day 1		Day 3		Day 7	
Temperature (°C)	25	4	25	4	25	4	25	4
5.7 μm coarse 42 μm beads 2 g beads								
5.7 μm coarse 99 μm beads 2 g beads								

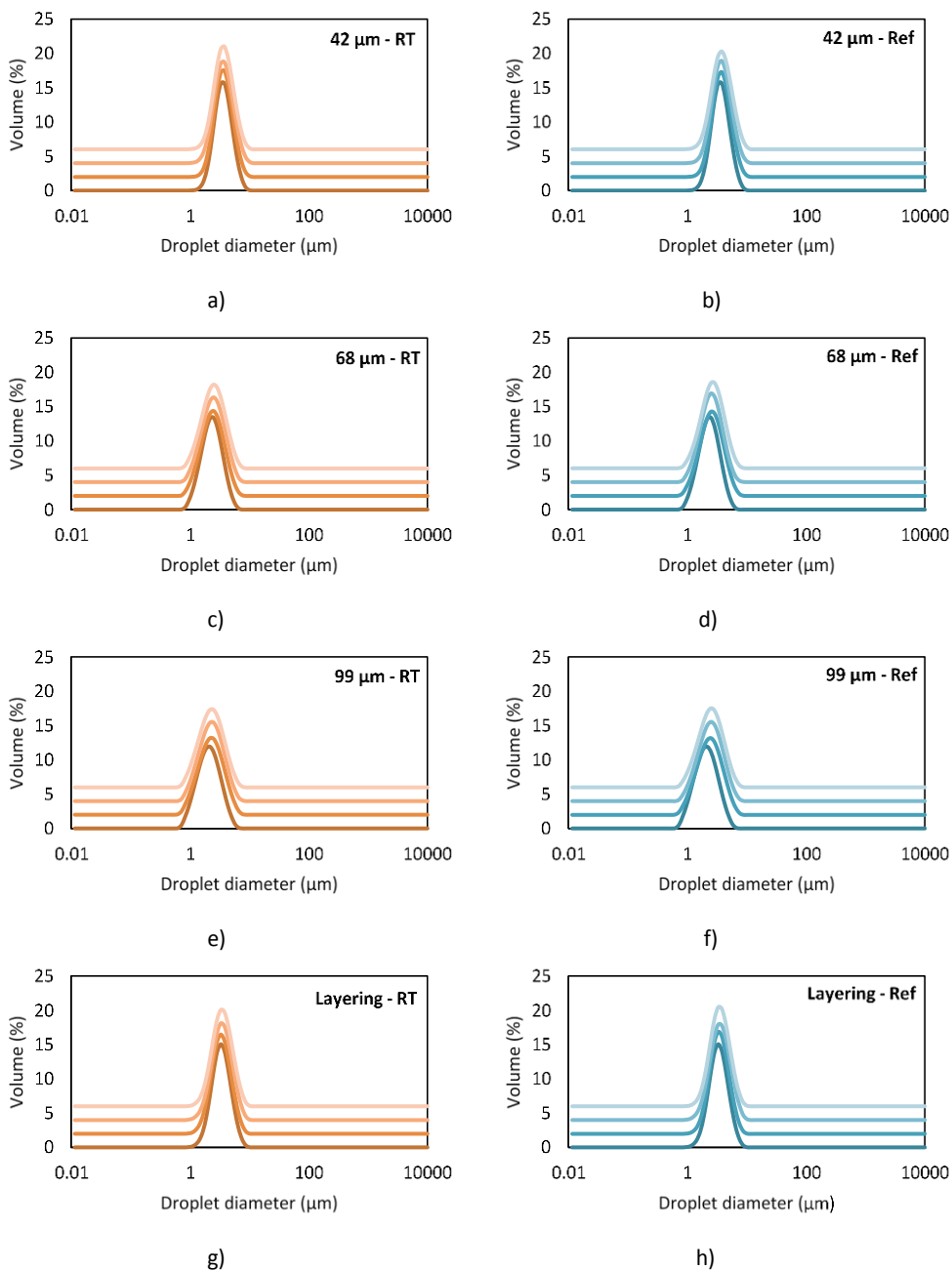


Figure 5.4. Droplet size distribution of 20% lemon oil emulsions, refined with 42, 68, 99 μm and layered micro-beads at constant bed height of 8.7mm, stored over a period of 7 days under refrigerated conditions (Ref) or at room temperature (RT). The color transparency scale indicates the number of days: from darkest to lightest refer to day 0 to 7.

The thickness of the dynamic membrane is also important for the emulsification process, since it is directly related with the resistance to the emulsion transport through the system. To study this parameter different amounts of the 99 μm micro-beads (0.5, 1, 2 and 4 g, average height reported in Table 5.1) were used to form the bed and refine a 20% LO emulsion, of coarse size 5.7 μm , at 450 kPa. As can be seen in Figure 5.2c, regardless of the thickness of the bed, the $d_{3,2}$ value kept decreasing after each emulsification cycle. However, the thicker the bed the bigger were the droplets obtained after five cycles. As mentioned previously regarding the relationship between the size of the micro-beads and the droplet size reduction, thicker beds present higher resistance thus lower breaking forces applied on droplets and, in turn, result in larger final droplets²².

As for the span value, there is no clear relationship between its variation and the thickness of the bed (Figure 5.2d), nevertheless the thinnest bed is the one giving the highest increase in the span value, and the thickest bed shows a reduction of this parameter after each emulsification cycle. With thicker beds, droplets reside in the system for a longer time thus having higher chance for the emulsifier to stabilize the droplet interface, and more uniform droplet sizes are obtained^{22,26,40}.

The stability of the four emulsions at two temperatures (Figure 5.3c and 5.3d) follows a similar trend as in the case of emulsions produced with different micro-bead sizes. The $d_{3,2}$ value remains almost constant for one week, while the span value increases after one day and remains almost constant the remaining time, except for the emulsion produced with the thinnest bed which continues to increase over the seven days period (Figure 5.5). This particular emulsion, by day 3, was destabilized faster at room temperature than at refrigerated conditions, but by day 7 the storage temperature didn't have an effect and a phase separation could be observed in both emulsions (Table 5.3).

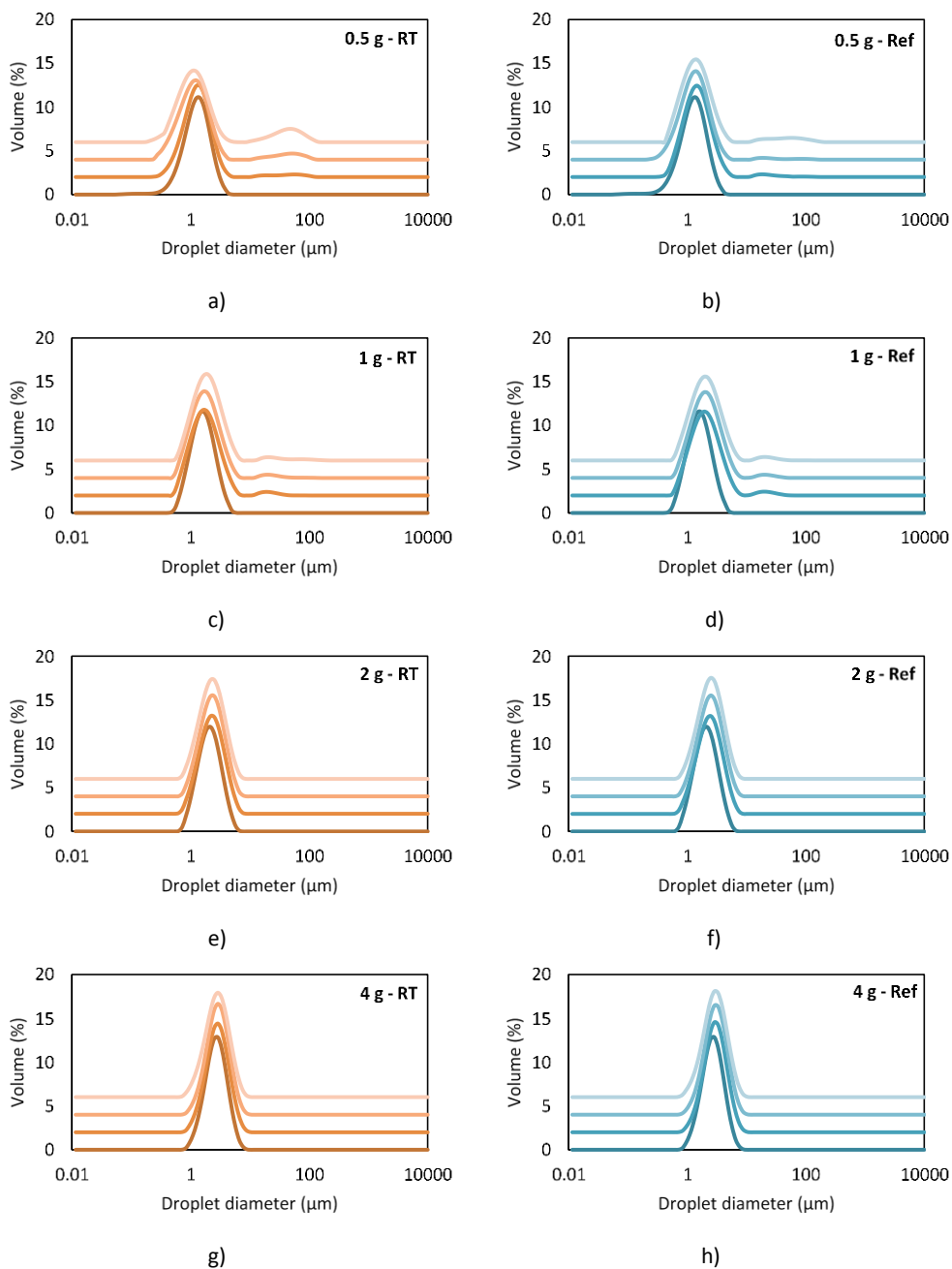
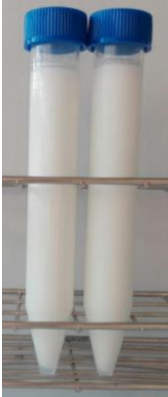


Figure 5.5. Droplet size distribution of 20% lemon oil emulsions, refined with 0.5, 1, 2 and 4 grams micro-beads beds, stored over a period of 7 days under refrigerated conditions (Ref) or at room temperature (RT). The color transparency scale indicates the number of days: from darkest to lightest refer to day 0 to 7.

Table 5.3. Stability of a 20% lemon oil emulsion prepared at two different bed heights.

	Day 0		Day 1		Day 3		Day 7	
Temperature (°C)	25	4	25	4	25	4	25	4
5.7 μm coarse 99 μm beads 0.5 g beads								
5.7 μm coarse 99 μm beads 4 g beads								

Neves, Wang, Kobayashi, & Nakajima (2017)¹³⁰ reported that emulsion viscosity at low temperature drops, reducing the mobility of oil droplets also reducing the exposure of these droplets to oxygen. This explains the more rapid phase separation occurring at room temperature.

It is also relevant to study the effect of the oil fraction and the emulsion coarse size in the performance of the DMTS system. For that reason, different coarse emulsions were prepared; two of them with 20% LO and coarse sizes of 5.7 and 24 μm , and another one with 40% LO and coarse size of 24 μm . These three emulsions were refined using a DMTS system with 2 g of micro-beads of 99 μm at 450 kPa,

showing that regardless of the oil fraction and the initial size of the emulsion, it was possible to reduce the droplet size by this technology (Figures 5.2e and 5.2f). This is important because, as discussed in section 4.2.1, using the nickel micro-sieve alone, with no silica micro-beads on top, for refining LO emulsions, causes considerable fouling problems. It was shown that a LO emulsion can pass through the nickel micro-sieve only if the oil fraction was 5% and the coarse size was 5.5 μm , and anything higher would foul the micro-sieve from the first emulsification cycle. Using a DMTS, however, made it possible to overcome all the pre-mentioned constraints. The results show that after the first emulsification cycle, the size of the coarse emulsion has been reduced by about 80% and 40% of its initial value for the emulsions with a coarse size of 24 and 5.7 μm , respectively. Nazir et al., (2013)⁴⁰ reports a size reduction of about 88% refining a 30 μm coarse hexadecane-in-water emulsion with 55 μm beads and at 500 kPa. This reduction is in the range of the value we report. Therefore, this kind of emulsification system enables to refine emulsions with big coarse sizes, which require lower mechanical energy input to be produced.

The other important feature of the DMTS system is that the droplet size reduction is obtained irrespective of the oil fraction (Figure 5.2e). As for the span value (Figure 5.2f), it seems that increasing the coarse size of the emulsion and/or the LO fraction, the span increases during the first emulsification cycle, when most of the droplet size reduction takes place, and as emulsification progresses, the span is reduced reaching a final value close to the one of the coarse emulsion. Being able to produce emulsions with high oil fraction is important especially when post-emulsification processes, like spray drying, are to be applied. Also, higher oil fractions in cases where active ingredients are encapsulated in the oil, allow higher encapsulation concentrations.

5.3.2. Effect of DMTS characteristics on emulsification throughput

As in all microporous systems, the transmembrane flux will depend on the size of the channels, the thickness, pressure applied and characteristics of the feed. In this study, the pressure applied was kept constant for all the experiments (450 kPa), while varying the d_v , thickness of the bed, oil fraction and coarse size of the emulsion. Transmembrane flux was measured for the experiments discussed in section 5.3.1 to understand the impact of the DMTS properties and emulsion characteristics on this important outcome of the process. First of all, the effect of the interstitial void diameter of the bed, which depends on the micro-bead size, was studied. As it can be seen in Figure 5.6a, a steady constant flux of about 200 $\text{m}^3 \cdot \text{m}^{-2} \cdot \text{h}^{-1}$ was obtained when the bed had the smallest d_v value. When the d_v increases (micro-beads of 68 and 99 μm) the transmembrane flux also increases,

but there is no difference between the values obtained for the two systems with wider channels.

As explained in section 5.3.1, different bed thicknesses were obtained using four different amounts of 99 μm micro-beads and the transmembrane fluxes were measured (Figure 5.6b). As expected, an increase in the thickness, higher resistance to the transport, results in a reduction of the flux. For the fifth cycle, the flux was about $1000 \text{ m}^3 \cdot \text{m}^{-2} \cdot \text{h}^{-1}$ for the thinnest DMTS system (0.5 g / 2.18 mm), while it was about $300 \text{ m}^3 \cdot \text{m}^{-2} \cdot \text{h}^{-1}$ for the thickest (4 g / 17.4 mm).

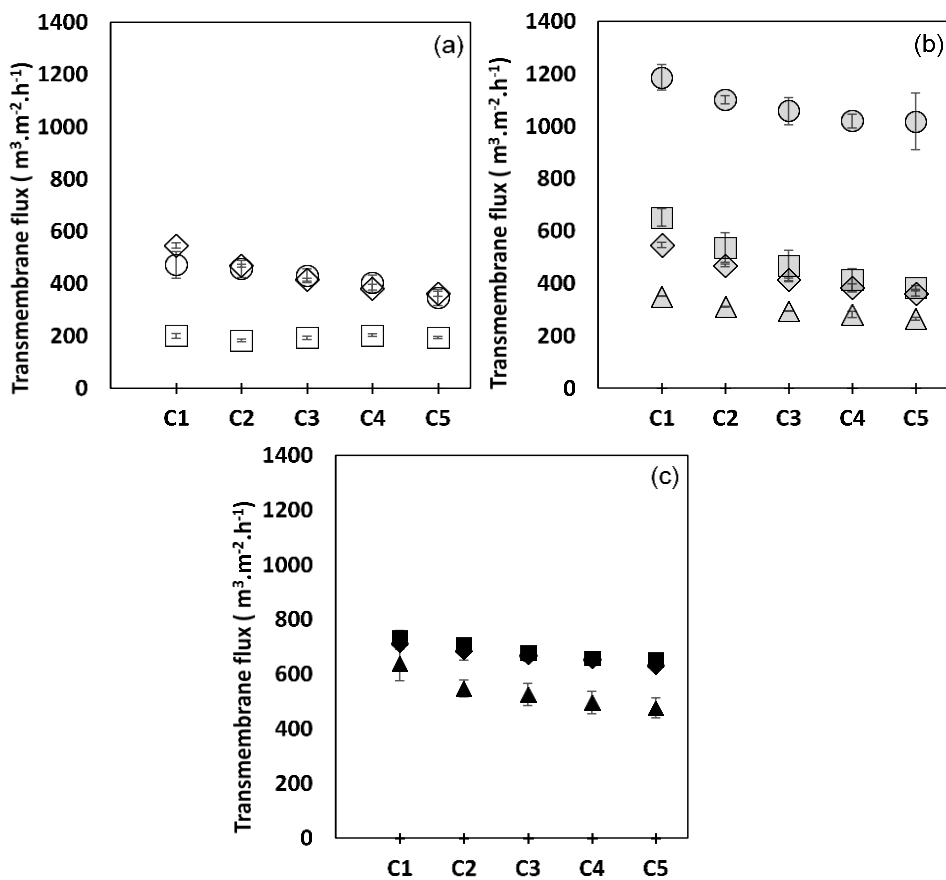


Figure 5.6. Effects on transmembrane flux of a) micro-beads size (\square : 42 μm , \circ : 68 μm , \diamond : 99 μm), b) bed height (\circ : 0.5 g, \square : 1 g, \diamond : 2 g, \triangle : 4g) and c) oil fraction and coarse emulsion droplet size (\blacklozenge : 99 μm –5.7 μm –20% LO, \blacksquare : 99 μm –24 μm –20% LO, \blacktriangle : 99 μm –24 μm –40% LO). The legend in (c) forms three parts: the micro-beads size used (99 μm), the size of the coarse emulsion (5.7 or 24 μm) and finally the lemon oil (LO) fraction (20 or 40%).

From Figures 5.6a and 5.6b it is clear that the thicker bed and the smaller the glass micro-beads size, the more resistance to emulsion flow, thus lower fluxes were obtained²². Figure 5.6b also shows another distinctive trend, that is transmembrane fluxes for 1, 2 and 4 g are more similar than the one for 0.5 g of micro-beads, which cannot be explained solely by the thickness of the bed. The resistance of the nickel micro-sieve has to be considered to fully explain the flux values. As can be seen in Table 5.1, the porosity of the nickel micro-sieve support ranges from 1.31 to 2.39%, which clearly has an impact on the emulsification productivity. It has to be pointed out that the variability in the porosity values of the nickel micro-sieves is related to the manufacturing process and cannot be avoided.

The effect of the nickel micro-sieve porosity was analyzed in-depth by conducting more experiments. Three micro-sieves were chosen with porosities of 1.3, 2.3 and 2.8%. A layer of silica micro-beads (99 μm , 2 g) was placed above the micro-sieve and the coarse emulsion (5.7 μm) was refined at 450 kPa for five consecutive cycles. It is clear from Figure 5.7a that the porosity of the micro-sieve influences the transmembrane flux; however, looking at droplet size and span values, no significant differences are seen (Figures 5.7b and 5.7c). This indicates that droplet break-up is occurring in the micro-beads bed only, and the nickel micro-sieve is adding resistance to the flow while acting as a support for the micro-beads. Thus, by choosing a sieve with a large pore size but still small enough to impede the passing of the micro-beads, the flux can be further optimized resulting in a larger emulsification throughput. It should be noted that the fluxes reported in this study and in literature (in emulsification processes with similar setups to the one used in this study) are comparable only if the porosities of the micro-sieves used are known.

To study the influence of the oil fraction and the size of the coarse emulsion on productivity, a DMTS system with 2 g of 99 μm micro-beads supported by a micro-sieve of 2.33% porosity was used to refine emulsions with 20 and 40% oil fraction and 5.7 and 24 μm coarse size. Increasing the oil fraction (from 20 to 40%, maintaining the size of the coarse emulsion at 24 μm), the fluxes dropped (from 653 $\text{m}^3\cdot\text{m}^{-2}\cdot\text{h}^{-1}$ to 476 $\text{m}^3\cdot\text{m}^{-2}\cdot\text{h}^{-1}$, Figure 5.6c) as expected, most probably due to the increase in emulsion viscosity. The increase in the coarse size of the emulsion has no significant effect on the flux value when the oil fraction is kept constant. Ladjal Ettoumi *et al.* (2017)⁴² reported an average flux of 100 $\text{m}^3\cdot\text{m}^{-2}\cdot\text{h}^{-1}$ for the refining of 20% sunflower oil-in-water emulsions at 300 kPa using a DMTS system. This value compared to the one we report is expected because of the differences in pressure, emulsions viscosity, micro-beads size, and micro-sieve porosity.

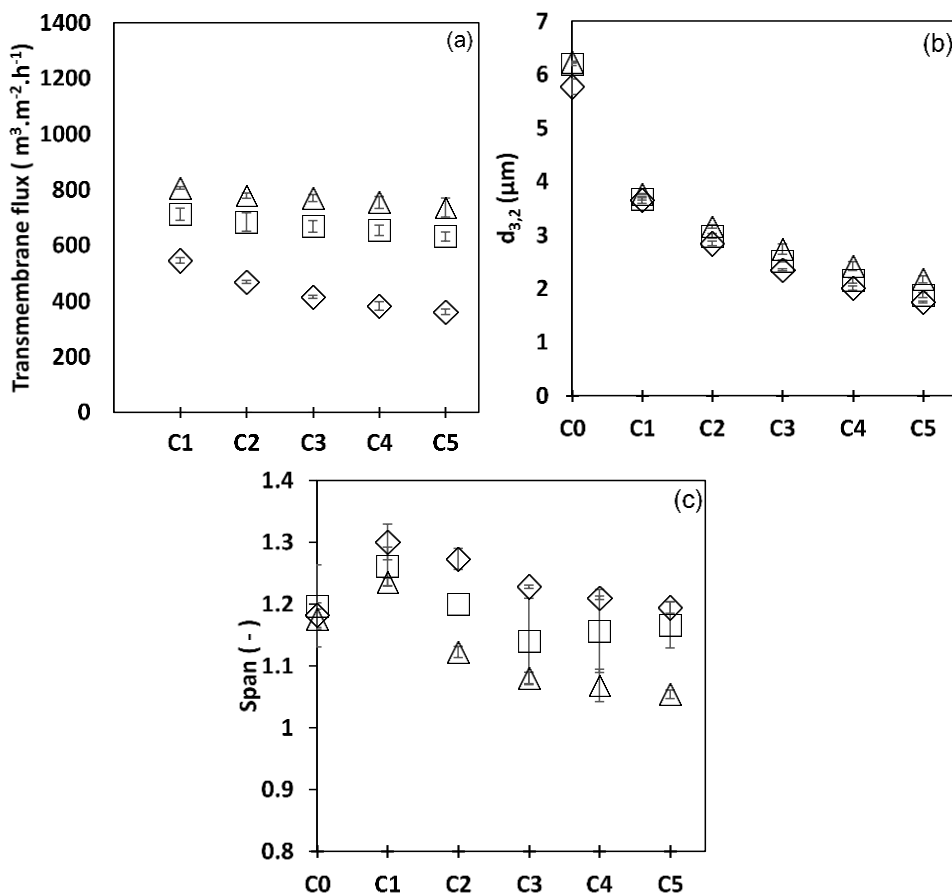


Figure 5.7. Effect of micro-sieve porosity on emulsion a) transmembrane flux, b) droplet size and c) span. Markers: ◇: 1.3%, □: 2.3%, Δ: 2.8%.

Comparing flux values obtained with the DMTS system with those obtained from only micro-sieve emulsification (no micro-beads), the main difference observed is due to the resistance that the glass micro-beads bed present. In section 4.3.3, and at the same pressure of 450 kPa, a flux of $\approx 990 \text{ m}^3 \cdot \text{m}^{-2} \cdot \text{h}^{-1}$ for refining 5% lemon oil-in-water emulsions with a nickel micro-sieve was obtained, but as previously demonstrated, DMTS fluxes typically range between 200-600 $\text{m}^3 \cdot \text{m}^{-2} \cdot \text{h}^{-1}$. Santos et al. (2015)⁸ have also produced LO emulsions with nickel micro-sieves however using a stirred cell but only attaining transmembrane fluxes of 2 $\text{m}^3 \cdot \text{m}^{-2} \cdot \text{h}^{-1}$. As for traditional premix membrane emulsification methods, like emulsification through a Shirasu porous-glass (SPG) membrane, the fluxes in the literature vary according to the effective area of the membrane. Since effective areas of SPG membranes can be as small as 3.2 cm^2 and as big as 30.7 cm^2 ³³, fluxes reported could be as large as 240 $\text{m}^3 \cdot \text{m}^{-2} \cdot \text{h}^{-1}$ and as small as 0.03 $\text{m}^3 \cdot \text{m}^{-2} \cdot \text{h}^{-1}$. These values lie on the low

range of the fluxes obtained with the DMTS system, mainly due to the SPG membrane's larger effective area.

In addition, it was shown in section 4.2.2 that using the same nickel micro-sieve (alone with no micro-beads) more than two times to produce an emulsion does not guarantee reproducibility. Using a DMTS however, and because of the lower flux values (shear) in the pores, it was possible to overcome all the pre-mentioned constraints. The nickel micro-sieve utilized to support the glass micro-beads could be used for more than 15 times without any damage to the pores while producing emulsions of a narrow droplet size distribution, high oil fractions and high throughput.

5.3.3. Effect of tuning the system porosity on the emulsion characteristics and productivity: layered DMTS

Results obtained so far prove that by tuning the DMTS system characteristics it is possible to overcome the limitations of other high-throughput membrane emulsification systems mentioned previously. Based on results from section 5.3.1, it was hypothesized that a bed of two superimposed layers of 99 and 42 μm micro-bead, could serve as a better dynamic membrane than the single, mono-sized, bed layer, helping in the reduction of the droplet size as well as the span value. The combination of layers of micro-beads of different size will be referred to as "layering" (L) from this point on in the paper.

To test the hypothesis about improving the performance characteristics of the system by layering, a DMTS system was formed with a micro-sieve of 2.33% porosity, supporting a layered bed. This layered DMTS system was used to refine two 20% LO emulsions, one with a coarse size of 5.7 μm and the other of 25 μm , and also another emulsion with 40% oil fraction of 24 μm coarse size, at 450 kPa.

The droplet size reduction, regardless of the oil fraction and the size of the coarse emulsion, was in the range of the one attained using a system of the same thickness with uniform channel size (Figure 5.8b).

Nevertheless, Figure 5.8b also shows that droplet size reduction is more efficient when starting with larger droplets, attaining 88% reduction of the droplet size after 3 cycles, compared to 56% with the smallest coarse emulsion. Another important feature of the DMTS system with layering is that for the three different emulsions produced, the span value was close to 1 after three emulsification cycles, and even below this value (0.96) for the emulsion with 20% LO and coarse size of 5.7 μm (Figure 5.8a), this value being in the range of the one obtained for the DMTS system with 2 g of 42 μm micro-beads (Figure 5.2b).

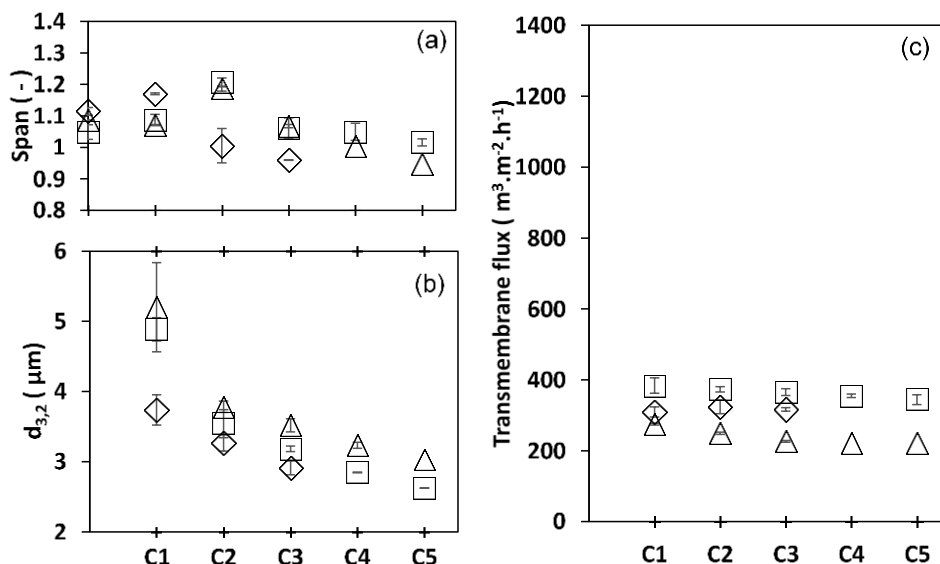


Figure 5.8. Effect of increasing coarse size and oil fraction on a) droplets span, b) droplets size and c) emulsification fluxes. The legend forms three parts: the micro-beads size used (layering: L), the size of the coarse emulsion (5.7 or 24 μm) and finally the lemon oil (LO) fraction (20 or 40%). Markers: \diamond : L-5.7 μm -20% LO, \square : L-24 μm -20% LO, Δ : L-24 μm -40% LO.

The span value is very important in emulsion production because, with monodispersed emulsions, stability is enhanced and post-processing steps (e.g. spray drying) become easier to carry out.

Regarding productivity of the DMTS system with layering, Figure 5.8c presents the flux values, which are intermediate values compared to the ones obtained for a monolayer of 99 or 42 μm micro-beads shown in Figure 5.6a. These results agree with the fact that the composition of the DMTS system has an upper layer with bigger channels (lower resistance) and a bottom layer with smaller channels (higher resistance). Consequently, using a layered DMTS, high-throughput was obtained and the number of emulsification cycles can be reduced to three, while still obtaining a final emulsion of about 3 μm of droplet size and achieving a final emulsion with narrow size distribution. Therefore, reducing the energy inputted into producing the coarse emulsions and saving energy with the emulsification cycles number will decrease the overall energy requirement of the process.

5.4. Conclusion

Stable LO emulsions, with oil fractions up to 40% and coarse size of 24 μm , were refined using DMTS systems. The final emulsion size ($d_{3,2}$) was in the range of 2-3 μm with span values that in most cases were below 1.2, and even below 1 for the

layered DMTS system. Emulsions' droplet size distribution remained stable at both room temperature and under refrigeration. The productivity with the DMTS was clearly much higher than the ones reported for other low energy emulsification techniques, and this was observed even when the oil fraction was up to 40%. Therefore, DMTS helps overcome limitations encountered with other low energy emulsification systems.

The performance of the DMTS systems was clearly influenced by the amount and size of the micro-beads. Increasing the micro-beads size resulted in an increase droplet size reduction but an increase in span. However, increasing the DMTS bed height resulted in a decrease in droplet size reduction and span. Layered DMTS has allowed a cut back (down to three) on the number of emulsification cycles required to obtain emulsions with small oil droplet sizes and narrow size distribution. Emulsions refined with the layered DMTS had comparable droplet size as the conventional monolayered DMTS but better span values (≤ 1). The DMTS in general, and the layered DMTS in particular, have the potential of replacing other low energy emulsification systems for further industrial production of food emulsions. It is a very robust system, that can be easily assembled, cleaned and tuned to produce stable emulsions with high throughput.

After optimizing the DMTS system specifically for the encapsulation of lemon oil, and as discussed in chapter 3, a better emulsifier is needed to stabilize the emulsions produced. The next chapter, will use the same DMTS system to produce lemon oil-in-water emulsions stabilized with conventional proteins as well as the WP-CMC complex.

6. Production of lemon oil emulsions stabilized by biopolymers with dynamic membranes of tunable pore size

This chapter has been submitted as:

W. Kaade, M. Ferrando, A. Ballon, S. De Lamo-Castellví, and C. Güell, *“Production of lemon oil emulsions stabilized by biopolymers with dynamic membranes of tunable pore size”, J. of Food Engineering.*

UNIVERSITAT ROVIRA I VIRGILI

LOW-ENERGY HIGH-THROUGHPUT MICROPOROUS EMULSIFICATION FOR LEMON OIL ENCAPSULATION

Wael Kaade

6.1. Introduction

Emulsions are encountered everywhere in our daily lives and especially in our food. From dressings to dairy products, margarines and spreads, emulsions can be found in different forms. More recently, emulsions have been used for encapsulation of flavors, antioxidants and other active ingredients. However, what is necessary for food emulsions in general is for them to remain stable, that is to maintain their physicochemical properties over time. One of the main features essential to lengthen emulsion stability is the presence of small and monodispersed droplets. To achieve this aim, energy intensive techniques like rotor stator systems, high-pressure homogenizers or colloid mills have been used traditionally^{49,69}. These methods, however, are not the best suited to produce emulsions encapsulating heat and shear sensitive ingredients, such as food aromas and proteins, respectively. The main drawbacks associated with these technologies are the difficulty to control droplet size, and more importantly that most of the inputted energy is dissipated in the form of heat⁵. Hence membrane emulsification (ME) has served as low shear replacement for the production of food emulsions in particular^{29,131}. With ME devices, the production of monodispersed emulsions at low shear conditions and minimum increase of working temperatures is possible¹².

One particular system of ME reported by Van Der Zwan *et al.* (2008)²⁶ is referred to as a dynamic membrane. It consists of a porous bed/layer of silica glass micro-beads supported by a porous nickel micro-sieve. This system is reported to yield high throughput ($\approx 1000 \text{ m}^3\text{m}^{-2}\text{h}^{-1}$), produce monodispersed emulsions and be easy to clean and re-use⁴⁰. A limited number of studies used this system for the production of food grade emulsions. Sunflower oil-in-water emulsions^{42,44}, $W_1/O/W_2$ double⁴⁵ emulsions and food foams⁴⁶ were reported in the literature to be produced with dynamic membranes. In chapter 5, dynamic membranes of tunable pore size (DMTS) have been used to produce food grade O/W emulsions encapsulating lemon oil (up to 40%wt), stabilized by small molecular weight surfactant polyoxyethylene sorbitan monolaurate (Tween 20). The DMTS system has been shown effective in the ease of tuning the emulsions' droplet sizes by controlling the micro-beads size and bed height. Besides, due to the particular nature of Tween 20, there was no noticeable fouling during the emulsification process.

Lemon oil is an essential oil that is currently being used mainly for flavoring purposes but it also has antimicrobial, antifungal and antioxidant properties, making its encapsulation of high interest^{132,133}. Encapsulating lemon oil allows its protection from oxidation and the production of off-flavors. The effective encapsulation of lemon oil, that often requires a final spray-drying step, can benefit from the use of biopolymers such as milk proteins or protein-polysaccharide

complexes, that will enhance the protection of the active ingredients during processing.

Traditional food grade emulsifiers are dairy proteins like whey protein (WP) and sodium caseinate (NaCaS). Proteins are considered as good emulsifiers because they contain hydrophobic parts that adsorb onto the oil phase while their hydrophilic part remains in the aqueous phase forming a bulky barrier at the interface⁸². However, due to their complicated structures and the interactions they have between each other, the way they adsorb to the interface changes resulting in a less coherent protein layer structure⁸³. Therefore other studies have reported using mixtures of proteins and polysaccharide that forms a bulkier complex⁸⁴⁻⁸⁶. One kind of complexation is electrostatic where the oppositely charged biopolymers interact. For example, Berendsen *et al.* (2014) have successfully produced a water soluble 0.5%wt whey protein – 0.25%wt carboxymethyl cellulose complex (WP-CMC) at a pH of 3.8. Below its isoelectric point, WP is positively charged and the polysaccharide (CMC) is negatively charged. Upon mixing, an over-all negatively charged complex is formed. In addition to having a thicker layer protecting the oil droplets and preventing their coalescence in O/W emulsions, CMC increases the viscosity of the continuous phase making it more difficult for droplets to move and retarding creaming. Another advantage of WP-CMC electrostatic complex is the possibility, in the presence of CMC, to reduce the concentration WP needed to stabilize an emulsion. Moreover, it has been reported that the WP-CMC complex increases the stability of emulsions^{84,87} and for these reasons this complex will be tested in this study.

The downside of using proteins or protein-polysaccharide complexes to stabilize emulsions by membrane systems is the interaction of these biopolymers with the membrane material that causes fouling. As a result, fluxes during emulsification can be reduced and the performance of the system to break-up the droplets can also be affected.

This chapter shows the first attempt to assess the effect of a protein-polysaccharide emulsifying complex, as compared to standard dairy proteins, on the properties and stability of lemon oil emulsions obtained with a DMTS system. A scaling relation to model the effect of the DMTS system characteristics on droplet break-up is developed. Finally, a modified DMTS system consisting of superimposed layers of different porosity was evaluated to reduce the energy input while maintaining the flux and the emulsion characteristics.

6.2. Materials and methods

For the production of the simple oil-in-water emulsions, distilled water was used, and the lemon oil was purchased from Dallant, Spain. The emulsifiers used were whey protein, WP, (Davisco Foods International, USA), sodium caseinate, NaCas, (Sigma-Aldrich Quimica SL, Spain) and a protein-polysaccharide electrostatic

complex: whey protein-carboxymethyl cellulose (CMC). The CMC was purchased from Sigma-Aldrich Quimica SL, Spain (CAS: 900-32-4). As for the DMTS, the nickel micro-sieves were donated by Stork Veco (Eerbeek, The Netherlands) and the micro-beads were purchased from Unicorn Industrial Cleaning Solutions (The Netherlands) (micro-beads size: 99 μm) and Microspheres-nanospheres (USA) (micro-beads sizes: 42 and 68 μm). Sodium hydroxide and 1M hydrochloric acid (HCl) were purchased from Fisher Scientific (UK) and acetic acid 96% was purchased from PanReac (Spain).

6.2.1. Continuous phase preparation

The continuous phases containing the proteins were prepared one day before using them for emulsification and stored overnight in the refrigerator (4 °C). The three emulsifiers used in this study were 1%wt. WP, 1%wt. NaCaS and 0.5%wt. WP - 0.25%wt. CMC electrostatic complex. Solutions (200 ml) of 2%wt. WP and NaCaS were prepared and diluted on the day of the experiment to 1%wt. As for the WP-CMC complex, 2%wt. WP and CMC solutions were prepared the day before, and the day of the experiment 200 ml of the complex were prepared by mixing the following: 22.5g of 2%wt. CMC, 22.5g of distilled water, 90g of 20mM acetic acid buffer and finally 45g of 2%wt. WP. At this point the pH of the complex was adjusted to 3.8 with 1M HCl. Berendsen *et al.* (2014)⁸⁷ have shown that this protein-polysaccharide 2:1 ratio is soluble at pH 3.8 and that the complex is negatively charged.

6.2.2. Interfacial tension measurement

The dynamic interfacial tension between the continuous phases, containing the proteins, and lemon oil was measured using an automated drop tensiometer (ADT, Teclis ITconcept, France). The method consists of a continuous phase drop (5-7 μl) suspended at the edge of a syringe inside a cuvette filled with lemon oil at 30 °C. All the protein solutions were diluted to a 0.1%wt. protein. Surface tension was calculated by the bubble shape analysis. Also, a measurement of lemon oil-distilled water interface was measured for reference.

6.2.3. Emulsification

To produce the 20% lemon oil-in-water emulsions, the same procedure reported in section 5.2.3 was followed. In short, the continuous phase (80%wt), containing one of the three emulsifiers, and lemon oil (20%wt) were mixed to form 120-200 g emulsions. These emulsions were first homogenized by a high shear mixer (IKA® T-18 basic Ultra-turrax) to produce a coarse emulsion (a.k.a. premix). The average oil droplet size ($d_{3,2}$) and span, measured as explained in section 6.2.4, of the three coarse emulsions prepared varied depending on the kind of emulsifier used and the values were: $13.08 \pm 0.76 \mu\text{m}$ and 0.97 ± 0.03 respectively for WP, 17.19 ± 0.45

μm and 0.93 ± 0.03 respectively for NaCaS and $19.95 \pm 0.96 \mu\text{m}$ and 0.93 ± 0.02 respectively for WP-CMC.

This premix was then passed, five consecutive times (cycles), under a constant pressure of 450 kPa, through a DMTS system to refine the emulsion that was then collected in an Erlenmeyer flask placed on a balance. Consequently, mass versus time information was collected. This information is used to calculate mass flow rate, φ . Then, transmembrane flux, J , can be calculated using Equation 6.1.

$$J = \frac{\varphi}{\rho_e A_{\text{column}}} \quad (6.1)$$

A_{column} is the area of the emulsification column (177 mm^2), ρ_e is the emulsion density (972 kg/m^3) and it is calculated using Equation 6.2. θ_d is the dispersed phase volume fraction and the continuous ($\rho_c = 1003 \text{ kg/m}^3$) and oil phase ($\rho_o = 846.2 \text{ kg/m}^3$) densities were measured using hydrometers.

$$\rho_e = \theta_d \rho_d + (1 - \theta_d) \rho_c \quad (6.2)$$

After each emulsification cycle, a sample was collected for particle size distribution measurements.

The DMTS system used in this chapter is the same shown in Figure 5.1, where a layer of silica glass micro-beads lay on top a nickel micro-sieve. In this study three micro-beads sizes were tested: 99, 68 and $42 \mu\text{m}$. Also, by controlling the mass of the micro-beads placed on top of the nickel micro-sieve, it is possible to control the height of the micro-beads layer. In that sense, by adding 0.5, 1, 2 and 4 g of micro-beads, bed heights of 2.18, 4.35, 8.7 and 17.4 mm were obtained and tested. The bed height can be calculated using Equation 6.3 ²⁶.

$$H = \frac{\text{mass of beads}}{\rho_p A_{\text{column}} (1 - \epsilon)} \quad (6.3)$$

The porosity of the bed, ϵ , is calculated as such:

$$\epsilon = 1 - \frac{\rho_b}{\rho_p} \quad (6.4)$$

Here ρ_b and ρ_p are the micro-beads bulk and particle density. All the values of these parameters are reported in Table 5.2. The tortuosity of a bed of spherical particles is calculated using Equation 6.5.

$$\tau = 1 + 0.41 \ln \left(\frac{1}{\epsilon} \right) \quad (6.5)$$

The pores in the microstructured system are assumed to have a diameter equivalent to the interstitial void diameter of the bed, d_v , defined by Equation 6.6⁴⁰. A_v is a ratio of a particle's surface area to its volume and it is given by: $A_v = 6/d_p$ where d_p is the bead diameter.

$$d_v = \frac{4 \epsilon}{A_v (1-\epsilon)} \quad (6.6)$$

A summary of all the experimental conditions used for refining coarse emulsions is reported in Table 6.1. In the first column of this table, experimental conditions reported in chapter 5 were also added for future references and comparisons.

An extra set of emulsions was also produced using a modified structure to the standard DMTS system. In this system, and instead of having only one layer of micro-beads on top of the micro-sieve, two superimposed layers of two different sizes are used. In this study, the modified DMTS comprised of, from bottom to top, of the nickel micro-sieve followed by 1g of 42 μm sized micro-beads followed by 1g of 99 μm sized micro-beads. The exact method of preparation is reported in section 5.2.1.

6.2.4. Particle size distribution measurement

Samples collected from the coarse emulsions and after each emulsification cycle (1 mL) were diluted with distilled water to a 1:10 ratio and used for particle size distribution analysis. These measurements were done laser diffraction (using a Malvern Mastersizer 2000). Three independent measurements were done for each sample and the equipment made three readings for each measurement, resulting in nine readings for each sample. An average was calculated, from which the Sauter mean diameter ($d_{3,2}$) and span were reported in this paper.

6.2.5. Stability

From each emulsion, after the fifth and last emulsification cycle, an equal volume of 14mL was placed in 6 plastic tubes to be used for stability measurements. All the tubes were wrapped with aluminum foil to prevent light oxidation and three were stored at room temperature (25 °C) and the other three were refrigerated (4 °C). Stability of the emulsions was studied over a period of 7 days, collecting samples on days 1, 3 and 7 after emulsification. In that sense, on the measurement day, one tube stored at room temperature and one that was refrigerated were collected, compared for differences in color, and then opened and used for particle size distribution measurements (as described in section 6.2.4).

Table 6.1. Experimental conditions (micro-beads mass, micro-beads size, coarse emulsion size) used to refine 20% lemon oil emulsions at 450 kPa. Also, the porosities of the sieves holding the silica beads are reported.

Tween20*	WP	NaCaS	WP-CMC
2g – 42 μm – 5.7 μm (Sieve porosity 2.39%)	2g – 42 μm – 13 μm (Sieve porosity 2.39%)	2g – 42 μm – 17 μm (Sieve porosity 2.39%)	Not possible
2g – 68 μm – 5.7 μm (Sieve porosity 2.39%)	2g – 68 μm – 13 μm (Sieve porosity 2.39%)	2g – 68 μm – 17 μm (Sieve porosity 2.39%)	2g – 68 μm – 20 μm (Sieve porosity 2.33%)
2g – 99 μm – 5.7 μm (Sieve porosity 1.31%)	2g – 99 μm – 13 μm (Sieve porosity 1.31%)	2g – 99 μm – 17 μm (Sieve porosity 1.31%)	2g – 99 μm – 20 μm (Sieve porosity 2.33%)
0.5g – 99 μm – 5.7 μm (Sieve porosity 2.39%)	0.5g – 99 μm – 13 μm (Sieve porosity 2.33%)	0.5g – 99 μm – 17 μm (Sieve porosity 2.39%)	0.5g – 99 μm – 20 μm (Sieve porosity 2.33%)
1 g – 99 μm – 5.7 μm (Sieve porosity 1.31%)	1g – 99 μm – 13 μm (Sieve porosity 1.31%)	1g – 99 μm – 17 μm (Sieve porosity 1.23%)	1g – 99 μm – 20 μm (Sieve porosity 2.33%)
4g – 99 μm – 5.7 μm (Sieve porosity 1.31%)	4g – 99 μm – 13 μm (Sieve porosity 1.31%)	4g – 99 μm – 17 μm (Sieve porosity 1.23%)	4g – 99 μm – 20 μm (Sieve porosity 2.33%)
2g – 99 μm – 5.7 μm (Sieve porosity 2.33%)			
2g – 99 μm – 5.7 μm (Sieve porosity 2.82%)			
2g – 99 μm – 24 μm (Sieve porosity 2.33%)			

* The experimental conditions in the first column are obtained from chapter 5.

6.3. Results and discussion

6.3.1. Effect of the DMTS system characteristics on the droplet size distribution of lemon oil emulsions stabilized with biopolymers

Lemon oil emulsions stabilized with Tween20 have been successfully produced using the DMTS system in chapter 5. To produce emulsions stabilized with WP, NaCaS and WP-CMC, pressure was maintained at 450 kPa and bed height and interstitial void diameter were changed. Figure 6.1 shows $d_{3,2}$ and span evolution during emulsification using these emulsifiers for (i) four different heights (2.18, 4.35, 8.70 and 17.40 mm) using micro-beads of 99 μm (interstitial void diameter = 57.97 μm) and (ii) for three different micro-beads sizes maintaining the bed height at 8.55 ± 0.8 mm. As previously seen for emulsions with Tween20, there is a reduction of $d_{3,2}$ during emulsification regardless of the emulsifier, bed height and bead size, with the highest size reduction occurring in the first cycle. Moreover, the droplet size of the coarse emulsion varies depending on the emulsifier, where emulsions stabilized with WP showed the smallest size (13.08 μm) and the WP-CMC complex gave the largest droplets (19.95 μm). This is most probably because looking at the proteins aggregates sizes, the following trend is reported: WP <

$\text{NaCaS} < \text{WP-CMC}$ ^{42,134}, so smaller sized molecules can stabilize newly formed droplets and pack more tightly at the interface ⁸⁷. In addition, from the dynamic interfacial tension profile (Figure 6.2), and especially in the first few seconds, WP seems to lower the interfacial tension quicker than the other proteins allowing the formation of smaller oil droplets. WP-CMC took a longer time to reach equilibrium because of the larger size of the complex molecule migrating to the oil-water interface.

It is noteworthy to mention that interfacial tension between lemon oil and water is lower than expected but that is due to the presence of emulsifying compounds in lemon oil like acetyl groups and methylesters ¹³⁵. Also, Rao and McClements, (2012b) reported a lemon oil-water equilibrium interfacial tension of $8.3 \text{ mN}\cdot\text{m}^{-1}$ due the high presence of surface-active compounds.

For the effect of the bed height, the highest size reduction always corresponds to the thinnest bed, and it is about 60% for the first cycle, regardless of the emulsifier. The increase in the thickness of the bed results in a lower size reduction, about 28-33%, again for the first cycle regardless of the emulsifier. Figure 6.1 shows the span values and here it should be noted that all the emulsions produced were monomodal by the 5th emulsification cycle. However, WP and NaCas stabilized emulsions show an increase in the span from the coarse emulsion to the one after the first emulsification cycle, followed by a slight decrease in the following emulsification cycles. Yet, for the emulsions stabilized with WP-CMC electrostatic complex, the span increases after each emulsification cycle, regardless of the thickness of the bed. So far, the results prove that the DMTS system is a powerful tool for producing emulsions with span values between 0.8 and 1.3, which is an important factor in terms of emulsion stability.

The size of the microbeads and the porosity of the bed determine the interstitial void diameter (Equation 6.6) which is related with the size of the open interconnected channels in the system. The microbead sizes used were 99, 68 and 42 μm , which correspond to d_v values of 57.97, 38.79 and 28.33 μm , respectively. It is important to note that the size of the coarse emulsions was always smaller than the interstitial void diameter, and even in this scenario significant droplet break-up occurs (Figure 6.1), which is indicative of the efficacy of the emulsification system. However, when the emulsions were stabilized with the WP-CMC complex, emulsion refinement was not possible when the microbead size was 42 μm . In this particular case, the pressure applied was not enough to overcome the resistance of the bed and the higher viscosity of the continuous phase.

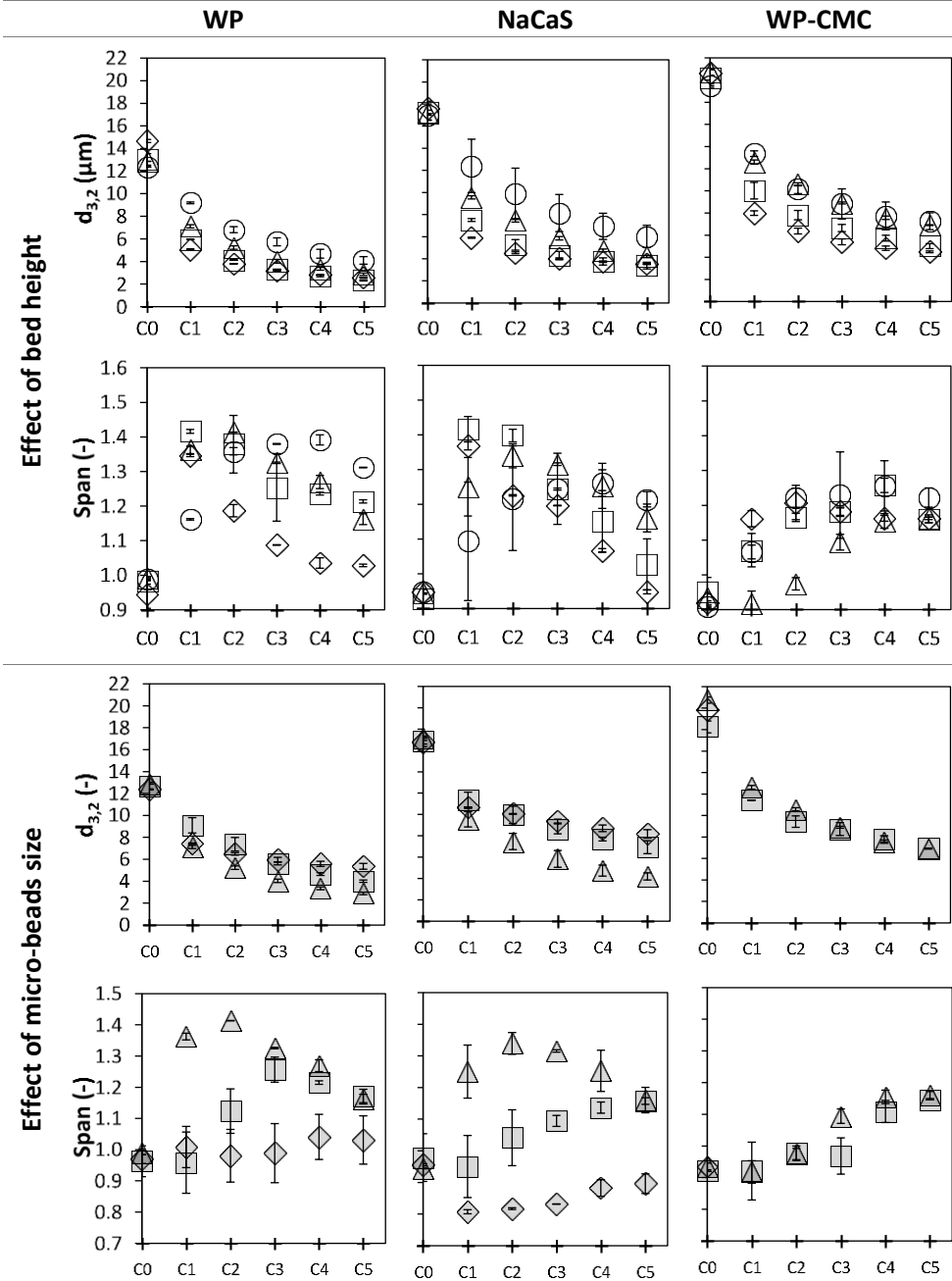


Figure 6.1. Effect of emulsifier type, micro-beads size, bed height and emulsification cycles on Sauter mean diameter and span. Markers: \circ : 2.18 mm, \triangle : 4.35 mm, \square : 8.70 mm, \diamond : 17.4 mm, ∇ : 42 μm , \square : 68 μm , \triangle : 98 μm

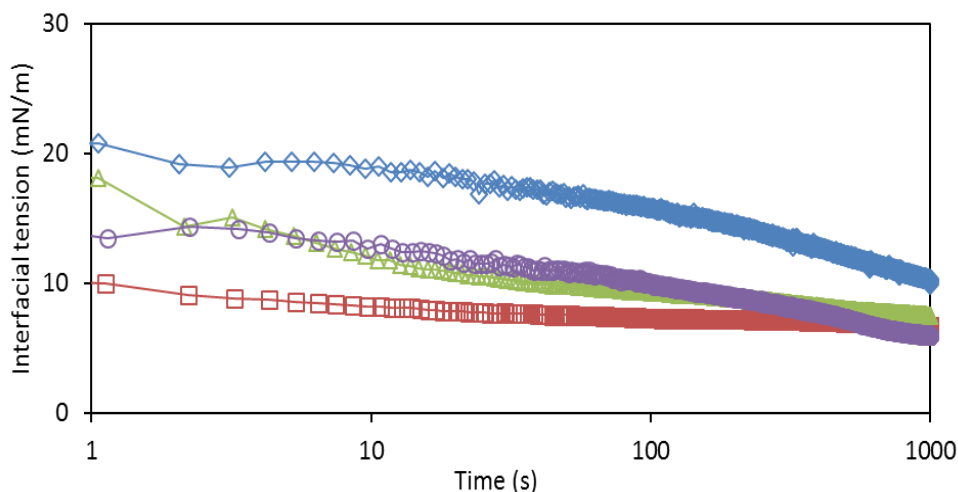


Figure 6.2. Dynamic interfacial tension profile of lemon oil with (\diamond) water, (\square) WP, (\triangle) NaCaS and (\circ) WP-CMC.

To better understand the effects of micro-beads size and bed height on droplet break-up, and homogenizing the results with respect to the coarse emulsions droplet size, $d_{3,2}/d_{coarse}$ and span values of the 5th emulsification cycle were plotted versus bed height and d_v (Figure 6.3). It is clear from Figures 6.3a and 6.3c that the thicker the bed and smaller the micro-beads size the less droplet break-up happens. However, it should be highlighted that with the thinnest bed, an 80% size reduction of the coarse emulsions was achieved, for the three emulsifiers.

When the DMTS system is composed of a thick bed and/or small micro-beads, transmembrane flux drops because of the higher resistance which also decreases the shear inside the bed pores responsible for deforming and breaking oil droplets^{22,40}. Regarding span values, Figure 6.3b shows that thicker beds gave higher span values probably because they allow droplets to reside in the bed for longer periods allowing them to coalesce⁹. Figure 6.3d indicates that large micro-beads sizes, which give the smallest droplets (Figure 6.3c), are less efficient in producing emulsions with a narrow droplet size distribution, that is, having higher span values.

Comparing the droplet size distribution of the emulsions obtained in this study to the literature is difficult since there are no results showing stabilization of lemon oil emulsions with proteins or protein-polysaccharide complexes. Berendsen *et al.* (2014)⁸⁷ produced sunflower O/W emulsions with a premix membrane emulsification technique (SPG membrane) stabilized with 1%wt WP and 0.5%wt WP - 0.25%wt CMC and obtained smaller droplets after four emulsification cycles (reported $d_{4,3}$ about 10 μm) but higher span values, 1.7 and 3.6 respectively, while

with the DMTS system lemon oil stabilized with WP or WP-CMC complex had span values of 1 and 1.1 for the same emulsifiers respectively.

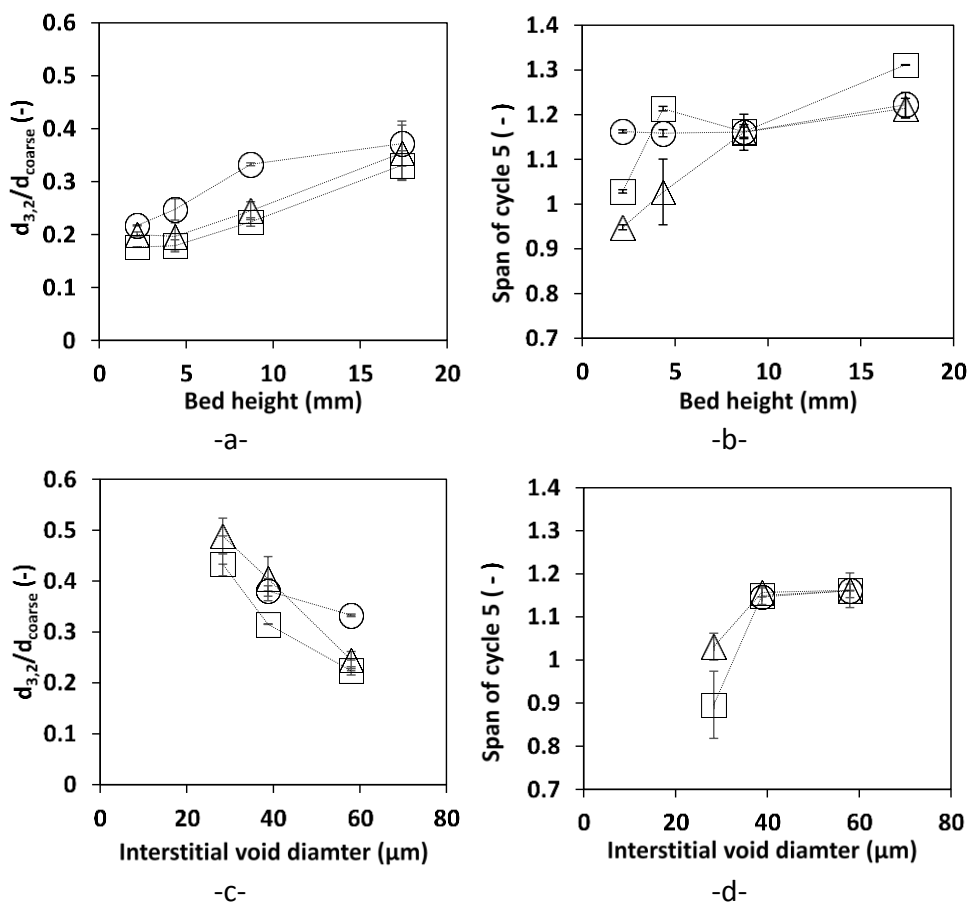


Figure 6.3. Effects of bed height (a,b), micro-beads size (c,d) and emulsifier type on the droplet break-up and span of the last emulsification cycle of 20% LO emulsions. Markers:

○ : WP-CMC; □ : WP; △ : NaCaS

This is yet another strong point for DMTS and its ability to produce narrow droplet size emulsions. As for DMTS systems, the literature shows applications in premix mode to produce O/W and W/O/W emulsions stabilized with WP. Ladjal Ettoumi et al., (2017)⁴² report producing 20% sunflower oil-in-water emulsions stabilized with WP using a 2 mm bed of 71 μm hydrophilic glass beads. They were able to refine a coarse emulsion ($d_{4,3} = 23 \mu\text{m}$) at 300 kPa with five emulsification cycles to a final size, $d_{4,3}$, of 5 μm . As in our study, droplet break-up occurred mainly in the first cycle. Eisinaite et al., (2016)⁴⁴ encapsulated beetroot juice in $W_1/O/W_2$ emulsions using 0.5 % WP to stabilize the sunflower oil/ W_2 interphase. As for the conditions of the DMTS system, they were exactly the same than the ones used by

Ladjal Ettoumi *et al.* (2017)⁴². Starting from a coarse emulsion, $d_{3,2}$, of 32 μm and span of 1.4, they were able to refine it down to 20 μm and span 5. These higher span values might be due to the higher viscosity of sunflower oil, also stable double emulsions being more difficult to form.

Moreover, to compare the extent of droplet break-up obtained in this study with previous literature, it is worth to use the ratio of the droplets' diameter ($d_{3,2}$) to the interstitial void diameter (d_v). It is clear that for all the emulsions the oil droplet sizes of the coarse emulsions are smaller than the interstitial void diameter ($d_{3,2}/d_v < 1$). Also, by the last emulsification cycle this ratio is $0.05 < d_{3,2}/d_v < 0.2$ which is in the lowest range reported for premix membrane emulsification^{9,22,27,36,40}. This again, shows the potential of the DMTS emulsification technique.

6.3.2. Effect of the DMTS system characteristics on the emulsification flux

As mentioned previously, 20% lemon oil emulsions were refined through the DMTS system with a constant pressure of 450 kPa, while varying micro-beads size (42, 68 and 99 μm), bead height (2.18, 4.35, 8.70 and 17.40 mm) and emulsifier type (WP, NaCaS and WP-CMC). Data collected during emulsification allows the calculation of the transmembrane flux (Equation 6.1). Figure 6.4 shows the fluxes as a function of the emulsification cycles for the different conditions.

Regarding the influence of the bed size, it is clear from Figure 6.4 a-c that the highest flux value is obtained when the DMTS system had the thinnest bed. The flux value obtained, at the fifth cycle, was around $1000 \text{ m}^3\text{m}^{-2}\text{h}^{-1}$ for emulsions stabilized with WP or WP-CMC, while it was close to $900 \text{ m}^3\text{m}^{-2}\text{h}^{-1}$ for emulsions stabilized with NaCas. These values are in the upper range of the ones reported for DMTS emulsification and very similar to the ones obtained with the exact same oil type and fraction, pressure and bed conditions but with Tween20 as emulsifier (chapter 5). Therefore, the use of proteins or a protein-polysaccharide complex does not seem to cause extensive fouling in the system reducing the productivity. A general trend can be seen in Figure 6.4 where the thicker the bed and the smaller the micro-beads sizes the lower are the transmembrane fluxes, which can be explained by the higher resistance to flow²². Nonetheless, some discrepancies are noticeable in the plots showing the flux values for WP and NaCaS. Figure 6.4 a-b show a much higher flux value for the system with the thinnest bed, while in Figure 6.4 d-e it can be seen that fluxes obtained with the 99 μm beads are in same range than the ones obtained with the 68 μm beads. This behavior can be explained by the different porosity of the micro-sieves used to support the bed (Table 6.1). The DMTS system consist of a bed with a porosity of about 50%, supported by a nickel micro-sieve with a much lower porosity (1.2-2.4%), exhibiting higher resistance.

As reported previously in section 5.3.2, for the same bed characteristics, higher porosities of the nickel sieve result in higher fluxes and the opposite is true. The effect of the porosity of the micro-sieve is overlooked in the DMTS emulsification literature, and controlling this factor has the potential of optimizing transmembrane flux, while maintaining all the other operational parameters.

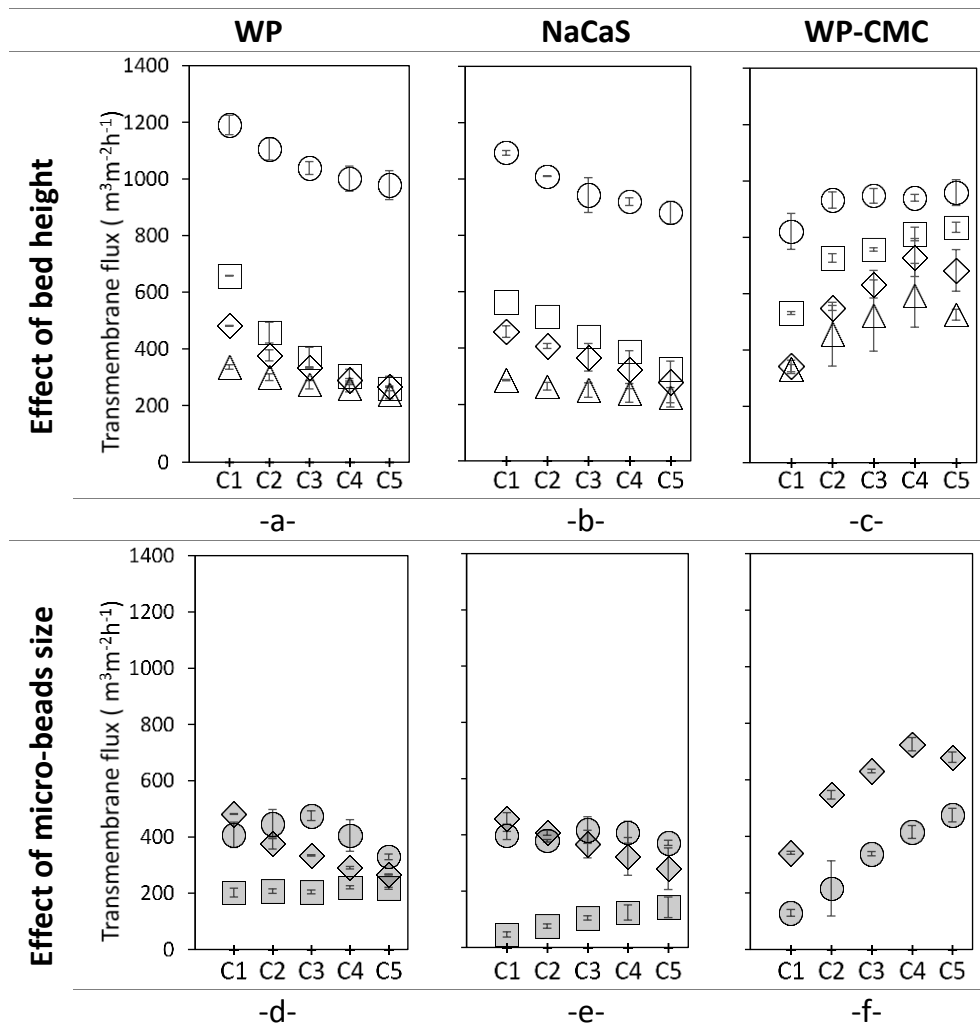


Figure 6.4. Effects of bed height (a,b,c) and micro-beads size (d,e,f) on transmembrane flux during emulsification of lemon oil (20%) stabilized with WP, NaCaS and WP-CMC complex. Markers: ○: 2.18mm; □: 4.35mm; ◇: 8.7mm; △: 17.4mm; ■: 42μm; ●: 68μm; ◆: 99μm.

Comparing the effect of the emulsifiers on the transmembrane fluxes, it is clear that emulsions with WP and NaCaS behaved similarly in comparison to emulsions with the protein-polysaccharide complex. This latter had flux values at the first emulsification cycle lower than the other two emulsifiers mainly because of the higher emulsion viscosity. As emulsification progresses, increasing the number of cycles, the flux values increased. Vladislavljević *et al.* (2004)²⁷ describe how the energy inputted into the system (in this case the constant applied pressure, P_m) is invested into (i) breaking the emulsion droplets (P_{disr}) and (ii) pushing the emulsion through the membrane (P_{flow}) (Equation 6.7).

$$P_m = P_{flow} + P_{disr} \quad (6.7)$$

It is possible that with emulsions prepared with WP-CMC, and taking the higher viscosity, energy was invested in the first cycles into breaking the comparatively large oil droplets. As these latter become smaller in the subsequent cycles, energy is invested more into flowing the emulsions which explains the increase in transmembrane flux. A more plausible explanation for the increasing flux, is that the emulsion is undergoing shear-thinning. Nor Hayati *et al.* (2009)¹³⁶ reports that O/W emulsions containing CMC exhibit shear thinning behavior. As for the emulsions with WP and NaCaS, and since the oil droplets in their emulsions are smaller than those with the complex, Sahin *et al.*, (2014) explains that with the increasing number of cycles, and thus decreasing size and increasing number of droplets, oil droplet might slightly accumulate in or before the bed, in turn lowering the flux values.

It should be noted that, as previously mentioned, the coarse emulsion stabilized with WP-CMC could not be refined at 450 kPa through the 9.25 mm layer of 42 μm sized micro-beads. Several trials were made but the emulsion was not able to pass through the bed. At a $d_v \approx 28 \mu\text{m}$ and a $d_{coarse} \approx 20 \mu\text{m}$, it seems that the inputted energy, along with the higher emulsion's viscosity, are not enough to push the emulsion through the bed. Because of the resistance of the bed, the $d_{coarse}/d_v = 0.71$ and the viscosity of the emulsion, the pressure applied is not enough to flow the emulsion through the bed. When the resistance can be overcome, then the emulsion is submitted to the shear forces and the shear thinning behavior which explains the increase in the flux in every cycle. With the micro-beads sizes of 68 and 99 μm the emulsion passed with no problems.

6.3.3. Emulsions stability

The stability of all the emulsions was studied over a period of 7 days at two different temperatures (4 and 25 °C). Figure 6.5 shows the particle size distributions of the fresh emulsions and after 7 days for the all the tested

conditions (micro-beads size, bed height, temperature, emulsifier type). All emulsions produced with WP and NaCaS appear to be stable with a small increase in $d_{3,2}$ and span after 7 days (more so for samples stored at room temperature). Emulsions stabilized with WP-CMC on the other hand show a stronger effect of storage temperature on stability. All the emulsions stored at room temperature destabilized by coalescence with a steep increase in droplets diameter and span.

However, refrigerated emulsions remained almost the same after 7 days. Figure 6.6 shows that creaming had occurred in all of the emulsions and a change in color due to oxidation was prominent in samples stored at room temperature.

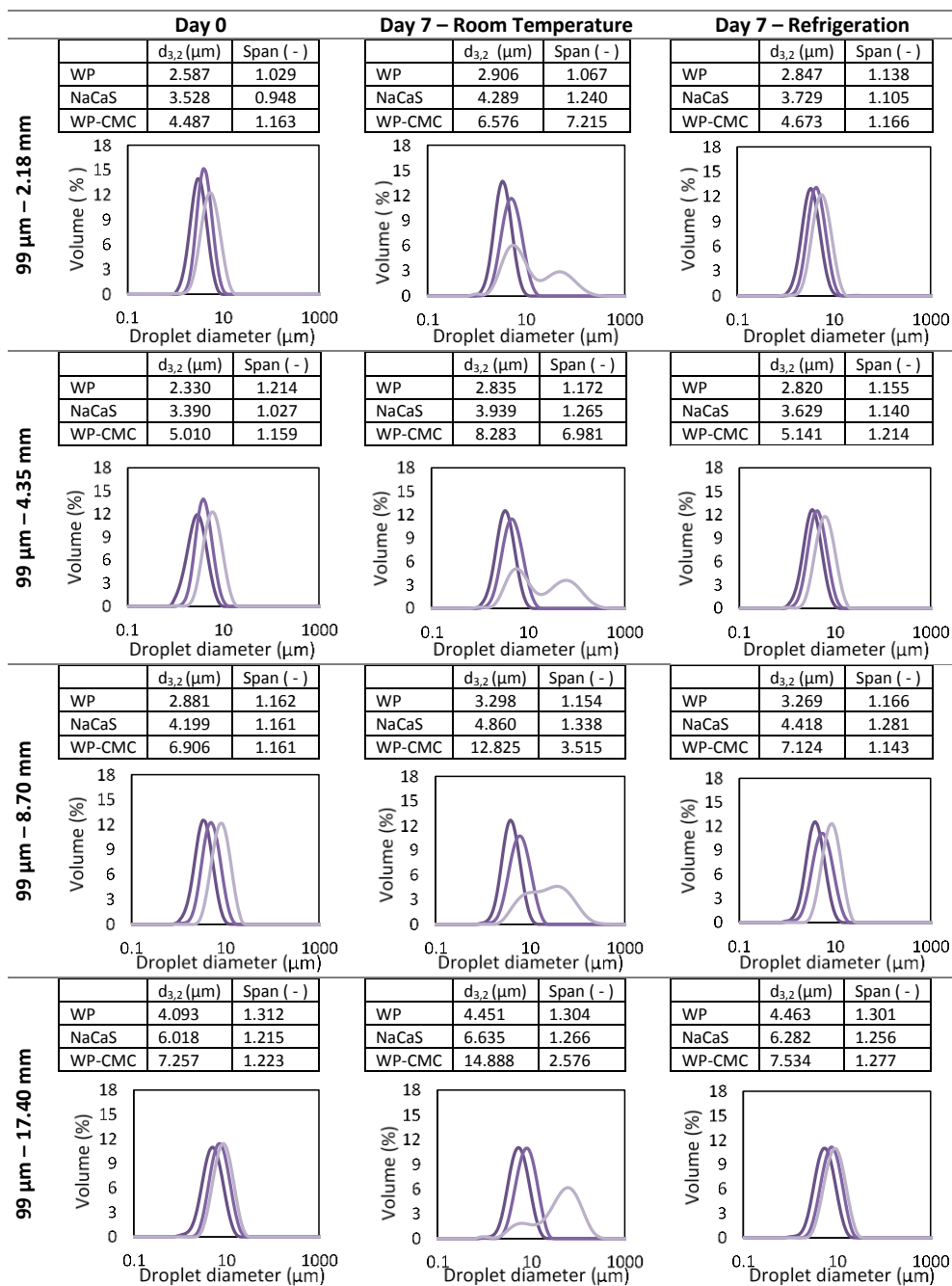
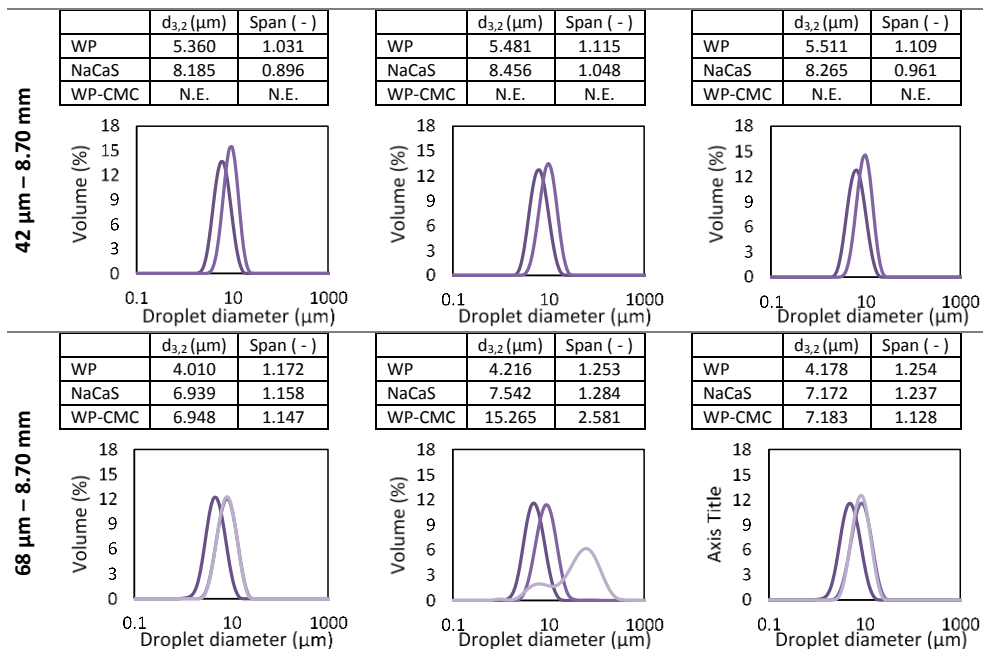


Figure 6.5. Effects of bed height (2.18, 4.35, 8.70, 17.40 mm), micro-beads size (42, 68 and 99 μm), emulsifier type (WP, NaCaS and WP-CMC) and storage temperature (room temperature or refrigeration) on 20% LO emulsion stability after 7 days. The color transparency scale indicates the type of emulsifier: from darkest to lightest refer WP, NaCaS and WP-CMC.



Continuation of Figure 6.5

At room temperature, lemon oil and the proteins are more prone to oxidation because at high temperatures emulsion viscosity is low (compared to the viscosity of the refrigerated emulsion) thus increasing the circulation of oxygen and its exposure to the droplets¹³⁰. What is interesting to point out is that no change in color was seen in emulsions stabilized with WP-CMC.

In these WP-CMC stabilized emulsions the creamy layer on top was harder to break than in the emulsions stabilized with single proteins, most probably due to the presence of a texture modifying agent, such as CMC. This thick layer on the top could have been responsible for protecting the emulsion from oxidation; however, only chemical stability studies can verify the extent of oxidation and this is out of the scope in the present study. In summary all the refrigerated emulsions remained stable after 7 days, which ensures that if emulsions are kept at low temperature, they can be stored for several days before any post-emulsification processes (e.g. spray drying) are applied. As for the WP-CMC complex it was able to keep the emulsions stable under refrigeration with no change in color.

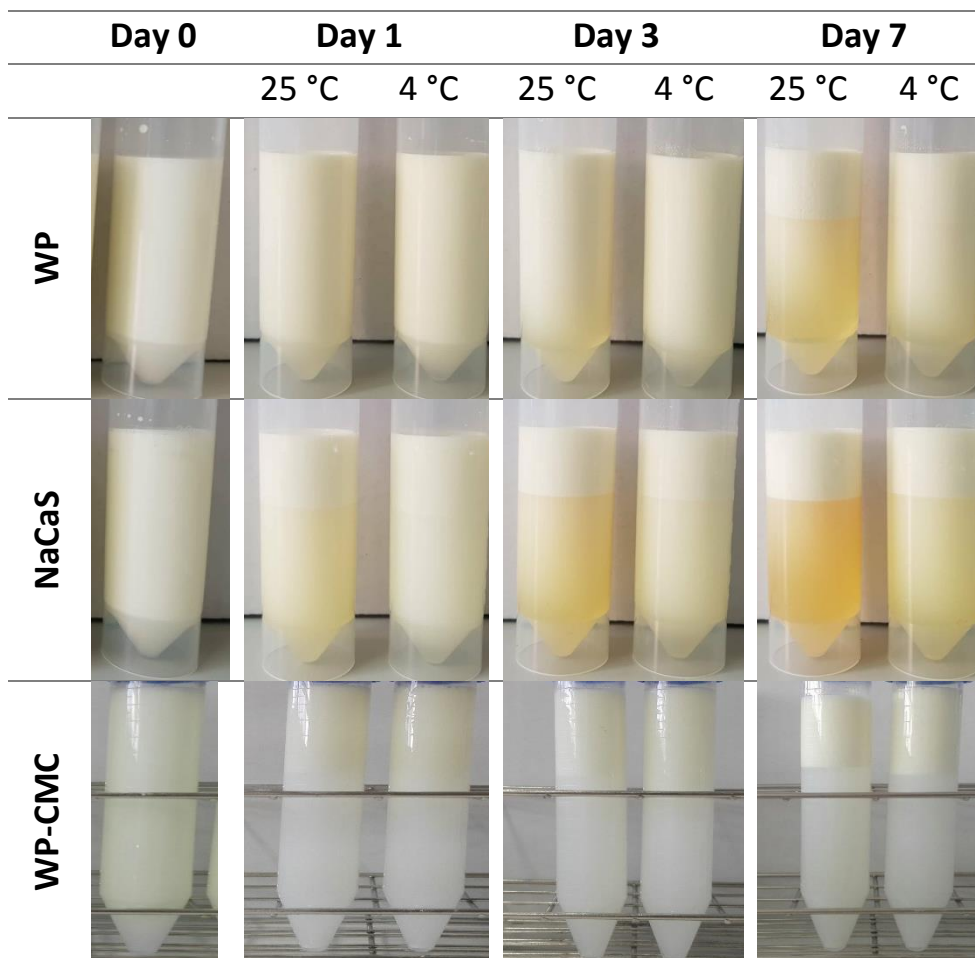


Figure 6.6. Stability of 20% lemon oil emulsion produced with 99 μ m-2g DMTS system with three emulsifiers.

In chapter 3, 20% lemon oil emulsions were prepared with an SPG membrane and stabilized with WP (pH: 6.8) and WP-CMC (pH: 3.8). Emulsions' stability was tested under accelerated conditions under UV light over a period of two weeks. Results are consistent with those reported in this chapter where emulsions stabilized with WP (pH:6.8) showed a change in color (yellowish) whereas emulsions stabilized with WP-CMC (pH: 3.8) inhibited this change in color. Regarding droplet size, emulsions stabilized with WP (pH: 6.8) and prepared with both the SPG and the DMTS systems, maintained a constant oil droplet size over 7 days. However, for droplet size distribution the behavior was not the same. Emulsions prepared with the SPG membrane and stabilized with WP (pH: 6.8) had a span of 0.8 after three emulsification cycles while the emulsions prepared with the DMTS system (99 μ m

beads size and 8.7 mm bed height) and stabilized with the same emulsifier, had a span of 1.16 after five emulsification cycles. Although the emulsions prepared with the SPG membrane had smaller droplet size distributions, the emulsions prepared with the DMTS system showed more stability and the distribution remained monomodal after 7 days unlike the emulsions prepared with the SPG membrane that showed signs of coalescence. This is probably due to the accelerated storage conditions where faster oxidation of the both the oil phase and whey protein occur. Muijlwijk *et al.* (2017)¹³⁷ reports that the oxidation of WP has decreased the coalescence stability of hexadecane oil droplets. Protein oxidation results in aggregates forming and peptides being released thus making the interfacial network less elastic. Also, these new products make the interface composition heterogeneous and by that reducing coalescence stability. As for emulsions stabilized with WP-CMC (pH:3.8), under UV light neither the droplet size nor the droplet size distribution was stable for emulsions produced with the SPG membrane, unlike the case reported in this chapter. This of course could be due to, again, the accelerated conditions but also the span of the emulsions produced by the SPG membrane was higher after three emulsification cycles (span = 1.4 with SPG vs. span = 1.1 with DMTS).

6.3.4. Scaling equation for droplet size versus applied pressure in the DMTS system

Several authors have related droplet break-up to applied energy through the energy density relation in emulsification systems to predict the droplet size based on the pressure applied^{26,40}. Since in this study the applied pressure was kept constant at 450 kPa, but the process parameters related to the structure of the microporous system and the nature of the emulsifier varied, an equation to include the effects of d_{coarse} , micro-beads size, bed height and number of emulsification cycles in the droplet size is proposed. The equation takes into account the number of the emulsification cycles (N) and the relationship between the height of the bed and the interstitial void diameter, as shown in Equation (6.8).

$$\frac{d_{3,2}}{d_{coarse}} = a \cdot N^{-b} \cdot \left(\frac{height}{d_v}\right)^c \quad (6.8)$$

where a , b and c are fitting parameters. The values of the three constants in Equation 6.8 were computed by the Solver tool in Microsoft Excel and verified with the Curve Fitting tool in Matlab (R2015a). To do so, the results from all the experimental conditions (Table 6.1) with the four emulsifiers (Tween 20, WP, NaCaS and WP-CMC), including all the replicates (255 points), were considered.

The fitting parameters are reported in Table 6.2, their p-values were: $p \ll 0.001$, which shows their statistical significance. Also, the general p-value of the equation was also: $p \ll 0.001$. The fit is very good ($R^2 \approx 0.83$) considering the extent of experimental variables. Figure 6.7 shows the experimental Sauter mean diameter plotted against the values obtained from Equation 6.8.

The importance of this equation is that it can be used to select the operating conditions of the DMTS system and calculate the expected droplet size regardless of the emulsifier used.

6.3.5. Tailored design of the DMTS system

As previously reported in section 5.3.3, it is possible to modify the DMTS system to maintain high emulsion through-put while decreasing the energy inputted, reducing the emulsification cycles, and still obtain narrow droplet size distributions during the production of lemon oil emulsions stabilized with Tween 20. This modified system, referred to from here on as layered DMTS, consists of two superimposed layers of beads of different size. As a result, the microstructured system has an upper layer (4.35 mm) of 57.97 μm of interstitial void diameter and a bottom layer of the similar thickness (4.63 mm) with an interstitial void diameter of about 28.33 μm (Table 5.2).

A set of experiments was designed to test the performance of the layered DMTS system with emulsions stabilized with WP, NaCaS or WP-CMC complex. Lemon oil emulsions (20%wt.) were prepared as described in section 6.2.3 and then they were refined at 450 kPa with the layered DMTS system. Figure 6.8 shows the droplet break-up ($d_{3,2}$, $d_{3,2}/d_{coarse}$ and span) as well as the transmembrane flux of the lemon emulsions stabilized with the three biopolymers.

Since one of the goals is to reduce the energy input, the emulsion refinement cycles with the layered DMTS system were reduced three, therefore the results can be compared with the ones obtained after three cycles using the standard DMTS system of similar thickness and intermediate interstitial void diameter.

Table 3. Regression parameters for Equation 6.8

	Coefficient	STD
a	0.1387	± 0.0100
b	0.372	± 0.0139
c	0.2902	± 0.0137
R²	0.8249	

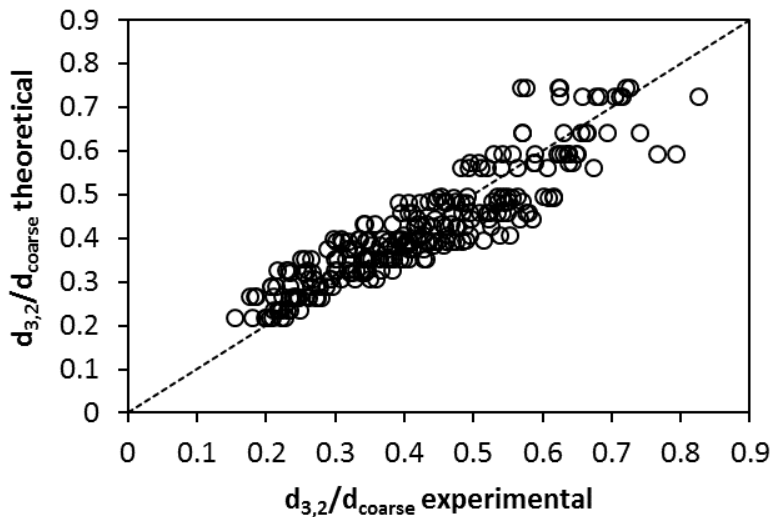


Figure 6.7. Experimental $d_{3,2}$ values plotted against the values obtained from Equation 6.8

Looking at Sauter mean diameter ($d_{3,2}$), different trends are observed for the emulsifiers: WP gave higher $d_{3,2}$ value than the one obtained using a 9.27 mm bed of mono-sized 68 μm beads, while for NaCas and WP-CMC the $d_{3,2}$ values were slightly lower or similar, respectively, to the ones with the mono-sized bed. It is interesting to point out that, with the WP-CMC complex, and as mentioned in section 6.3.1, the emulsion was not able to pass through 42 μm micro-beads, but with the layering arrangement this problem is overcome and the emulsions were able to be refined to a $d_{3,2}$ value of about 9 μm . It may be that the first layer of the 99 μm beads refines the WP-CMC lemon oil emulsion down to a droplet size that allows the emulsion to move through the tighter channels of the bottom layer, where they are further refined. Looking at Figure 6.8b, and by the third cycle, the droplet size reduction was the same regardless of the emulsifier type.

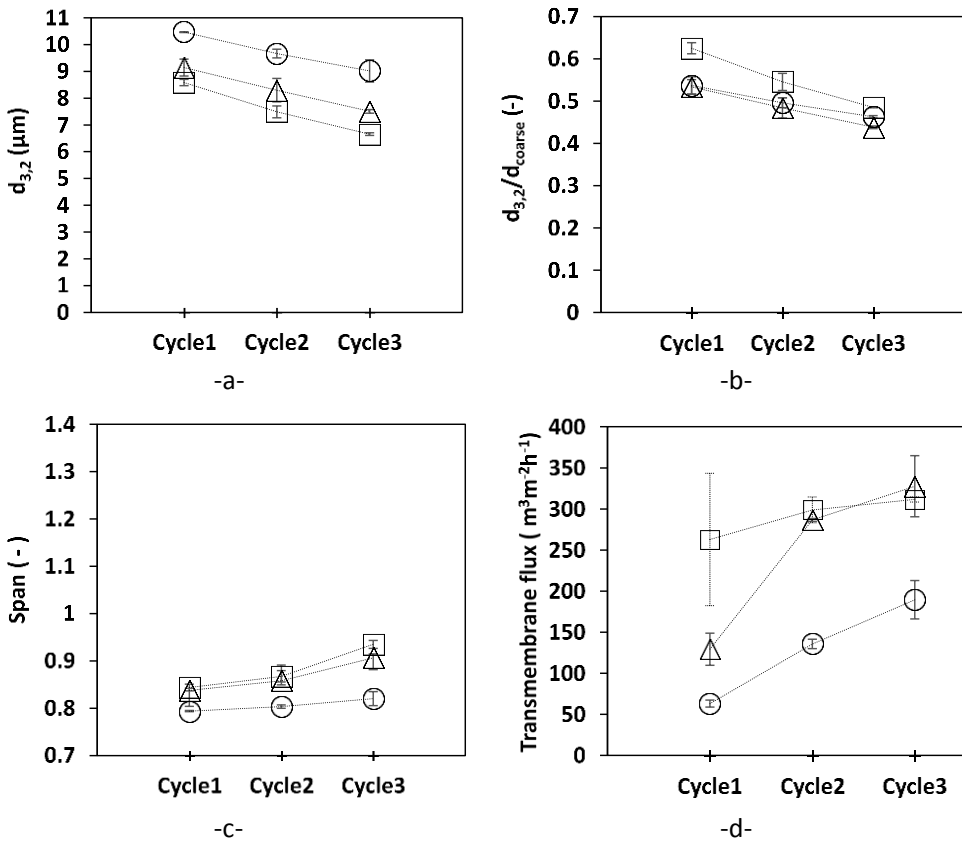


Figure 6.8. Effects of using a layered DMTS system and a different emulsifier on (a,b) droplet break-up, (b) span and (c) transmembrane flux during the production of 20% LO emulsions. Markers: ○ : WP-CMC; □ : WP; △ : NaCaS

As for the span values, all of them were lower than the ones resulting after three emulsification cycles with the 9.27 mm mono-sized bed, showing the potential of tailoring the microstructured system to obtain narrower droplet size distributions. To the authors' knowledge no other study has reported producing emulsions stabilized with WP-CMC with a span value as small as 0.82.

Emulsion refinement leading to narrow droplet size distributions while reducing the energy input need to be accompanied by high productivities to scale-up the process. Figure 6.8d shows the flux evolution during emulsification in the layered DMTS system for the three emulsifiers. The flux values at the 3rd cycle are of around $300 \text{ m}^3\cdot\text{m}^{-2}\cdot\text{h}^{-1}$ for emulsions stabilized with WP and NaCaS, and about $200 \text{ m}^3\cdot\text{m}^{-2}\cdot\text{h}^{-1}$ for emulsions stabilized with WP-CMC. Even though these values are 40% lower than the ones obtained with the 9.27 mm bed of $68 \mu\text{m}$ micro-beads, they

are still comparable to flux values reported for Shiratsu porous glass membranes².

The stability of the emulsions produced with the layered DMTS system was monitored for 7 days at 4 and 25 °C. As reported in section 6.2.5, emulsions were less stable when stored at room temperature but very stable at 4 °C. In fact, the refrigerated emulsions that were produced by layering, were the most physically stable between all the emulsions (Figure 6.9) most probably due to the low span values. For that reason, layering is a promising tool for obtaining emulsions with narrow droplet size distributions and high through-put while reducing inputted energy.

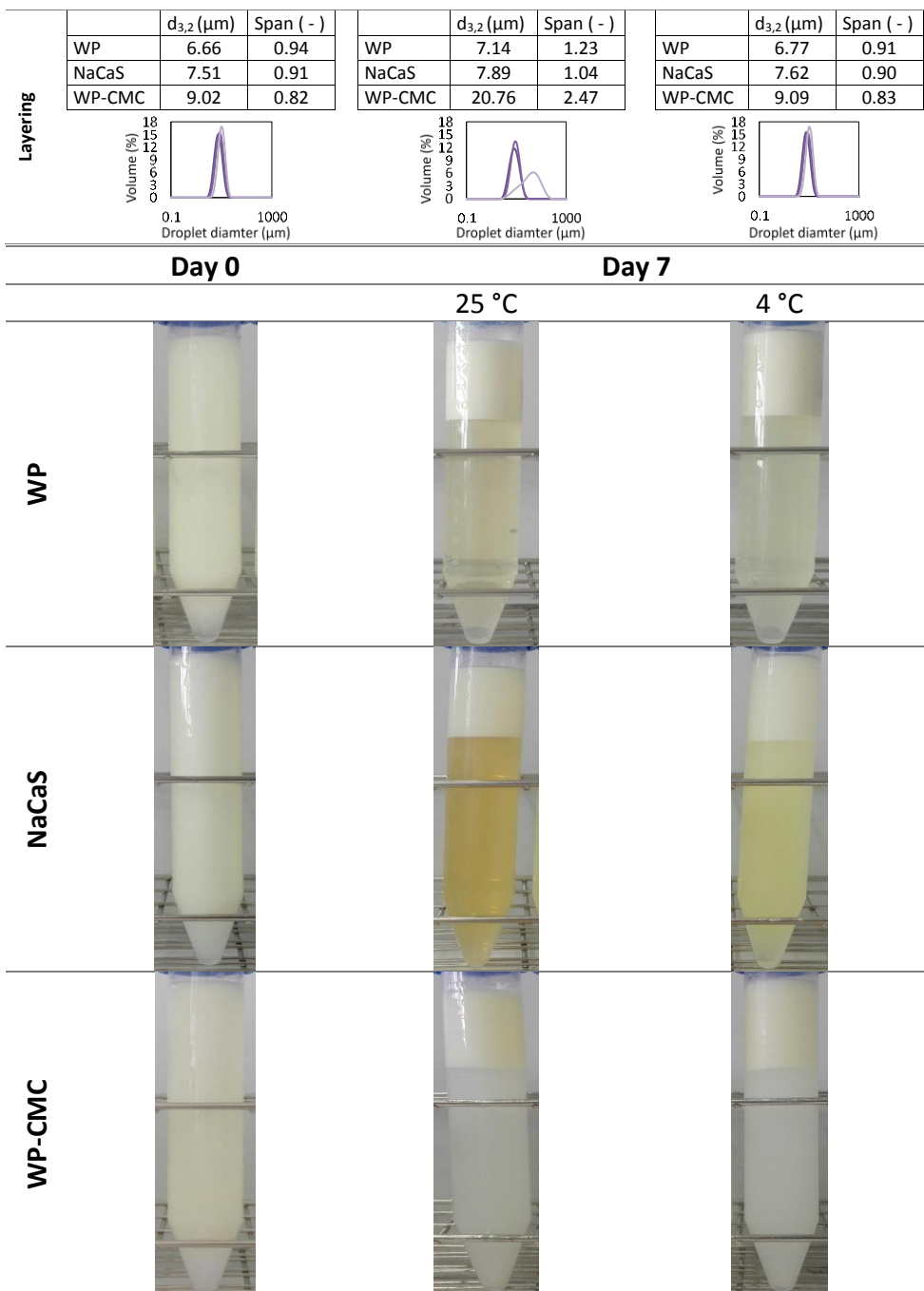


Figure 6.9. Effects of layering, emulsifier type (WP, NaCaS and WP-CMC) and storage temperature (room temperature or refrigeration) on 20% LO emulsion stability after 7 days. The color transparency scale (top image) indicates the type of emulsifier: from darkest to lightest refer WP, NaCaS and WP-CMC.

6.4. Conclusions

This study has proven the feasibility of using standard and layered DMTS systems to produce lemon oil emulsions stabilized by two milk proteins (whey protein and sodium caseinate) and a protein-polysaccharide electrostatic complex (WP-CMC). It has been established that tailoring the operating parameters of the DMTS system (interstitial void diameter, bed height, nickel micro-sieve porosity) enabled to control the droplet size distribution while maintaining the emulsion productivity. Overall, for the three emulsifiers, the thinner the bed the smaller and narrower size distribution of the droplets. As for the interstitial void diameter, it was clear that increasing this parameter, droplet size decreased and increased the droplet size distribution. A scaling relation to predict the droplet size based on the size of the coarse emulsion, the number of emulsification cycles and the ratio between bed height and interstitial void diameter, and regardless of the emulsifier, was established. The results show the potential of the DMTS system to refine emulsions stabilized with biopolymers, since at the fifth emulsification cycle the values of $d_{3,2}/d_v$ are in the lowest range reported for premix emulsification, while maintaining the productivity at $300\text{-}200\text{ m}^3\text{m}^{-2}\text{h}^{-1}$. The layered DMTS system allows to tailor the microstructure to refine the emulsion while reducing the energy input. The layered DMTS allowed the production of a monodispersed emulsion, stabilized with WP-CMC complex, with the lowest reported span value (0.82) so far. Regarding stability, emulsions prepared with the conventional and layered DMTS systems tended to be more stable at 4°C compared to the ones stored at room temperature. All emulsions stabilized with WP and NaCaS had a yellowish tint after 7 days (more so the ones stored at room temperature) that can be attributed to oxidation. However, emulsions stabilized with WP-CMC CMC did not show any significant change in color, even though they were not stable at room temperature. Although the complex seems to better protect the emulsions against oxidation (visually), a chemical stability study should be performed.

7. Pea protein for the stabilization of O/W emulsions: A microfluidics approach

Parts of this chapter have been published as:

Hinderink, E. B. A., Kaade, W., Sagis, L., Schroën, K., & Berton-Carabin, C. C. (2020). Microfluidic investigation of the coalescence susceptibility of pea protein-stabilised emulsions: Effect of protein oxidation level. *Food Hydrocolloids*, 102, 105610.

UNIVERSITAT ROVIRA I VIRGILI

LOW-ENERGY HIGH-THROUGHPUT MICROPOROUS EMULSIFICATION FOR LEMON OIL ENCAPSULATION

Wael Kaade

7.1. Introduction

Food emulsions make up many products that are often used like dressings, ice-cream and spreads. Simple emulsions can be in the form of oil-in-water or water-in-oil emulsions. In both cases, emulsions need emulsifiers to keep them kinetically stable and a popular choice is dairy protein. However, with the increase of the global human population to 9.5 billion by 2050, the demand for protein is expected to double. For that reason, research is turning to plant proteins as another protein source. Plant proteins are safer for human consumption (low allergenicity) and more sustainable, not to mention they are a preference for people following a vegan or vegetarian diet. A downside to plant proteins is their strong taste and low solubility in water. In the year 2019 alone more than fifteen studies have reported using plant proteins as emulsifiers to stabilize O/W emulsions.

Pea protein (PP) in particular has been much researched in the last year. PP's major components (65-80%) are the globular proteins: 11S legumin and 7S vicilin^{88,89}. Compared to other plant proteins like soy, PP have lower allergenic potential and higher nutritional value. Similarly to milk proteins, PP are amphiphilic and by that can be used to stabilize emulsions. Burger & Zhang, (2019)⁸⁹ report that the process for PP to stabilize an oil/water interface starts by migration of the protein to the interface, adhesion, partial denaturation and reorientation (the hydrophilic portion facing the water and the hydrophobic one inside the oil) and finally the formation of a viscoelastic film at the interface. This film stabilizes oil droplets through electrostatic repulsion and steric hindrance.

Since PP are considered a new protein source, the way they stabilize oil droplets in O/W emulsions hasn't been studied much. The mechanism of droplet formation and coalescence cannot be measured using conventional emulsification techniques. In these latter, droplet size measurements are done minutes after emulsification while droplet break-up and coalescence occur within milliseconds of emulsification. Using microfluidics, however, allows the observation of droplet formation in the sub-second range. A microfluidics chip developed by Krebs *et al.* (2012)¹³⁸ is formed of three sections: a T-shaped junction where the oil and aqueous phase meet and the droplets form, a meandering channel where the oil droplets get stabilized by the emulsifier, and finally a long coalescence chamber where the oil droplets meet and interact. This chip has been used for stabilizing oil droplets with sodium dodecyl sulphate¹³⁸, β -lactoglobulin and whey protein¹³⁷. Muijlwijk *et al.* (2017)¹³⁷ used chips with different meandering channel length while maintaining the same flow rate. This allows to control the time the oil droplets have in contact with the continuous phase and thus the amount of droplet coverage. For instance, they reported that hexadecane droplets need at least 100 ms in contact with 0.005% β -lactoglobulin in the meandering channel to be

stabilized and not coalesce in the coalescence chamber. Other variables tested are the emulsifier's type and concentration, the flow rates of the continuous and dispersed phase and the pH of the continuous phase.

The aim of this chapter is to open a scope on new sustainable plant-based emulsifiers, pea protein in particular, for droplets stabilization in microfluidics. Droplets' stability was studied as a function of protein concentration, meandering channel length, and continuous phase flow rate.

7.2. Materials and methods

Pea protein isolate was bought from Roquette (80–90% purity, NUTRALYS, s85F, France). Sodium phosphate dibasic (Na_2HPO_4), sodium phosphate monobasic (NaH_2PO_4), hexadecane, were all purchased from Sigma Aldrich (Saint Louis, Missouri, USA). The bicinchoninic acid (BCA) assay kit was obtained from Sigma-Aldrich (BCA1-1 KT, Saint Louis, USA).

7.2.1. Preparation of pea protein solution

A 6%wt pea protein solution was prepared with 10mM phosphate buffer (pH: 7.0) and stirred for 24h at 4 °C. The solution was then centrifuged at 16,000xg for 30min, the supernatant was separated and centrifuged again in the same way. The protein content of the supernatant was measured through a standard BCA assay at 562 nm using a DU 720 UV–vis spectrophotometer (Beckman Coulter, Woerden, the Netherlands)¹³⁹. The supernatant contained 15 g/L soluble protein. This protein solution was frozen in 1 ml vials for future use.

7.2.2. Microfluidics experiments

The borosilicate glass microfluidics chips (Figure 7.1) were custom made by Micronit Microtechnologies B.V. (Enschede, the Netherlands). On the left side of the chip are the continuous and dispersed phase entrances (width = 100 μm) where they meet at a T-shaped junction and an oil droplet is formed. The droplet then passes through the meandering channel before reaching the coalescence chamber (width = 500 μm , length = 26.2 mm). Different chips having meandering channels of different lengths were used. Consequently, the residence time of a droplet in the meandering channel was 11, 31, 65, 100 or 173 ms depending on the shape of that channel. The different shapes are shown in Figure 7.1. All the channels of a chip have a depth of 45 μm .

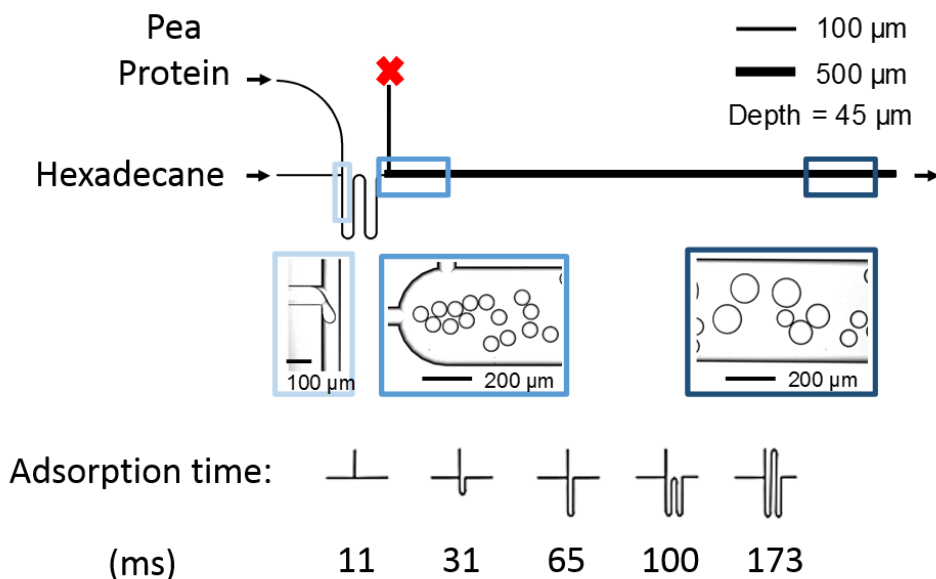


Figure 7.1. Microfluidic coalescence chip with an adsorption time of 100 ms (top). The extra inlet in the coalescence channel is closed as indicated by **X**. At the bottom of the figure, an overview of the different meandering channels and the corresponding adsorption times is given.

The microfluidics chip was placed in its holder and connected to the continuous phase (pea protein solution) and the dispersed phase (n-hexadecane) sources via glass capillary tubes. The continuous phase was filtered with a 0.22 μm filter before using it. The continuous and dispersed phase were pressurized into the microfluidics chips by means of a pressure system (OB1, Elveflow, France) and the flow rates were controlled with a CORI-Flow sensor (Bronkhorst B.V., Netherlands). The flow rate of hexadecane was maintained constant throughout all the experiments at 2 μL/min while the continuous phase was varied between 20 and 70 μL/min.

For image capturing, a light microscope (Axiovert 200 MAT, Carl Zeiss B.V.) connected to a high-speed camera (MotionPro Y4-A2) was utilized. A 1000 images were collected at a rate of 30 frames/s at the inlet and outlet of the coalescence chamber. A custom-made ImageJ macro¹³⁷ was used to determine the two dimensional area of the droplet. From that, a mean droplet area (A_f) at any position and a mean initial droplet area (A_i) at the inlet on the coalescence chamber were calculated. Then, the number of coalescence occurrences (N_{coal}) can be calculated using Equation 7.1.

$$N_{coal} = \frac{A_f}{A_i} - 1 \quad (7.1)$$

7.3. Results and discussion

7.3.1. Effect of pea protein concentration on droplet stability

Hexadecane droplets were formed at a flow rate of 2 $\mu\text{L}/\text{min}$ and the protein solution was flowing at a constant 40 $\mu\text{L}/\text{min}$ rate which brings the total flow rate to 42 $\mu\text{L}/\text{min}$. Protein concentration was varied from 0.1 to 1 g/L to test its effect on oil droplets' stability. The microfluidics chip used in this section is one have a 100 ms adsorption time in the meandering channel. It should be notes that changing protein concentration had no effect on the size of the oil droplet which remained constant at around 60 μm .

For all the experiments, the coalescence occurrences at the front of the coalescence chamber were lower than at the end of it. That alone shows that coalescence started occurring immediately after entering the chamber and that the adsorption time throughout the chamber was not enough to further stabilize the droplets. Figure 7.2 shows the relationship between pea protein concentration and the number of coalescence occurrences.

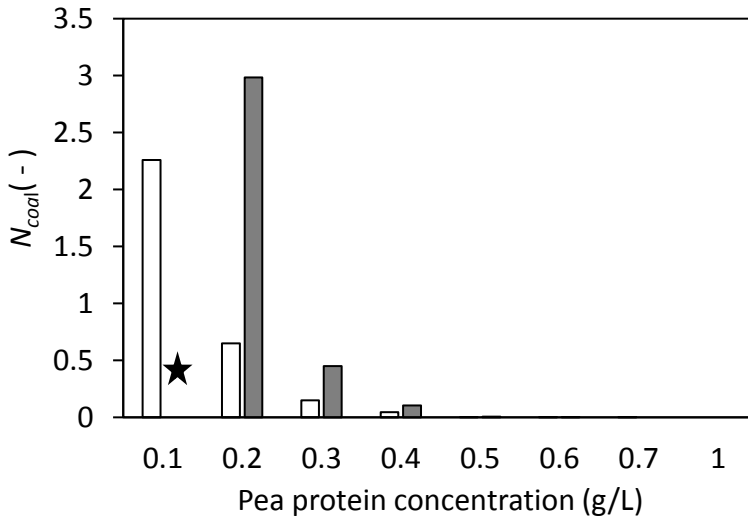


Figure 7.2. Number of coalescence occurrences in the chip with 100 ms adsorption time for different concentrations (0.1-1 g/L) of PP measured at the front (empty marker) and the end (grey marker) of the coalescence chamber. ★ indicates that the coalesced droplets were too large to measure as seen in Figure 7.3.

It is clear that the higher the PP concentration, the less coalescence events are registered. In particular, PP concentration above 0.5 g/L successfully stabilized the droplets while passing through the meandering channel (100 ms) by sufficiently covering the surface. This is clearer in Figure 7.3 where only below the PP concentration of 0.4 g/L droplets A_f larger than A_i could be seen.

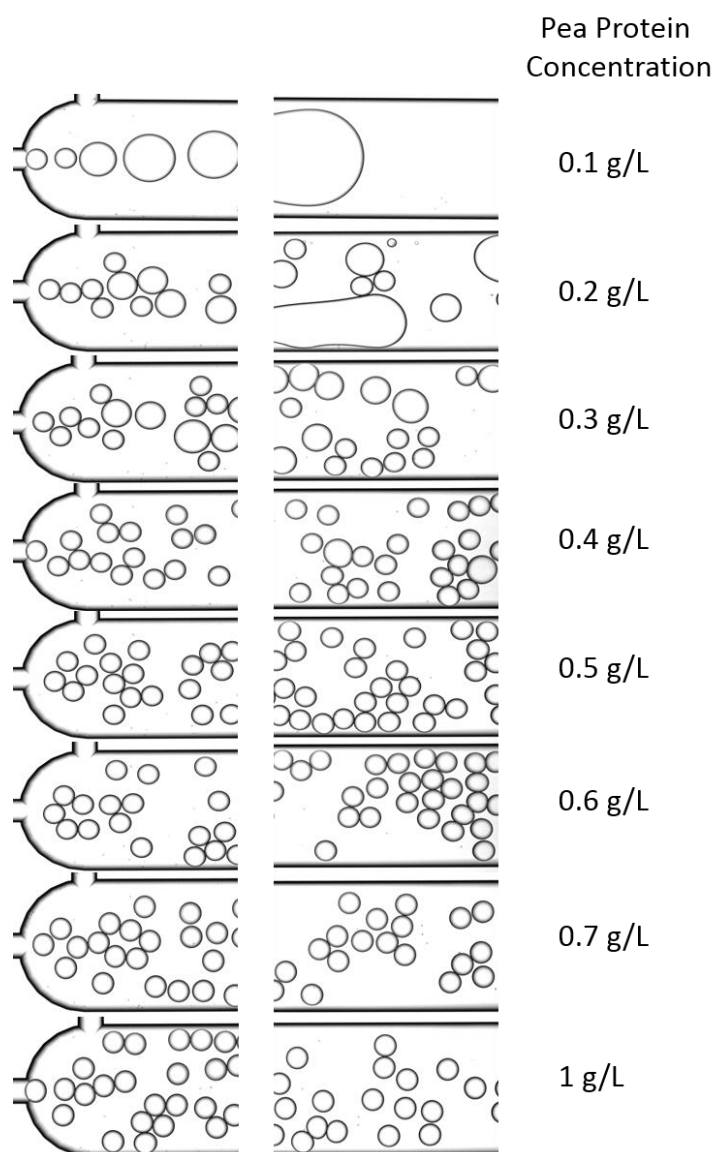


Figure 7.3. Microscopic images of the effect of pea protein concentration on droplet stability taken at the front and end of the coalescence chamber.

7.3.2. Effect of meandering channel length on droplet stability

Five different chips with different meandering channels lengths were used to test the effect of the PP adsorption time (11-173 ms) on droplet stability. As it can be seen in Figure 7.4, and as discussed in section 7.3.1, for all the chips, increasing PP concentration increases droplet stability. Also, it is clear that for any given PP concentration, a longer adsorption time resulted in less coalescence events. Taking a PP concentration of 0.3 g/L for example, Figure 7.5 shows how the number of coalescence occurrences decreases when more time is allowed for the droplets' surface to be covered.

Muijlwijk *et al.* (2017)¹³⁷ reports that using β -lactoglobulin (major whey protein in cow milk) as emulsifier, a concentration as low as 0.05 g/L was enough to stabilize hexadecane droplet in 31 ms chip. This indicates that unlike dairy protein, a much higher concentration of PP (0.5 g/L with a 65 ms chip) and/or a longer adsorption time are needed to stabilize the oil droplets. Also, Hendrick reports that pea protein's high molecular weight and their soluble aggregate's state might be why a higher concentration of PP is needed.

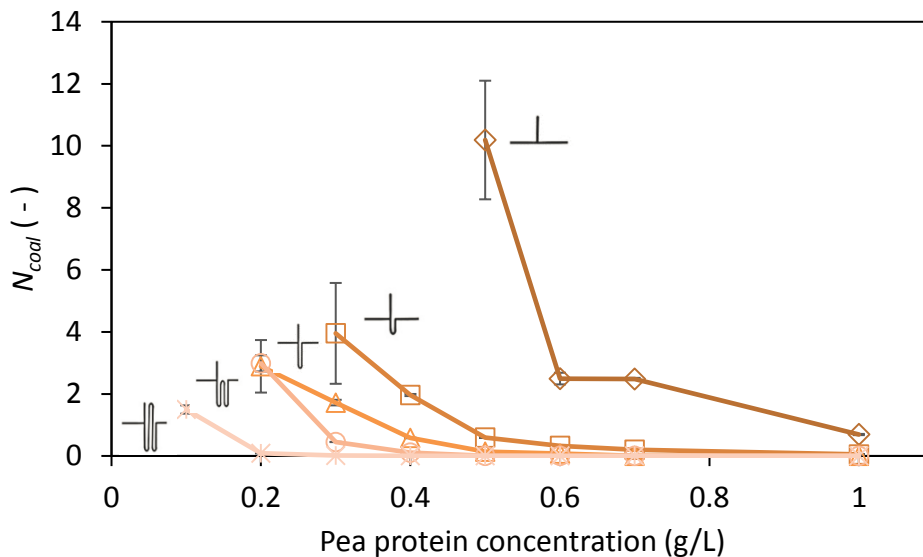


Figure 7.4. Number of coalescence occurrences at the outlet of the coalescence chamber measured in chips with different adsorption times 11 (◇), 31 (□), 65 (△), 100 (○) and 173 (*) ms and protein concentrations (0.1–1 g/L).

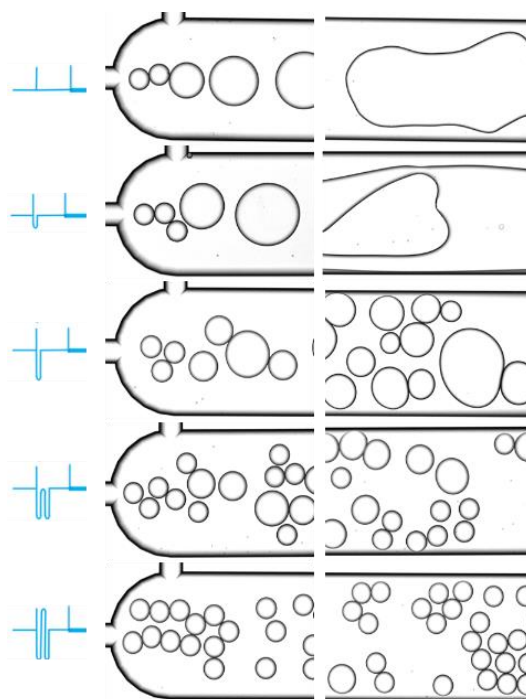


Figure 7.5. Microscopic images taken at the front and end of the coalescence chamber showing the effect of adsorption time (11, 31, 65, 100, 173 ms) on droplet stability with PP concentration of 0.3 g/L.

7.3.3. Effect of continuous phase flow rate on droplet stability

The 100 ms chip was used to test the effect of the continuous phase flow rate on the hexadecane droplets stability. The oil flow rate was maintained at 2 $\mu\text{L}/\text{min}$ and the PP concentration used was 0.2 g/L. The continuous phase flow rate was varied between 20 and 70 $\mu\text{L}/\text{min}$. Figure 7.6 shows the results. It is clear that regardless of the flow rate used, coalescence started immediately after entering the coalescence chamber. Increasing the continuous phase flow rates has several consequences. First the shear applied on the forming droplets at the T-shaped junction is higher. This is reflected by the decreasing droplet size. The mean droplet size decreased from 78 μm to 53 μm with the increase of flow rate from 20 and 70 $\mu\text{L}/\text{min}$. Also, because of the higher continuous phase flow rate, the pressure applied on the oil inlet was higher leading to a decrease in oil volume fraction (less droplets) from 10% to 4%. As for coalescence, it seems from Figure 7.6 that a higher flow rate leads to less coalescence events. Muijlwik *et al.* (2016)¹⁴⁰ reported a similar trend while stabilizing hexadecane droplets with 0.005 g/L β -lactoglobulin.

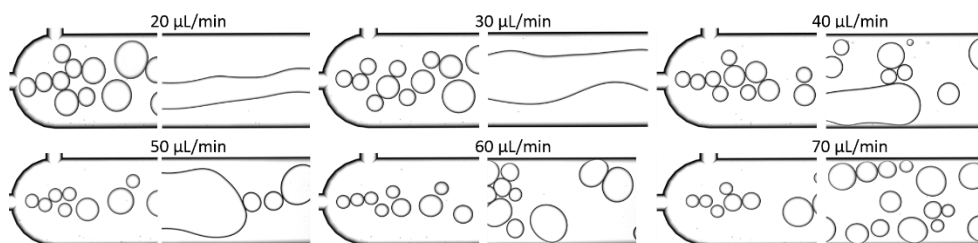


Figure 7.6. Microscopic images taken at the front and end of the coalescence chamber showing the effect of continuous phase flow rate on droplet stability.

These authors gave the following explanations: 1) at low flow rates, the droplets spend more time in the coalescence chamber thus increasing chances of collision, 2) at low flow rates, droplets' collision time is longer and may exceed film drainage time, 3) at low flow rates, convective transport of proteins is low thus not sufficient surface coverage will be reached. Moreover, and in this study's case also it is possible that the higher oil volume fraction at low flow rates, thus higher droplets' collision chances, can lead to higher coalescence events.

7.4. Conclusion

Microfluidics technology is a powerful tool that helps understand droplet formation and stabilization mechanisms that would be otherwise impossible to measure in high-throughput emulsification techniques. This chapter shows the potential of using a plant-based protein, pea protein in particular, for O/W emulsions' stabilization. A higher concentration of pea protein and longer adsorption times will be required to rapidly stabilize droplets as compared to whey protein. Also, continuous phase flow rate controls droplets' protein coverage rate, droplets' size, oil volume fraction and overall emulsion stability. It would definitely be worth trying stabilizing lemon oil emulsions with pea protein.

8. Conclusions

UNIVERSITAT ROVIRA I VIRGILI

LOW-ENERGY HIGH-THROUGHPUT MICROPOROUS EMULSIFICATION FOR LEMON OIL ENCAPSULATION

Wael Kaade

8.1. General conclusion

This work demonstrates the feasibility of producing stable lemon oil-in-water emulsions with narrow droplet size distribution with high-throughput and low-energy premix microporous emulsification systems.

A WP-CMC electrostatic complex (pH: 3.8) was used to stabilize lemon emulsions produced by microporous emulsification with SPG membranes and compared to WP at neutral and acidic pH (Chapter 3). Although the physical stability of the emulsions in terms of droplet size distribution was not improved, the use of an electrostatic WP-CMC complex increased the protection against deterioration of d-limonene and hindered the reduction of citral isomers under acidic and accelerated oxidation conditions. Tailor-made interfaces are thought to be preserved during emulsification using SPG membranes, thus being an effective strategy to control the complex chemical reactions underpinning the degradation of aroma compounds in lemon oil.

Lemon oil emulsification was also tried with a low-cost ceramic membrane, however results showed that this kind of microporous system is not adequate (Chapter 3). On one hand, ceramic membranes are fragile which impede using higher pressures and on the other, they seem to function better for emulsion separation rather than formation for they retain the oil phase.

Nickel micro-sieves have been tested for the first time to produce lemon oil emulsions in premix mode (Chapter 4). Lemon oil emulsions were successfully refined with nickel micro-sieves; however, several considerations have to be taken into account. The oil fraction of Tween 20 stabilized emulsions has to be maintained low (about 5%wt.) and the relationship between the droplet size of the coarse emulsion and the hydraulic diameter of the pores (d_{coarse}/d_h) has to be lower than 1 to allow emulsion refinement. The nickel micro-sieves need to go through a mild cleaning process to maintain the physical integrity and to be reused. Following these limitations, lemon oil emulsions with 0.5 μm droplet size can be produced at transmembrane fluxes that can reach 1000 $\text{m}^3 \cdot \text{m}^{-2} \cdot \text{h}^{-1}$ at 450 kPa.

An alternative microporous system consisting of a layer of silica beads added on top of the nickel micro-sieve, referred to as DMTS system, was tested to encapsulate lemon oil (Chapter 5). With the DMTS system, it was possible to increase the oil fraction of Tween 20 stabilized emulsions up to 40%wt., moreover,

24 μm sized coarse emulsions could be easily refined. An extra advantage of the DMTS system is that in this configuration, the nickel micro-sieve kept its integrity and could be reused up to 20 times. With the DMTS system, stable emulsions of 2-3 μm were produced with very narrow droplet size distribution. The main asset of the DMTS system is the ability to control the outcoming droplet size of the emulsion by controlling the interstitial void diameter of the bed (silica beads size) and layer height (beads amount). This is especially the case with the layered DMTS system, which is composed by two superimposed layers of different porosity. The layered DMTS system has allowed a cut-back on the energy inputted to the system while maintaining a high throughput and droplet size reduction with span values ≤ 1 .

Conventional dairy proteins, such as whey protein and sodium caseinate, and a WP-CMC electrostatic complex successfully stabilized 20% wt. lemon oil emulsions produced with the DMTS system (Chapter 6). In general, it can be seen that an increase in the bed height and a reduction of the interstitial void diameter reduces the extend of droplet break up, owing to a reduction in the velocity in the channels of the microporous system. The emulsion fluxes obtained with biopolymer stabilized emulsions with the DMTS system are still in the upper range of the values reported for emulsions stabilized with proteins obtained with premix membrane emulsification. As for the physical stability, the emulsions stabilized with WP or NaCaS were stable for 7 days at 4 and 25 $^{\circ}\text{C}$, while the emulsions stabilized with WP-CMC complex were stable if maintained under refrigeration. Since it has been previously established that WP-CMC electrostatic complex increases protection against deterioration of certain key volatile components of lemon oil aroma, finding a robust emulsification technique with high fluxes at low energy input is highly relevant for industrial scale-up. Moreover, the use of the layered DMTS system allowed to refine lemon oil emulsions stabilized with the electrostatic complex having lowest span value, of 0.82, reported.

In general, the DMTS system, and the layered DMTS in particular, is a low-energy, high-throughput microporous emulsification technology that has more potential for scaling-up than other low-energy emulsification systems such as SPG membranes. It can be tuned according to the specifications of the emulsion to obtain a narrow droplet size distribution. It allows the use of biopolymers as stabilizing agents, maintaining emulsification fluxes over $200 \text{ m}^3 \cdot \text{m}^{-2} \cdot \text{h}^{-1}$, and finally it is easy to clean and reuse.

The potential of using other type of biopolymers, such as plant proteins, to stabilize oil/water emulsions is assessed using pea protein with microfluidics (Chapter 7). A microfluidics study showed, on a micro-level scale, that a minimum of 0.5 g/L pea protein concentration with minimum of 65ms adsorption time are required to stabilize oil droplets. Continuous phase flow rate also proved to be able to control oil droplet size and stability.

8.2. Future work

This thesis covered the physical stability of emulsions produced with the DMTS system. However, a chemical stability of the emulsions is also necessary so verify if the improvement in droplet size dispersity, over span values obtained from conventional membrane affected the aroma profile. More importantly, the DMTS produces emulsions with all the predispositions to be follow up with a spray drying step.

The emulsifiers tested for stabilizing LO emulsions in the DMTS system include, but are not limited to: WP (pH: 6.8) and WP-CMC (pH:3.8). It would have been interesting to form emulsions stabilized with WP (pH:3.8) to have a reference of a positively charged surfactant and its effects on stability.

On a broader point of view, it was shown that the DMTS renders a high-throughput. But tests of durability would have given a more complete view of its scale up potential. At the moment emulsions of about 200 mL have been refined. It would be interesting to produce 2L emulsions and observed if the system fouls. Another option would also be refining 200 mL emulsions many times monitoring if the end product flows at the same rate, and the droplet size and size distribution remain the same. That would show how often the cleaning step is required and if there a possibility in economizing in that step.

Nevertheless, it is still necessary to figure out the droplet break-up mechanisms in the DMTS system and especially with the modified DMST. Having two superimposed layers of beads of different sizes results in two different Reynolds numbers in along the bed. Being able to measure and calculate the different pore velocities would allow the calculation of the dimensionless Reynolds number. The calculation of such number is imperative for understanding droplet break-up mechanisms and for scale-up. Moreover, it cannot be stressed enough the importance of controlling the porosity of the nickel micro-sieve in the DMTS

system. For experiments that need to be compared the same micro-sieve has to be used otherwise it will be difficult later on to homogenize the results and observe trends.

Finally, plant protein and more and more studied with the increasing demand on proteins. It would be interesting to try stabilizing lemon oil droplets in the microfluidics chip. From these results, lemon oil emulsions stabilized with pea proteins can be produced with the DMTS systems and the droplet stabilization mechanism understood furtherly.

References

1. Charcosset, C. Preparation of emulsions and particles by membrane emulsification for the food processing industry. *J. Food Eng.* **92**, 241–249 (2009).
2. Vladislavljević, G. T., Shimizu, M. & Nakashima, T. Production of multiple emulsions for drug delivery systems by repeated SPG membrane homogenization: Influence of mean pore size, interfacial tension and continuous phase viscosity. *J. Memb. Sci.* **284**, 373–383 (2006).
3. Vladislavljević, G. T., Lambrich, U., Nakajima, M. & Schubert, H. Production of O/W emulsions using SPG membranes, ceramic α -aluminium oxide membranes, microfluidizer and a silicon microchannel plate - A comparative study. *Colloids Surfaces A Physicochem. Eng. Asp.* **232**, 199–207 (2004).
4. Zhang, Y. *et al.* Investigation on the uniformity and stability of sunflower oil/water emulsions prepared by a Shirasu porous glass membrane. *Ind. Eng. Chem. Res.* **47**, 6412–6417 (2008).
5. Vladislavljević, G. T. Structured microparticles with tailored properties produced by membrane emulsification. *Adv. Colloid Interface Sci.* **225**, 53–87 (2015).
6. McClements, D. J. *Food emulsions: Principles, practices, and techniques: Second edition. Food Emulsions: Principles, Practices, and Techniques, Second Edition* (2004).
7. Håkansson, A. Can high-pressure homogenization cause thermal degradation to nutrients? *J. Food Eng.* **240**, 133–144 (2019).
8. Santos, J., Vladislavljević, G. T., Holdich, R. G., Dragosavac, M. M. & Muñoz, J. Controlled production of eco-friendly emulsions using direct and premix membrane emulsification. *Chem. Eng. Res. Des.* **98**, 59–69 (2015).
9. Laouini, A., Charcosset, C., Fessi, H. & Schroen, K. Use of dynamic membranes for the preparation of vitamin E-loaded lipid particles: An alternative to prevent fouling observed in classical cross-flow emulsification. *Chem. Eng. J.* **236**, 498–505 (2014).
10. Schadler, V. & Windhab, E. J. Continuous membrane emulsification by using a membrane system with controlled pore distance. *Desalination* **189**,

- 130–135 (2006).
11. Pu, X., Wolf, B. & Dragosavac, M. Generation of magnesium enriched water-in-oil-in-water food emulsions by stirred cell membrane emulsification. *J. Food Eng.* **247**, 178–187 (2019).
 12. Dragosavac, M. M., Holdich, R. G., Vladisavljević, G. T. & Sovilj, M. N. Stirred cell membrane emulsification for multiple emulsions containing unrefined pumpkin seed oil with uniform droplet size. *J. Memb. Sci.* **392–393**, 122–129 (2012).
 13. Piacentini, E., Giorno, L., Dragosavac, M. M., Vladisavljević, G. T. & Holdich, R. G. Microencapsulation of oil droplets using cold water fish gelatine/gum arabic complex coacervation by membrane emulsification. *Food Res. Int.* **53**, 362–372 (2013).
 14. Holdich, R. G., Dragosavac, M. M., Vladisavljević, G. T. & Piacentini, E. Continuous membrane emulsification with pulsed (oscillatory) flow. *Ind. Eng. Chem. Res.* **52**, 507–515 (2013).
 15. Kosvintsev, S. R., Gasparini, G., Holdich, R. G., Cumming, I. W. & Stillwell, M. T. Liquid - Liquid membrane dispersion in a stirred cell with and without controlled shear. *Ind. Eng. Chem. Res.* **44**, 9323–9330 (2005).
 16. Pan, X., York, D., Preece, J. A. & Zhang, Z. Size and strength distributions of melamine-formaldehyde microcapsules prepared by membrane emulsification. *Powder Technol.* **227**, 43–50 (2012).
 17. Egidi, E., Gasparini, G., Holdich, R. G., Vladisavljević, G. T. & Kosvintsev, S. R. Membrane emulsification using membranes of regular pore spacing: Droplet size and uniformity in the presence of surface shear. *J. Memb. Sci.* **323**, 414–420 (2008).
 18. Holdich, R. G., Dragosavac, M. M., Vladisavljević, G. T. & Kosvintsev, S. R. Membrane emulsification with oscillating and stationary membranes. *Ind. Eng. Chem. Res.* **49**, 3810–3817 (2010).
 19. Holzapfel, S., Rondeau, E., Mühlich, P. & Windhab, E. J. Drop detachment from a micro-engineered membrane surface in a dynamic membrane emulsification process. *Chem. Eng. Technol.* **36**, 1785–1794 (2013).
 20. Nazir, A., Schroën, K. & Boom, R. High-throughput premix membrane emulsification using nickel sieves having straight-through pores. *J. Memb. Sci.* **383**, 116–123 (2011).

21. Nazir, A., Schroën, K. & Boom, R. The effect of pore geometry on premix membrane emulsification using nickel sieves having uniform pores. *Chem. Eng. Sci.* **93**, 173–180 (2013).
22. Sawalha, H., Sahin, S. & Schroën, K. Preparation of polylactide microcapsules at a high throughput with a packed-bed premix emulsification system. *J. Appl. Polym. Sci.* **133**, 3–9 (2016).
23. Cheetangdee, N. & Fukada, K. Protein stabilized oil-in-water emulsions modified by uniformity of size by premix membrane extrusion and their colloidal stability. *Colloids Surfaces A Physicochem. Eng. Asp.* **403**, 54–61 (2012).
24. Trentin, A., Ferrando, M., López, F. & Güell, C. Premix membrane O/W emulsification: Effect of fouling when using BSA as emulsifier. *Desalination* **245**, 388–395 (2009).
25. Lloyd, D. M., Norton, I. T. & Spyropoulos, F. Processing effects during rotating membrane emulsification. *J. Memb. Sci.* **466**, 8–17 (2014).
26. Van Der Zwan, E. A., Schroën, C. G. P. H. & Boom, R. M. Premix membrane emulsification by using a packed layer of glass beads. *AIChE J.* **54**, 2190–2197 (2008).
27. Vladislavljević, G. T., Shimizu, M. & Nakashima, T. Preparation of monodisperse multiple emulsions at high production rates by multi-stage premix membrane emulsification. *J. Memb. Sci.* **244**, 97–106 (2004).
28. Surh, J., Jeong, Y. G. & Vladislavljević, G. T. On the preparation of lecithin-stabilized oil-in-water emulsions by multi-stage premix membrane emulsification. *J. Food Eng.* **89**, 164–170 (2008).
29. Kandori, K. Chapter 7 - Applications of microporous glass membranes: Membrane emulsification. in *Food Processing* (ed. Gaonkar, A. G.) 113–142 (Elsevier Science B.V., 1995). doi:<https://doi.org/10.1016/B978-044481500-2/50009-8>
30. SUZUKI, K., SHUTO, I. & HAGURA, Y. Characteristics of the Membrane Emulsification Method Combined with Preliminary Emulsification for Preparing Corn Oil-in-Water Emulsions. *Food Sci. Technol. Int. Tokyo* **2**, 43–47 (1996).
31. Matos, M., Gutiérrez, G., Iglesias, O., Coca, J. & Pazos, C. Characterization, stability and rheology of highly concentrated monodisperse emulsions

- containing lutein. *Food Hydrocoll.* **49**, 156–163 (2015).
32. Mugabi, J. *et al.* Preparation of small droplet size monodispersed emulsions at high production rate by continuous intramembrane premix emulsification method. *J. Chem. Eng. Japan* **52**, 259–266 (2019).
 33. Alliod, O. *et al.* Preparation of oil-in-water nanoemulsions at large-scale using premix membrane emulsification and Shirasu Porous Glass (SPG) membranes. *Colloids Surfaces A Physicochem. Eng. Asp.* **0–1** (2018). doi:10.1016/j.colsurfa.2018.04.045
 34. Vladisavljević, G. T., Kobayashi, I. & Nakajima, M. Production of uniform droplets using membrane, microchannel and microfluidic emulsification devices. *Microfluid. Nanofluidics* **13**, 151–178 (2012).
 35. Vladisavljević, G. T. Preparation of microemulsions and nanoemulsions by membrane emulsification. *Colloids Surfaces A Physicochem. Eng. Asp.* **579**, 123709 (2019).
 36. Vladisavljević, G. T., Surh, J. & McClements, J. D. Effect of emulsifier type on droplet disruption in repeated Shirasu porous glass membrane homogenization. *Langmuir* **22**, 4526–4533 (2006).
 37. Matos, M., Suárez, M. A., Gutiérrez, G., Coca, J. & Pazos, C. Emulsification with microfiltration ceramic membranes: A different approach to droplet formation mechanism. *J. Memb. Sci.* **444**, 345–358 (2013).
 38. Zwan, E., Schroën, K. & Boom, R. M. Premix Membrane Emulsification by Using a Packed Layer of Glass Beads. *IFAC Proc. Vol.* **7**, 405–410 (2009).
 39. Nazir, A., Schroën, K. & Boom, R. High-throughput premix membrane emulsification using nickel sieves having straight-through pores. *Chem. Eng. Sci.* **93**, 173–180 (2013).
 40. Nazir, A., Boom, R. M. & Schroën, K. Droplet break-up mechanism in premix emulsification using packed beds. *Chem. Eng. Sci.* **92**, 190–197 (2013).
 41. Nazir, A., Boom, R. M. & Schroën, K. Influence of the emulsion formulation in premix emulsification using packed beds. *Chem. Eng. Sci.* **116**, 547–557 (2014).
 42. Ladjal Ettoumi, Y., Berton-Carabin, C., Chibane, M. & Schroën, K. Legume Protein Isolates for Stable Acidic Emulsions Prepared by Premix

- Membrane Emulsification. *Food Biophys.* **12**, 119–128 (2017).
43. Laouini, A., Charcosset, C., Fessi, H. & Schroen, K. Use of dynamic membranes for the preparation of vitamin E-loaded lipid particles: An alternative to prevent fouling observed in classical cross-flow emulsification. *Chem. Eng. J.* **236**, 498–505 (2014).
 44. Eisinaite, V., Juraite, D., Schroën, K. & Leskauskaite, D. Preparation of stable food-grade double emulsions with a hybrid premix membrane emulsification system. *Food Chem.* **206**, 59–66 (2016).
 45. Sahin, S., Sawalha, H. & Schroën, K. High throughput production of double emulsions using packed bed premix emulsification. *Food Res. Int.* **66**, 78–85 (2014).
 46. Nazir, A., Maan, A. A., Sahin, S., Boom, R. M. & Schroën, K. Foam preparation at high-throughput using a novel packed bed system. *Food Bioprod. Process.* **94**, 561–564 (2015).
 47. Yasuda, M., Goda, T., Ogino, H., Glomm, W. R. & Takayanagi, H. Preparation of uniform monomer droplets using packed column and continuous polymerization in tube reactor. *J. Colloid Interface Sci.* **349**, 392–401 (2010).
 48. Cortés-Camargo, S. *et al.* Microencapsulation by spray drying of lemon essential oil: Evaluation of mixtures of mesquite gum–nopal mucilage as new wall materials. *J. Microencapsul.* **34**, 395–407 (2017).
 49. Bai, L., Huan, S., Li, Z. & McClements, D. J. Comparison of emulsifying properties of food-grade polysaccharides in oil-in-water emulsions: Gum arabic, beet pectin, and corn fiber gum. *Food Hydrocoll.* **66**, 144–153 (2017).
 50. BANGS, W. E. & REINECCIUS, G. A. Characterization of Selected Materials for Lemon Oil Encapsulation by Spray Drying. *J. Food Sci.* **55**, 1356–1358 (1990).
 51. Bhandari, B. R., Arcy, B. R. D., Le, L. & Bich, T. Lemon Oil to -Cyclodextrin Ratio Effect on the Inclusion Efficiency of -Cyclodextrin and the Retention of Oil Volatiles in the Complex. *Analysis* **8561**, 1494–1499 (1998).
 52. Park, S.-J., Shin, Y.-S. & Lee, J.-R. Preparation and Characterization of Microcapsules Containing Lemon Oil. *J. Colloid Interface Sci.* **241**, 502–508 (2001).

53. Treesuwan, W., Neves, M. A., Uemura, K., Nakajima, M. & Kobayashi, I. Preparation characteristics of monodisperse oil-in-water emulsions by microchannel emulsification using different essential oils. *LWT - Food Sci. Technol.* **84**, 617–625 (2017).
54. Santos, J., Trujillo-Cayado, L. A., Calero, N., Alfaro, M. C. & Muñoz, J. Development of eco-friendly emulsions produced by microfluidization technique. *J. Ind. Eng. Chem.* **36**, 90–95 (2016).
55. Trujillo-Cayado, L. A., Alfaro, M. C., García, M. C. & Muñoz, J. Comparison of homogenization processes for the development of green O/W emulsions formulated with N,N-dimethyldecanamide. *J. Ind. Eng. Chem.* **46**, 54–61 (2017).
56. Lou, Z. *et al.* The antioxidant, antibacterial, antibiofilm activity of essential oil from *Citrus medica* L. var. *sarcodactylis* and its nanoemulsion. *LWT - Food Sci. Technol.* **80**, 371–377 (2017).
57. Zhao, S. *et al.* The stability of three different citrus oil-in-water emulsions fabricated by spontaneous emulsification. *Food Chem.* **269**, 577–587 (2018).
58. Ramakrishnan, S., Ferrando, M., Aceña-Muñoz, L., De Lamo-Castellví, S. & Güell, C. Fish Oil Microcapsules from O/W Emulsions Produced by Premix Membrane Emulsification. *Food Bioprocess Technol.* **6**, 3088–3101 (2013).
59. Leimann, F. V., Gonçalves, O. H., Machado, R. A. F. & Bolzan, A. Antimicrobial activity of microencapsulated lemongrass essential oil and the effect of experimental parameters on microcapsules size and morphology. *Mater. Sci. Eng. C* **29**, 430–436 (2009).
60. Fang, Z., Comino, P. R. & Bhandari, B. Effect of encapsulation of d-limonene on the moisture adsorption property of β -cyclodextrin. *LWT - Food Sci. Technol.* **51**, 164–169 (2013).
61. Bhandari, B. R., D’Arcy, B. R. & Padukka, I. Encapsulation of lemon oil by paste method using β -cyclodextrin: Encapsulation efficiency and profile of oil volatiles. *J. Agric. Food Chem.* **47**, 5194–5197 (1999).
62. Yuliani, S., Torley, P. J., D’Arcy, B., Nicholson, T. & Bhandari, B. Extrusion of mixtures of starch and D-limonene encapsulated with β -cyclodextrin: Flavour retention and physical properties. *Food Res. Int.* **39**, 318–331 (2006).

63. Reineccius, T. A., Reineccius, G. A. & Peppard, T. L. Utilization of β -Cyclodextrin for Improved Flavor Retention in Thermally Processed Foods. *J. Food Sci.* **69**, (2004).
64. Chen, Y. *et al.* Effect of zein-based microencapsules on the release and oxidation of loaded limonene. *Food Hydrocoll.* **84**, 330–336 (2018).
65. Koh, A. & Gross, R. A versatile family of sophorolipid esters: Engineering surfactant structure for stabilization of lemon oil-water interfaces. *Colloids Surfaces A Physicochem. Eng. Asp.* **507**, 152–163 (2016).
66. Santos, J., Trujillo-Cayado, L. A., Calero, N. & Muñoz, J. Physical characterization of eco-friendly O/W emulsions developed through a strategy based on product engineering principles. *AIChE J.* **60**, 2644–2653 (2014).
67. Cortés-Camargo, S. *et al.* Effect of chia mucilage addition on oxidation and release kinetics of lemon essential oil microencapsulated using mesquite gum – Chia mucilage mixtures. *Food Res. Int.* **116**, 1010–1019 (2019).
68. Rao, J. & McClements, D. J. Food-grade microemulsions, nanoemulsions and emulsions: Fabrication from sucrose monopalmitate & lemon oil. *Food Hydrocoll.* **25**, 1413–1423 (2011).
69. Rao, J. & McClements, D. J. Lemon oil solubilization in mixed surfactant solutions: Rationalizing microemulsion & nanoemulsion formation. *Food Hydrocoll.* **26**, 268–276 (2012).
70. Xue, F., Gu, Y., Wang, Y., Li, C. & Adhikari, B. Encapsulation of essential oil in emulsion based edible films prepared by soy protein isolate-gum acacia conjugates. *Food Hydrocoll.* **96**, 178–189 (2019).
71. Sabik, H. *et al.* Study of chemical stability of lemon oil components in sodium caseinate-lactose glycoconjugate-stabilized oil-in-water emulsions using solid-phase microextraction-gas chromatography. *Food Funct.* **5**, 1495–1505 (2014).
72. Huynh, T. V., Caffin, N., Dykes, G. & Bhandari, B. Optimization of the microencapsulation of lemon myrtle oil using response surface methodology. *Dry. Technol.* **26**, 357–368 (2008).
73. Choi, S. J., Decker, E. A., Henson, L., Popplewell, L. M. & McClements, D. J. Influence of Droplet Charge on the Chemical Stability of Citral in Oil-in-Water Emulsions. *J. Food Sci.* **75**, C536–C540 (2010).

74. Nirmal, N. P., Mereddy, R., Li, L. & Sultanbawa, Y. Formulation, characterisation and antibacterial activity of lemon myrtle and anise myrtle essential oil in water nanoemulsion. *Food Chem.* **254**, 1–7 (2018).
75. Galindo-Pérez, M. J., Quintanar-Guerrero, D., de los Ángeles Cornejo-Villegas, M. & de la Luz Zambrano-Zaragoza, M. Optimization of the emulsification-diffusion method using ultrasound to prepare nanocapsules of different food-core oils. *LWT* **87**, 333–341 (2018).
76. Rao, J. & McClements, D. J. Impact of lemon oil composition on formation and stability of model food and beverage emulsions. *Food Chem.* **134**, 749–757 (2012).
77. Jo, Y.-J., Choi, M.-J., Hong, G.-P. & Kwon, Y. J. A comparison of physicochemical stabilities of β -carotene-loaded nanoemulsions prepared with different food proteins. *J. Food Meas. Charact.* **13**, 1373–1381 (2019).
78. Yi, J., Zhu, Z., McClements, D. J. & Decker, E. A. Influence of Aqueous Phase Emulsifiers on Lipid Oxidation in Water-in-Walnut Oil Emulsions. *J. Agric. Food Chem.* **62**, 2104–2111 (2014).
79. Djordjevic, D., Cercaci, L., Alamed, J., McClements, D. J. & Decker, E. A. Stability of citral in protein- and gum arabic-stabilized oil-in-water emulsions. *Food Chem.* **106**, 698–705 (2008).
80. Srinivasan, M., Singh, H. & Munro, P. A. Sodium Caseinate-Stabilized Emulsions: Factors Affecting Coverage and Composition of Surface Proteins. *J. Agric. Food Chem.* **44**, 3807–3811 (1996).
81. Alves, A. C. & Tavares, G. M. Mixing animal and plant proteins: Is this a way to improve protein techno-functionalities? *Food Hydrocoll.* **97**, (2019).
82. Grigoriev, D. O. & Miller, R. Mono- and multilayer covered drops as carriers. *Curr. Opin. Colloid Interface Sci.* **14**, 48–59 (2009).
83. Mun, S., Decker, E. A. & McClements, D. J. Influence of emulsifier type on in vitro digestibility of lipid droplets by pancreatic lipase. *Food Res. Int.* **40**, 770–781 (2007).
84. Malinauskytė, E. *et al.* Impact of Interfacial Composition on Emulsion Digestion Using In Vitro and In Vivo Models. *J. Food Sci.* **83**, 2850–2857 (2018).
85. Bakry, A. M. *et al.* Stability of tuna oil and tuna oil/peppermint oil blend

- microencapsulated using whey protein isolate in combination with carboxymethyl cellulose or pullulan. *Food Hydrocoll.* **60**, 559–571 (2016).
86. Dickinson, E. Interfacial structure and stability of food emulsions as affected by protein–polysaccharide interactions. *Soft Matter* **4**, 932–942 (2008).
 87. Berendsen, R., Güell, C., Henry, O. & Ferrando, M. Premix membrane emulsification to produce oil-in-water emulsions stabilized with various interfacial structures of whey protein and carboxymethyl cellulose. *Food Hydrocoll.* **38**, 1–10 (2014).
 88. Barac, M. *et al.* Profile and functional properties of seed proteins from six pea (*Pisum sativum*) genotypes. *Int. J. Mol. Sci.* **11**, 4973–4990 (2010).
 89. Burger, T. G. & Zhang, Y. Recent progress in the utilization of pea protein as an emulsifier for food applications. *Trends Food Sci. Technol.* **86**, 25–33 (2019).
 90. Hinderink, E. B. A., Münch, K., Sagis, L., Schroën, K. & Berton-Carabin, C. C. Synergistic stabilisation of emulsions by blends of dairy and soluble pea proteins: Contribution of the interfacial composition. *Food Hydrocoll.* **97**, 105206 (2019).
 91. Zha, F., Dong, S., Rao, J. & Chen, B. Pea protein isolate-gum Arabic Maillard conjugates improves physical and oxidative stability of oil-in-water emulsions. *Food Chem.* **285**, 130–138 (2019).
 92. Liu, C., Bhattarai, M., Mikkonen, K. S. & Heinonen, M. Effects of Enzymatic Hydrolysis of Fava Bean Protein Isolate by Alcalase on the Physical and Oxidative Stability of Oil-in-Water Emulsions. *J. Agric. Food Chem.* **67**, 6625–6632 (2019).
 93. Nikbakht Nasrabadi, M., Goli, S. A. H., Sedaghat Doost, A., Dewettinck, K. & Van der Meeren, P. Bioparticles of flaxseed protein and mucilage enhance the physical and oxidative stability of flaxseed oil emulsions as a potential natural alternative for synthetic surfactants. *Colloids Surfaces B Biointerfaces* **184**, 110489 (2019).
 94. Le Priol, L. *et al.* Comparative study of plant protein extracts as wall materials for the improvement of the oxidative stability of sunflower oil by microencapsulation. *Food Hydrocoll.* **95**, 105–115 (2019).
 95. Pan, X. *et al.* Covalent Interaction between Rice Protein Hydrolysates and

- Chlorogenic Acid: Improving the Stability of Oil-in-Water Emulsions. *J. Agric. Food Chem.* **67**, 4023–4030 (2019).
96. Li, R. *et al.* Bioaccessibility and stability of β -carotene encapsulated in plant-based emulsions: impact of emulsifier type and tannic acid. *Food Funct.* 7239–7252 (2019). doi:10.1039/c9fo01370a
 97. Chen, J., Mu, T., Zhang, M. & Goffin, D. Effect of heat treatments on the structure and emulsifying properties of protein isolates from cumin seeds (*Cuminum cyminum*). *Food Sci. Technol. Int.* **24**, 673–687 (2018).
 98. Karefyllakis, D., Octaviana, H., van der Goot, A. J. & Nikiforidis, C. V. The emulsifying performance of mildly derived mixtures from sunflower seeds. *Food Hydrocoll.* **88**, 75–85 (2019).
 99. Silva, J. V. C. *et al.* Heat-induced gelation of micellar casein / plant protein oil-in-water emulsions. **569**, 85–92 (2019).
 100. Nikbakht Nasrabadi, M. *et al.* Plant based Pickering stabilization of emulsions using soluble flaxseed protein and mucilage nano-assemblies. *Colloids Surfaces A Physicochem. Eng. Asp.* **563**, 170–182 (2019).
 101. Chen, Y., Zhang, R., Xie, B., Sun, Z. & McClements, D. J. Lotus seedpod proanthocyanidin-whey protein complexes: Impact on physical and chemical stability of β -carotene-nanoemulsions. *Food Res. Int.* **127**, (2020).
 102. Walia, N. & Chen, L. Pea protein based vitamin D nanoemulsions: Fabrication, stability and in vitro study using Caco-2 cells. *Food Chem.* **305**, 125475 (2020).
 103. Wang, Y., Ghosh, S. & Nickerson, M. T. Effect of pH on the formation of electrostatic complexes between lentil protein isolate and a range of anionic polysaccharides, and their resulting emulsifying properties. *Food Chem.* **298**, (2019).
 104. Taha, A. *et al.* Effects of different ionic strengths on the physicochemical properties of plant and animal proteins-stabilized emulsions fabricated using ultrasound emulsification. *Ultrason. Sonochem.* **58**, (2019).
 105. Schieberle, P. & Grosch, W. Identification of potent flavor compounds formed in an aqueous lemon oil/citric acid emulsion. *J. Agric. Food Chem.* **36**, 797–800 (1988).
 106. Nguyen, H., Campi, E. M., Roy Jackson, W. & Patti, A. F. Effect of oxidative

- deterioration on flavour and aroma components of lemon oil. *Food Chem.* **112**, 388–393 (2009).
107. Shaw, P. E. Review of Quantitative Analyses of Citrus Essential Oils. *J. Agric. Food Chem.* **27**, 246–257 (1979).
 108. Pérez-López, A. J., Saura, D., Lorente, J. & Carbonell-Barrachina, A. A. Limonene, linalool, α -terpineol, and terpinen-4-ol as quality control parameters in mandarin juice processing. *Eur. Food Res. Technol.* **222**, 281–285 (2006).
 109. Qian, C. & McClements, D. J. Formation of nanoemulsions stabilized by model food-grade emulsifiers using high-pressure homogenization: Factors affecting particle size. *Food Hydrocoll.* **25**, 1000–1008 (2011).
 110. Yang, Y. *et al.* A soy protein-polysaccharides Maillard reaction product enhanced the physical stability of oil-in-water emulsions containing citral. *Food Hydrocoll.* **48**, 155–164 (2015).
 111. Xiang, J., Liu, F., Fan, R. & Gao, Y. Physicochemical stability of citral emulsions stabilized by milk proteins (lactoferrin, α -lactalbumin, β -lactoglobulin) and beet pectin. *Colloids Surfaces A Physicochem. Eng. Asp.* **487**, 104–112 (2015).
 112. Su, J., Guo, Q., Mao, L., Gao, Y. & Yuan, F. Effect of gum arabic on the storage stability and antibacterial ability of β -lactoglobulin stabilized D-limonene emulsion. *Food Hydrocoll.* **84**, 75–83 (2018).
 113. Wang, J., Oussama Khelissa, S., Chihib, N. E., Dumas, E. & Gharsallaoui, A. Effect of drying and interfacial membrane composition on the antimicrobial activity of emulsified citral. *Food Chem.* **298**, 1–7 (2019).
 114. Guzey, D. & McClements, D. J. Formation, stability and properties of multilayer emulsions for application in the food industry. *Adv. Colloid Interface Sci.* **128–130**, 227–248 (2006).
 115. Berendsen, R., Güell, C. & Ferrando, M. A procyanidin-rich extract encapsulated in water-in-oil-in-water emulsions produced by premix membrane emulsification. *Food Hydrocoll.* **43**, 636–648 (2015).
 116. Estévez, M., Güell, C., De Lamo-Castellví, S. & Ferrando, M. Encapsulation of grape seed phenolic-rich extract within W/O/W emulsions stabilized with complexed biopolymers: Evaluation of their stability and release. *Food Chem.* **272**, 478–487 (2019).

117. Kim, H. J., Decker, E. A. & McClements, D. J. Impact of protein surface denaturation on droplet flocculation in hexadecane oil-in-water emulsions stabilized by β -lactoglobulin. *J. Agric. Food Chem.* **50**, 7131–7137 (2002).
118. McCLEMENTS, D. J., MONAHAN, F. J. & KINSELLA, J. E. Disulfide Bond Formation Affects Stability of Whey Protein Isolate Emulsions. *J. Food Sci.* **58**, 1036–1039 (1993).
119. Uçan, F., Ağçam, E. & Akyildiz, A. Bioactive compounds and quality parameters of natural cloudy lemon juices. *J. Food Sci. Technol.* **53**, 1465–1474 (2016).
120. Xi, W., Lu, J., Qun, J. & Jiao, B. Characterization of phenolic profile and antioxidant capacity of different fruit part from lemon (*Citrus limon* Burm.) cultivars. *J. Food Sci. Technol.* **54**, 1108–1118 (2017).
121. Murase, T., Ohn, T. & Kamimura, K. Dynamic Microfiltration of Dilute O/W Emulsion in Rotating Cylindrical Membrane Filter. *KAGAKU KOGAKU RONBUNSHU* **22**, 120–126 (1996).
122. Nazir, A., Schroën, K. & Boom, R. Premix emulsification: A review. *J. Memb. Sci.* **362**, 1–11 (2010).
123. Güell, C., Ferrando, M. & Schroën, K. Membranes for Enhanced Emulsification Processes. in *Innovative Food Processing Technologies Extraction, Separation, Component Modification and Process Intensification* 429–453 (2016). doi:10.1016/B978-0-08-100294-0.00017-1
124. Sahin, S., Bliznyuk, O., Rovalino Cordova, A. & Schroën, K. Microfluidic EDGE emulsification: the importance of interface interactions on droplet formation and pressure stability. *Sci. Rep.* **6**, 26407 (2016).
125. Schroën, K., Ferrando, M., de Lamo-Castellví, S., Sahin, S. & Güell, C. Linking Findings in Microfluidics to Membrane Emulsification Process Design: The Importance of Wettability and Component Interactions with Interfaces. *Membranes (Basel)*. **6**, 26 (2016).
126. Eunok, C. & B., Min, D. Mechanisms and Factors for Edible Oil Oxidation. *Compr. Rev. Food Sci. Food Saf.* **5**, 169–186 (2006).
127. Gromponea, M. A. & Moynab, P. Geometric Isomerization of Fatty Acids with Nickel Catalyst. *J. Am. Oil Chem. Soc.* **63**, 550–551 (1986).
128. MALACRIDA, C. R., KIMURA, M. & JORGE, N. Phytochemicals and

- Antioxidant Activity of Citrus Seed Oils. *Food Sci. Technol. Res.* **18**, 399–404 (2012).
129. Suárez, M. A., Gutiérrez, G., Coca, J. & Pazos, C. Stirred tank membrane emulsification using flat metallic membranes: A dimensional analysis. *Chem. Eng. Process. Process Intensif.* **69**, 31–43 (2013).
130. Neves, M. A., Wang, Z., Kobayashi, I. & Nakajima, M. Assessment of Oxidative Stability in Fish Oil-in-Water Emulsions: Effect of Emulsification Process, Droplet Size and Storage Temperature. *J. Food Process Eng.* **40**, (2017).
131. Joscelyne, S. M. & Trägårdh, G. Food emulsions using membrane emulsification: Conditions for producing small droplets. *J. Food Eng.* **39**, 59–64 (1999).
132. Di Vaio, C. *et al.* Essential oils content and antioxidant properties of peel ethanol extract in 18 lemon cultivars. *Sci. Hortic. (Amsterdam)*. **126**, 50–55 (2010).
133. Singh, P. *et al.* Chemical profile, antifungal, antiaflatoxic and antioxidant activity of Citrus maxima Burm. and Citrus sinensis (L.) Osbeck essential oils and their cyclic monoterpene, DL-limonene. *Food Chem. Toxicol.* **48**, 1734–1740 (2010).
134. Bonilla-Reyna, B., Sosa-Herrera, M. G. & Martínez-Padilla, L. P. Interfacial adsorption and shear flow properties of gum arabic-sodium caseinate mixtures. *Procedia Food Sci.* **1**, 12–16 (2011).
135. Verkempinck, S. H. E. *et al.* Emulsion stabilizing properties of citrus pectin and its interactions with conventional emulsifiers in oil-in-water emulsions. *Food Hydrocoll.* **85**, 144–157 (2018).
136. Nor Hayati, I., Che Man, Y. Bin, Tan, C. P. & Nor Aini, I. Droplet characterization and stability of soybean oil/palm kernel olein O/W emulsions with the presence of selected polysaccharides. *Food Hydrocoll.* **23**, 233–243 (2009).
137. Muijlwijk, K. *et al.* Coalescence of protein-stabilised emulsions studied with microfluidics. *Food Hydrocoll.* **70**, 96–104 (2017).
138. Krebs, T., Schroën, K. & Boom, R. Coalescence dynamics of surfactant-stabilized emulsions studied with microfluidics. *Soft Matter* **8**, 10650–10657 (2012).

139. Smith, P. K. *et al.* Measurement of protein using bicinchoninic acid. *Anal. Biochem.* **150**, 76–85 (1985).
140. Muijlwijk, K., Huang, W., Vuist, J. E., Berton-Carabin, C. & Schroën, K. Convective mass transport dominates surfactant adsorption in a microfluidic Y-junction. *Soft Matter* **12**, 9025–9029 (2016).
141. SUZUKI, K., FUJIKI, I. & HAGURA, Y. Preparation of Corn Oil/Water and Water/Corn Oil Emulsions Using PTFE Membranes. *Food Sci. Technol. Int. Tokyo* **4**, 164–167 (1998).
142. Zhou, Q. Z., Ma, G. H. & Su, Z. G. Effect of membrane parameters on the size and uniformity in preparing agarose beads by premix membrane emulsification. *J. Memb. Sci.* **326**, 694–700 (2009).
143. Shima, M. *et al.* Preparation of fine W/O/W emulsion through membrane filtration of coarse W/O/W emulsion and disappearance of the inclusion of outer phase solution. *Food Hydrocoll.* **18**, 61–70 (2004).
144. Jing, W., Wu, J., Xing, W., Jin, W. & Xu, N. Emulsions prepared by two-stage ceramic membrane jet-flow emulsification. *AIChE J.* **51**, 1339–1345 (2005).
145. Sawalha, H., Purwanti, N., Rinzema, A., Schroën, K. & Boom, R. Polylactide microspheres prepared by premix membrane emulsification-Effects of solvent removal rate. *J. Memb. Sci.* **310**, 484–493 (2008).

UNIVERSITAT ROVIRA I VIRGILI

LOW-ENERGY HIGH-THROUGHPUT MICROPOROUS EMULSIFICATION FOR LEMON OIL ENCAPSULATION

Wael Kaade

UNIVERSITAT ROVIRA I VIRGILI

LOW-ENERGY HIGH-THROUGHPUT MICROPOROUS EMULSIFICATION FOR LEMON OIL ENCAPSULATION

Wael Kaade